Habilitation à Diriger des Recherches

Université Sorbonne Paris Nord

Bérangère Delourme

Quelques contributions à l'étude théorique et numérique des phénomènes de propagation des ondes dans des milieux périodiques

---

date de soutenance : 04/10/2023

Composition du jury :

Mme Anne-Sophie BONNET-BEN DHIA
M. Eric CANCES
M. Simon CHANDLER-WILDE
M. Nicolas CROUSEILLES
Mme Marion DARBAS
Mme Laurence HALPERN
Mme Pauline LAFITTE
M. Grégory VIAL

Remerciements

Je remercie tout d'abord l'ensemble des membres du jury. Je suis très honorée de pouvoir présenter mes travaux devant eux. Un grand merci aux rapporteurs, Simon Chandler-Wilde, Marion Darbas et Grégory Vial pour leur travail de relecture.

Je remercie également tous les membres du laboratoire de mathématiques de Paris Nord. J'ai la chance de travailler au LAGA depuis onze ans dans un climat calme et chaleureux. Une grand merci aux équipes de direction et à l'équipe administrative, tout particulièrement à Yolande Jimenez et à Leïla Segarel, toujours efficaces et attentionnées. Je remercie aussi les membres de l'équipe Modélisation et Calcul Scientifique : les différents responsables de l'équipe, Laurence Halpern, qui a œuvré pour mon intégration au sein du laboratoire, Emmanuel Audusse binôme enthousiaste pour organiser le séminaire, Marion Darbas toujours dynamique et encourageante, Igor Chollet, mon co-bureau et dernier arrivé dans l'équipe et Jérôme Le Rousseau. J'ai bien entendu une pensée pour toute l'équipe de la formation MACS, tout particulièrement Hakim Boumaza, Olivier Lafitte et Laurent Tournier. Échanger avec eux est toujours un réel plaisir. Je remercie par ailleurs Linda El Alaoui-Lakhnati et Gwenola Madec qui m'ont appris à diversifier et renouveler mes pratiques pédagogiques. Je souhaite enfin remercier les responsables pédagogiques et administratifs avec qui j'ai pu travailler à l'Institut Galilée mais aussi à l'UFR de sciences économiques et de gestion. Merci particulièrement à Liliana Cano, Elisabeth Christiny, Charles El Nouty, Sophie Toulouse et Laurent Vernac.

Je souhaite remercier les stagiaires de master, doctorants et post-doctorant que j'ai eu le plaisir d'encadrer ou de co-encadrer. Ces expériences ont enrichi ma pratique professionnelle sur le plan scientifique et humain. Un très grand merci à Elizaveta Vasilevskaya, qui a énormément contribué aux résultats présentés dans ce manuscrit, et avec qui j'ai beaucoup appris. Merci aussi à Bui Duc Quang dont le travail est présenté dans le dernier chapitre.

Je remercie tous mes collaborateurs scientifiques: Agnès Maurel, Jean-Francois Mercier, Kim Pham, qui m'expliquent avec enthousiasme les phénomènes physiques et mécaniques, David P. Hewett suffisamment patient pour discuter de développements asymptotiques malgré mon anglais médiocre, Xavier Claeys dont l'étendue de la culture mathématique m'impressionne toujours et Kersten Schmidt. Plus récemment, j'ai eu la chance d'échanger avec David Gontier et Antonin Coutand sur les questions de physique et de topologie ainsi que Felix Kwok sur les méthodes de décomposition de domaines. Un immense merci à l'équipe POEMS qui m'a accueillie deux semestres en délégation, tout particulièrement à Anne-Sophie Bonnet Ben-Dhia qui m'a beaucoup soutenue. Je tiens à remercier Sonia Fliss, avec qui j'ai le plaisir de collaborer depuis plus de dix ans, qui me fait confiance malgré les lenteurs de mon travail : une grande partie de mon activité de recherche n'aurait pu être réalisée sans son aide. Merci enfin à mes deux directeurs de thèse Houssem Haddar et Patrick Joly, qui m'ont transmis avec générosité et bienveillance un socle important de connaissances mathématiques et de précieuses méthodes de travail.

Pour terminer, je remercie mes proches pour leur soutien indéfectible. D'abord mes parents, mon frère Thibaud et ma soeur Maud. Et bien entendu Lucas ainsi que nos deux filles Suzanne et Bertille.

Introduction

This report aspires to make a summary of ten years of research activities at LAGA, mainly on the numerical and theoretical study of periodic media. It has been made possible thanks to the help and the work of different collaborators in and outside my laboratory.

The first chapter, which appears as a natural prolongation of my PhD work, presents pieces of work I have made on the modeling of periodic meta-surfaces. A periodic meta-surface consists of a periodic arrangement of homogenous materials along a curve (or a surface in three dimensions). In the low frequency regime, we assume that both the period and the thickness of the layer are much smaller than the wavelength (of the associated incident wave). It permits to analyse their effective behavior through asymptotic techniques based on periodic homogenization. On that topic, I have followed three research axis: first, in a collaborative project with K. Schmidt and A. Semin, we investigated the homogenization of meta-surfaces of finite length. It is well-known that a periodic meta-surface is responsable for the existence of an oscillatory and strongly localized boundary layer. In the case of a finite meta-surface (which is of course often the case in practice), we prove the existence of additional corner boundary layers appearing at the extremities of the meta-surface. In a second axis, developed with D.P. Hewett, we have studied the Faraday Cage effect, namely the ability of a wire mesh to block electromagnetic waves. Although the phenomenon is well-known by physicists, there is very few mathematical results on that topic, especially in three dimensional problems. Considering three 3D model configurations (Time harmonic Maxwell's equations), where the periodic layer comprises (i) discrete obstacles, (ii) parallel wires, (iii) wire mesh, we verify that the effective behaviour depends strongly on the topology of the periodic layer, with total shielding occurring only in the case of a wire mesh. Finally, I mention a collaborative work with the mechanical researchers A. Maurel, J.F. Mercier and K. Pham on the validity of high order asymptotic models (wherein the meta-surface is replaced by transmission conditions) in the presence of resonances. We formally show that, under certain hypothesis, high order approximative models remain valid around the resonance frequencies, although the limit problems are not.

In the second chapter, I collect some results on the existence of guided waves in periodic 'graph-like' structures. If this section is still dedicated to the study of periodic configurations, there are not seen in the low frequency homogenization limit: the wavelength of the wave is of the same order of magnitude than the period of the structure, which produces constructive and destructive interferences. As a result, their investigation requires additional mathematical tools, for instance spectral theory and Floquet-Bloch transform. This work has been initiated by the PhD work of Elizaveta Vasilevskaya (LAGA, 2012-2016) supervised by P. Joly (in collaboration with S. Fliss). We have proven the existence of guided waves and bounded states in perturbed square 'lattice'-like structures: we use, here again, asymptotic arguments, since, as the thickness of the domain goes to 0, the spectrum of the underlaying operator tends to the spectrum of an operator posed on the limit graph (its spectrum can be explicitly determined). More recently, S. Fliss and I have extended the approach to honeycomb graph-like domains, proving for instance, the existence of Dirac points (special points wherein the dispersion surfaces of the underlying operator are locally conical).

Finally, the third and last chapter, shorter, deals with the entirely different topic of domain decomposition methods for control problems that I started to look into as a participant of the A.N.R. project Allowap (ALgorithms for Large-scale optimisation of WAve Propagation). This project, led by L. Halpern

(LAGA), F. Kwok (Université Laval) and J. Salomon (Inria-Paris), aims to design space-time parallel algorithms for optimisation problems that arise when modeling wave phenomena. My contribution to this project focus on the conception of optimized Schwarz methods for control problems. We first studied with L. Halpern a preliminary elliptic case. Then, in collaboration with Dang Thanh Vuong (PhD, LAGA, 2020-2023, supervision L. Halpern) and Bui Duc Quang (Post-doctoral researcher at LAGA since Sept-2021, co-supervision L. Halpern), we aim to extend it for transport and wave optimal control problems, investigating first time domain decomposition methods.

List of publications

1. Delourme, B., Haddar, H., and Joly, P. *Approximate models for wave propagation across thin periodic interfaces.* Journal de mathématiques pures et appliquées, 2012, vol. 98, no 1, p. 28-71.

2. Delourme, B., Haddar, H., and Joly, P. *On the well-posedness, stability and accuracy of an asymptotic model for thin periodic interfaces in electromagnetic scattering problems.* Mathematical Models and Methods in Applied Sciences, 2013, vol. 23, no 13, p. 2433-2464.

3. Claeys, X. and Delourme, B. *High order asymptotics for wave propagation across thin periodic interfaces.* Asymptotic Analysis, 2013, vol. 83, no 1-2, p. 35-82.

4. Bruno, O.-P. and Delourme, B. *Rapidly convergent two-dimensional quasi-periodic Green function throughout the spectrum—including Wood anomalies.* Journal of Computational Physics, 2014, vol. 262, p. 262-290.

5. Delourme, B. *High-order asymptotics for the electromagnetic scattering by thin periodic layers.* Mathematical Methods in the Applied Sciences, 2015, vol. 38, no 5, p. 811-833.

6. Delourme, B., Schmidt K., and Semin, A. *On the homogenization of thin perforated walls of finite length.* Asymptotic Analysis, 2016, vol. 97, no 3-4, p. 211-264.

7. Delourme, B., Fliss, S., Joly P., and Vasilesvksaya, E. *Trapped modes in thin and infinite ladder like domains. Part 1: Existence results.* Asymptotic analysis, 2017, vol. 103, no 3, p. 103-134.

8. Delourme, B., Joly P., and Vasilevskaya, E. *Existence of guided waves due to a lineic perturbation of a 3D periodic medium.* Applied Mathematics Letters, 2017, vol. 69, p. 146-152.

9. Delourme, B., Halpern, L., and Nguyen, B.- T.. *Optimized Schwarz methods for elliptic optimal control problems.* International Conference on Domain Decomposition Methods. Springer, Cham, 2017. p. 215-222.

10. Semin, A., Delourme, B., and Schmidt, K. *On the homogenization of the Helmholtz problem with thin perforated walls of finite length.* ESAIM: Mathematical Modelling and Numerical Analysis, 2018, vol. 52, no 1, p. 29-67.

11. Delourme, B., Fliss, S., Joly P., and Vasilesvksaya, E. *Trapped modes in thin and infinite ladder like domains. Part 2: asymptotic analysis and numerical application.* Asymptotic Analysis, 2020, vol. 119, no 1-2, p. 117-152.

12. Delourme, B. and Hewett, D.-P. *Electromagnetic shielding by thin periodic structures and the Faraday cage effect.* Comptes Rendus. Mathématique, 2020, vol. 358, no 7, p. 777-784.

13. Delourme, B., Duyckaerts , T., and Lerner, N. *On integrals over a convex set of the Wigner distribution.* Journal of Fourier Analysis and Applications, 2020, vol. 26, no 1, p. 1-40.

14. Delourme, B., Lunéville, E., Marigo, J.-J., Maurel, A., Mercier, J.-F. and Pham, K., *A stable, unified model for resonant Faraday cages.* Proceedings of the Royal Society A, 2021, vol. 477, no 2245, p. 20200668.

15. Delourme, B. and Halpern, L. *A Complex Homographic Best Approximation Problem. Application to Optimized Robin–Schwarz Algorithms, and Optimal Control Problems.* SIAM Journal on Numerical Analysis, 2021, vol. 59, no 3, p. 1769-1810.

16. Bui, D.-C., Delourme, B. and Kwok, F. *Optimized Schwarz Methods in Time for Transport Control.* International Conference on Domain Decomposition Methods, 2023, to appear.

17. Delourme, B. and Fliss, S. *Guided modes in a hexagonal periodic graph like domain*, submitted.

Publication [9] and [16] are conference proceedings. In [13], my participation is limited to only a small section.

Supervision activities

Master's Thesis

- 2013: Lê Tung (co-supervision with V. Milisik): asymptotic models for thin layer.

- 2014: Thanh Binh Nguyen (co-supervision with L. Halpern): mathematical study of an elliptic control problem.

- 2017 : Tan Binh Phan (co-supervision with S. Fliss): numerical and theoretical investigation of hexagonal graph models.

- 2019: Doan Trang Nguyen Tung: numerical computation for the Faraday Cage effect

- 2023: Huynh Le Nhat Linh (co-supervision with Bui Duc Quang): dispersion properties of Brick wall structures.

PhD and postdoctoral students

- 2012-2016: Co-Supervision of Elizabeta Vasilevskaya (with P. Joly and S.Fliss) (bourse de l'école Doctorale Galilée)

- 2020-2023: Co-Supervision of Dang Thanh Vuong (with L. Halpern) (bourse de l'école Doctorale Galilée)

- 2021-2023: Co-supervision of the post-doctoral project of Bui Duc Quang (with L. Halpern) (ANR Allowap)

Contents

Chapter 1

Asymptotic models for meta-surfaces

1.1 Context

Metamaterials are artificially designed materials exhibiting specific behaviors that do not exist in nature (for instance negative permeability, permittivity, near zeros index). There are typically made of a three-dimensional periodic arrangement of small scatterers or resonators (dielectric or metallic), cf. Fig. 1.1. Effective properties of such materials are derived using asymptotic techniques. Because the size, the shape or the nature of the inclusions can be tuned by the designer, electromagnetic response can be controlled. For instance, the use of resonating scatterers permits to create doubly negative materials, whose effective permeability and effective permittivity are negative (in a range of frequencies) [224, 253, 145]: at the interface between a classical medium and such meta-material, incoming and refracted waves live in the same side of the normal (Fig. 1.2). Because they allow for controlling the wave propagation, the design of such materials opens a wide range of applications: shielding, cloaking, low-reflexion materials, antennas, resonators...

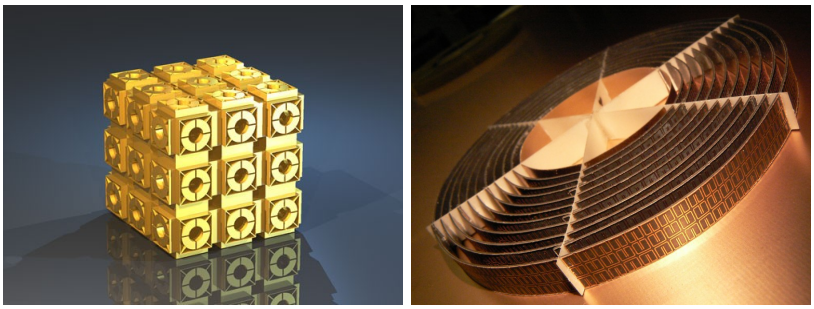

Figure 1.1: Examples of metamaterial (D. Schurig, Duke University (left),C. Soukoulis, Ames Laboratory (right))

Meta-surfaces (or single layer metamaterials) can be seen as the bi-dimensional counterpart of those meta-materials: they consists of a two dimensional array of scatterers, whose period and thickness are small in comparaison with the wavelength (of the illuminated wave). They can surround an obstacle or be disposed at the interface between two media. By contrast with 3D meta-materials, they cannot be described by effective materials. However, those surfaces can be rigorously approximated by transmission or impedance conditions, leading to approximate reflexion and transmission coefficients. Tuning those coefficients by designing the shape and the nature of the scatterers yields, as for the 3D metamaterial to specific properties. Because they take less physical space than their 3D counterpart and appear to be relatively simpler to build (with lithography and nano-printing), they are a promising alternative to meta-materials and has been widely investigated in the last decade. Applications such as frequency selective surfaces bases

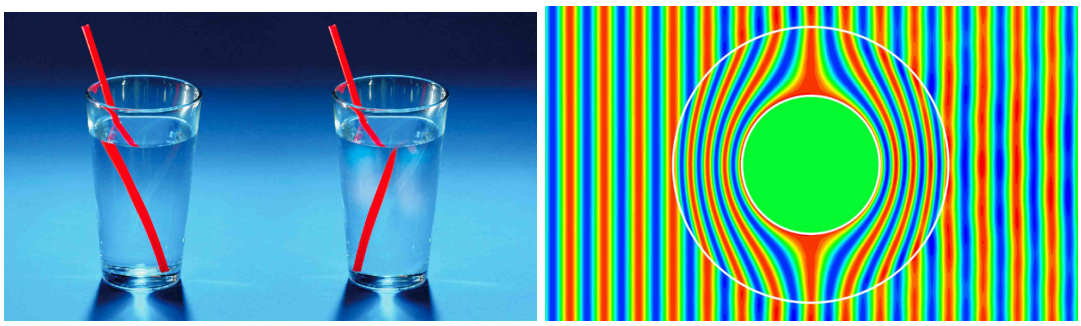

Figure 1.2: Negative refractive index, Cloaking of a plane wave

meta-surfaces, meta-surfaces antennas, polarization conversion can be found in [146, 45, 41, 59].

The derivation of the aforementioned approximate transmissions relies on multi-scale asymptotic analysis (see e.g [236, 11, 82, 38, 6, 185, 62, 186]). The main idea is to decompose the electric field into a macroscopic one (which lives far from the meta-surface) and a boundary layer corrector term in the vicinity of the meta-surface. Strongly localized, it decays exponentially fast as the distance to the periodic layer increases. Identifying the limit but also the higher order terms of the far field allows us to identify macroscopic effects of the meta-surfaces.

The pieces of work of this chapter explores this methodology to study the following problems:

1. **Asymptotic behavior of meta-surfaces of finite length** (Section 1.2). In most of the mathematical studies, the meta-surfaces are infinitely long (or surrounding a closed curve). This is not the case in applications, wherein the meta-surfaces are usually of finite length. Therefore, it is interesting to understand the influence of the end points on the macroscopic behavior of the structure. We prove that the presence of end points is responsable for the appearing of corners singularities in the neighborhood of their extremities.

2. **Identification of full three-dimensional behavior for the time Harmonic Maswell's Equations** (Section 1.3). Although the average problems for the 2D Helmholtz equation has ben widely investigated, the 3D Maxwell's equations is less known. We prove that the limit problem depends on the geometry of the meta-surface (this result is just the well known Faraday Cage effect). On the one hand, if the surface has a fishnet topology, it behaves as a perfect conductor at the limit. The meta-surface acts as a 'metascreen'. In the other hand, if the meta-surface is made of simply connected obstacles (that does not touch from one periodicity cell to the neighbor one), then the meta-surface disappears at the limit, and is denoted as a meta-screen. Partial shielding is obtained for intermediate situations like, grating of parallel wires.

3. **Validity of the approximate models in the resonant regime** (Section 1.4). For closed meta-screen, there are frequencies where the limit problem is not well posed. This is due to the Dirichlet eigenvalues of the interior problem, responsible for complex resonances. However, we can prove that, under certain assumptions, high order transmission models remain valid and accurate in the vicinity of those resonance frequencies.

1.2 'Finite' meta-surfaces

This work has been doing in collaboration with K. Schmidt and A. Semin. The associated results are published in the items [6] and [10] of the list of publications.

1.2.1 Description of the problem and main results

The objective of this work is to identify the impact of the end points of meta-surfaces on the macroscopic scale. To illustrate the problematic, we investigated a model problem made of a two dimensional meta-surface joining two re-entrant corners (see Fig. 1.3b). More specifically, let $\delta > 0$ be a small parameter and let us consider a domain Ω^δ consisting of a polygonal domain which excludes a set of similar small obstacles equi-spaced along the line between two re-entrant corners. The size of the obstacles and the distance between two consecutive ones are of same order of magnitude δ. Note, that as δ goes to 0, the repetition of holes degenerates to the interface Γ (of finite length), while the domain Ω^δ goes to the domain $\Omega_{\mathrm{T}} \cup \Omega_{\mathrm{B}}$ (see Fig. 1.3a).

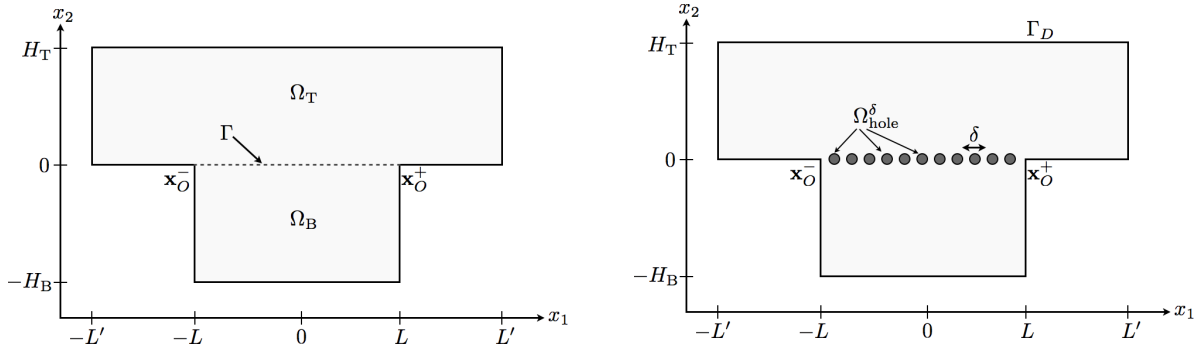

(a) The domain $\Omega = \Omega_{\mathrm{T}} \cap \Omega_{\mathrm{B}} \cap \Gamma$.

(b) The domain of interest $\Omega^\delta = \Omega \backslash \overline{\Omega^\delta_{\mathrm{hole}}}$.

Figure 1.3: Illustration of the polygonal domain Ω and the domain of interest Ω^δ.

On the domain Ω^δ , we consider the following problem: Seek u^δ solution to

$$\begin{cases} -\Delta u^\delta = f, & \text{in } \Omega^\delta \ , \\ \nabla u^\delta \cdot \mathbf{n} = 0, & \text{on } \partial\Omega^\delta_{\mathrm{hole}}, \\ u^\delta = 0, & \text{on } \partial\Omega \ , \end{cases} \tag{1.1}$$

where $f \in L^2(\Omega^\delta)$ is such that its support does not intersect the corners points $\mathbf{x}_O^\pm$. Using Lax-Milgram Theorem, it is easily seen that for any $\delta > 0$, there exists a unique solution $u^\delta \in \mathrm{H}^1(\Omega^\delta)$ of problem (1.1), and there exists a constant C (independent of δ) such that

$$\left\| u^\delta \right\|_{\mathrm{H}^1(\Omega^\delta)} \leqslant C \ \|f\|_{\mathrm{L}^2(\Omega^\delta)} \ . \tag{1.2}$$

The presence of the thin periodic layer of holes is responsible for the appearance of two different kinds of singular behaviors:

- First, a highly oscillatory boundary layer appears in the vicinity of the periodic layer. Strongly localized, it decays exponentially fast as the distance to the periodic layer increases.
- Additionally, since the thin periodic layer has a finite length and ends in corners of the boundary, corners singularities come up in the neighborhood of its extremities.

The boundary layer effect occurring in the vicinity of the periodic layer is well-known. It can be described using a two-scale asymptotic expansion (inspired by the periodic homogenization theory) that superposes slowly varying macroscopic terms and periodic correctors that have a two-scale behavior: these functions are the combination of highly oscillatory and decaying functions (periodic of period δ with respect to the tangential direction of the periodic interface and exponentially decaying with respect to d/δ, d denoting the distance to the periodic interface) multiplied by slowly varying functions. This boundary

layer effect has been widely investigated since the work of Sanchez-Palencia [237, 236], Achdou [4, 5] and Artola-Cessenat [11, 12]. In particular, high order asymptotics have been derived in [6, 185, 62, 42] for the Laplace equation and in [225, 226] for the Helmholtz equation.

On the other hand, corner singularities appearing when dealing with singularly perturbed boundaries have also been widely investigated. Among the numerous examples of such singularly perturbed problems, we can mention the cases of small inclusions (see [194, chapter 2] for the case of one inclusion and [34] for the case of several inclusions), perturbed corners [69], propagation of waves in thin slots [153, 154], the diffraction by wires [63], or the mathematical investigation of patched antennas [25]. Again, this effect can be depicted using two-scale asymptotic expansion methods that are the method of multi-scale expansion (sometimes called compound method) and the method of matched asymptotic expansions (see [251, 194, 147]). Following these methods, the solution of the perturbed problem may be seen as the superposition of slowly varying macroscopic terms that do not see directly the perturbation and microscopic terms that take into account the local perturbation.

The combination of the two types of singular behaviors have been investigated by Vial and co-authors [254, 48] for a Poisson problem in a polygonal domain surrounded by a thin and homogeneous layer, while Nazarov [204] studied the resolution of a general elliptic problem in a polygonal domain with periodically changing boundary. In their studies they have combined the two different kinds of asymptotic expansions mentioned above in order to deal with both corner singularities and the boundary layer effect. Based on the multi-scale method, the authors of [254, 48] constructed and justified a complete asymptotic expansion for the case of the homogeneous layer. For the periodic oscillatory boundary in [204] the first terms of the asymptotic expansion have been constructed and error estimates have been carried out. This asymptotic expansion relies on a sophisticated analysis of solution behavior at infinity for the Poisson problem in an infinite cone with oscillating boundary with Dirichlet boundary conditions by Nazarov [202], where he published an analysis for Neumann boundary conditions in [205].

We have complemented the two previous the work by constructing explicitly and rigorously justifying asymptotic an expansion for the above mentioned periodic layer transmission problem to any order (with Neumann boundary conditions on the perforations of the layer). Moreover, the study was extended to the Helmholtz equation for more generic domains with angles.

Description of the asymptotic expansion

Due to the periodic layer, it seems not possible to write a simple asymptotic expansion valid in the whole domain. We have to take into account both the boundary layer effect in the vicinity of Γ and the additional corner singularities appearing in the neighborhood of the two reentrant corners. To do so, we shall distinguish a *far field area* located ' far' from the reentrant corners $\mathbf{x}_O^{\pm}$ and two *near field zones* located in the vicinity of them (see Fig. 1.4).

Far field expansion Far from the two corners $\mathbf{x}_O^{\pm}$ (hatched area in Fig. 1.4), we shall see that u^δ is the superposition of a macroscopic part (that is not oscillatory) and a boundary layer localized in the neighborhood of the thin periodic layer. More precisely, we choose the following ansatz:

$$u^\delta(\mathbf{x}) = \sum_{(n,q)\in\mathbb{N}^2} \delta^{\frac{2}{3}n+q}\, u^\delta_{FF,n,q}(\mathbf{x}), \tag{1.3}$$

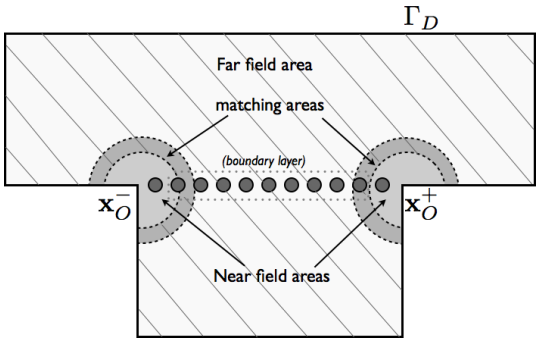

Figure 1.4: Schematic representation of the overlapping subdomains for the asymptotic expansion. The far field area (*hatched*) away from the corners $\mathbf{x}_O^{\pm}$ is overlapping the near field area (*light grey*) in the matching zone (*dark grey*).

where $\mathbf{x} = (x_1, x_2)$, and for $(n, q) \in \mathbb{N}^2$

$$u^{\delta}_{FF,n,q}(\mathbf{x}) = \begin{cases} u^{\delta}_{n,q}(\mathbf{x}) & \text{if } |x_1| > L, \\ \chi\left(\frac{x_2}{\delta}\right) u^{\delta}_{n,q}(\mathbf{x}) + \Pi^{\delta}_{n,q}(x_1, \frac{\mathbf{x}}{\delta}) & \text{if } |x_1| < L. \end{cases} \tag{1.4}$$

Here $\chi : \mathbb{R} \mapsto (0, 1)$ denotes a smooth cut-off function satisfying

$$\chi(t) = \begin{cases} 1 & \text{if } |t| > 2, \\ 0 & \text{if } |t| < 1. \end{cases} \tag{1.5}$$

The *macroscopic terms* $u^{\delta}_{n,q}$ are defined in the limit domain $\Omega_{\mathrm{T}} \cup \Omega_{\mathrm{B}}$. A priori, they are not continuous across Γ. As for the *boundary layer correctors* $\Pi^{\delta}_{n,q}(x_1, X_1, X_2)$ (also sometimes denoted *periodic correctors*), and as usual in the periodic homogenization theory, there are 1-periodic with respect to the scaled tangential variable X_1. Consequently, they are defined in $(-L, L) \times \mathcal{B}$, where $\mathcal{B}$ is the infinite periodicity cell (see Fig. 1.5a):

$$\mathcal{B} = \{(0, 1) \times \mathbb{R}\} \setminus \overline{\widehat{\Omega}_{\mathrm{hole}}}. \tag{1.6}$$

Moreover, the periodic correctors are super-algebraically decaying as the scaled variable X_2 tends to $\pm\infty$ (they decay faster than any power of X_2), more precisely, for any $(k, \ell) \in \mathbb{N}^2$,

$$\lim_{|X_2| \to +\infty} X_2^k \partial^{\ell}_{X_2} \Pi^{\delta}_{n,q} = 0. \tag{1.7}$$

The macroscopic terms as well as the boundary layer corrector terms might have a polynomial dependence with respect to $\ln \delta$: there is $N(n, q) \in \mathbb{N}$ such that

$$u^{\delta}_{n,q} = \sum_{s=0}^{N(n,q)} (\ln \delta)^s \, u_{n,q,s}, \quad \text{and} \quad \Pi^{\delta}_{n,q} = \sum_{s=0}^{N(n,q)} (\ln \delta)^s \Pi_{n,q,s},$$

where $u_{n,q,s}$ and $\Pi_{n,q,s}$ do not depend on δ.
Finally, in order to take into account the corner singularities, the far field terms $u^{\delta}_{FF,n,q}$ can blow up in the vicinity of the corners.

Remark 1. *Note that, although it might be surprising, we call far field expansion the expansion* (1.3)*, i.e., the superposition of the macroscopic terms and the boundary layer correctors. Besides, it should also be noted that, for any $k \in \mathbb{N}$, we consider $\delta^{\frac{2(n+3k)}{3}+q}$ and $\delta^{\frac{2n}{3}+(q+2k)}$ as different scales as they would be different powers of δ. In fact, the integers n and q play a different role in the asymptotic procedure. Finally, the consideration of the more general case of two angles of measure α, would yield to an expansion of the form (1.3) substituting $\delta^{\frac{2n}{3}+q}$ for $\delta^{\frac{\pi n}{\alpha}+q}$ (see [48]).*

Near field expansions In the vicinity of the two corners $\mathbf{x}_O^{\pm}$ (light grey areas in Fig. 1.4), the solution varies rapidly in all directions. Therefore, we shall see that

$$u^\delta(\mathbf{x}) = \sum_{(n,q)\in\mathbb{N}^2} \delta^{\frac{2n}{3}+q} U^\delta_{n,q,\pm}\left(\frac{\mathbf{x}-\mathbf{x}_O^{\pm}}{\delta}\right), \tag{1.8}$$

for some near field terms $U^\delta_{n,q,\pm}$ defined in the fixed unbounded domains

$$\widehat{\Omega}^- = \mathcal{K}^- \setminus \bigcup_{\ell\in\mathbb{N}} \left\{\overline{\widehat{\Omega}_{\rm hole}} + \ell\mathbf{v}_1\right\}, \quad \widehat{\Omega}^+ = \mathcal{K}^+ \setminus \bigcup_{\ell\in\mathbb{N}^*} \left\{\overline{\widehat{\Omega}_{\rm hole}} - \ell\mathbf{v}_1\right\} \tag{1.9}$$

shown in Figure 1.5b and 1.5c, where $\mathcal{K}^\pm$ are the unbounded angular domains

$$\mathcal{K}^\pm = \left\{\mathbf{X} = R^\pm(\cos\theta^\pm, \sin\theta^\pm), R^\pm \in \mathbb{R}_+^*, \theta^\pm \in I^\pm\right\} \in \mathbb{R}^2$$

of angular sectors $I^+ = (0, \frac{3\pi}{2})$ and $I^- = (-\frac{\pi}{2}, \pi)$. If the domain $\widehat{\Omega}_{\rm hole}$ is symmetric with respect to the axis $X_1 = 1/2$, then the domain $\widehat{\Omega}^-$ is nothing but the domain $\widehat{\Omega}^+$ mirrored with respect to the axis $X_1 = 0$. However, this is not the case in general. Similarly to the far field terms the near field terms might also have a polynomial dependence with respect to $\ln\delta$, i.e., for all $(n,q) \in \mathbb{N}^2$, there is $N(n,q) \in \mathbb{N}$ such that

$$U^\delta_{n,q,\pm} = \sum_{s=0}^{N(n,q)} (\ln\delta)^s U_{n,q,\pm,s}\ ,$$

where the functions $U_{n,q,\pm,s}$ do not depend on δ.

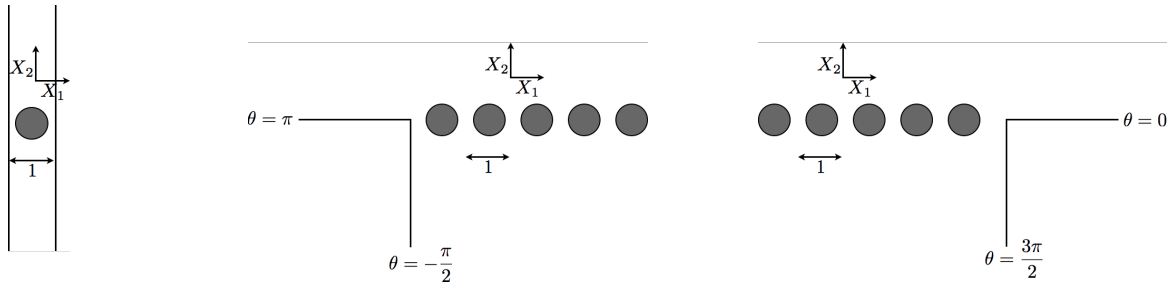

(a) The periodicity cell $\mathcal{B}$. (b) The domain $\widehat{\Omega}^-$. (c) The domain $\widehat{\Omega}^+$.

Figure 1.5: The periodicity cell $\mathcal{B}$ and the normalized domains $\widehat{\Omega}^\pm$.

Matching principle To link the two different expansions, we assume that they are both valid in two intermediate areas $\Omega^{\delta,\pm}_{\mathcal{M}}$ (dark shaded in Fig. 1.4) of the following form:

$$\Omega^{\delta,\pm}_{\mathcal{M}} = \left\{\mathbf{x} = (x_1, x_2) \in \Omega, \sqrt{\delta} \le d(\mathbf{x}, \mathbf{x}_O^{\pm}) \le 2\sqrt{\delta}\right\},$$

where d denotes the usual Euclidian distance. These intermediate areas correspond to a neighborhood of the corners $\mathbf{x}_O^{\pm}$ of the reentrant corners for the far field terms (macroscopic and boundary layer correctors) and to $R^\pm$ going to $+\infty$ for the near field terms (expressed in the scaled variables).

Main result:

Theorem 1. *Let $N_0 > 0$ such that $3N_0$ is an integer and let D_{N_0} denote the set of couples $(n,q) \in \mathbb{N}^2$ such that $\frac{2}{3}n + q \le N_0$. Furthermore, for a given number $\alpha > 0$, let*

$$\Omega_\alpha = \Omega^\delta \setminus (-L-\alpha, L+\alpha) \times (-\alpha, \alpha).$$

Then, there exist $\delta_0 > 0$,$C = C(\alpha, \delta_0) > 0$, *and* $k = k(N_0) \geq 0$, *such that for any* $\delta \in (0, \delta_0)$

$$\|u^\delta - \sum_{(n,q)\in D_{N_0}} \delta^{\frac{2}{3}n+q} u^\delta_{n,q}\|_{H^1(\Omega_\alpha)} \leq C\, \delta^{N_0+\frac{1}{3}} (\ln \delta)^k. \tag{1.10}$$

Main lines of the proof. The proof of Theorem 1 relies on the following arguments:

1. For each $(n, q) \in \mathbb{N}^2$, we justify the existence of the macroscopic terms $u^\delta_{n,q}$, the boundary layer corrector $\Pi^\delta_{n,q}$ and the near field terms $U^\delta_{n,q}$ up to $2n$ given constants. It requires to use weighted Sobolev spaces that allow polynomial blow up in the vicinity of the corners for $u^\delta_{n,q}$ and for large R for $U^\delta_{n,q}$.

2. We exhibit very precisely the behaviour of all the macroscopic terms $u^\delta_{n,q}$ in the vicinity of the corners and $U^\delta_{n,q}$ for large R.

3. We formally match the different expansions in the matching zones and provide a complete algorithm to construct all the terms of the asymptotic.

4. Once all the terms are constructed, we provide error estimates : it is based on the estimation of the construction of an approximation of u^δ in the whole domain and the stability estimate (1.2).

□

Because the overall procedure is very technical, in this report, we shall only focus on the investigation of near field problems, and more specifically on their precise behavior for large R. This might be the most original contribution of the work.

1.2.2 Microscopic terms

Inserting the near field ansatz (1.8) into the Laplace equation (1.1) and separating formally the different powers of δ, it is easily seen that the near field term $U^\delta_{n,q}$ satisfies

$$\begin{cases} -\Delta_{\mathbf{X}} U^\delta_{n,q} = 0 & \text{in } \widehat{\Omega}^\pm, \\ U^\delta_{n,q} = 0 & \text{on } \partial\mathcal{K}^\pm, \\ \partial_n U^\delta_{n,q} = 0 & \text{on } \partial\widehat{\Omega}^\pm_{\text{hole}} = \partial\widehat{\Omega}^\pm \setminus \partial\mathcal{K}^\pm. \end{cases} \tag{1.11}$$

We decide to write $U^\delta_{n,q}$ as a linear combination of so called 'near field' singularities $S^\pm_k$

$$U^\delta_{n,q,\pm} = \sum_{k=1}^{n} \mathscr{L}_k(U^\delta_{n,q,\pm}) S^\pm_k, \tag{1.12}$$

where, for any $q \in \mathbb{N}$, the n constants $\mathscr{L}_k(U^\delta_{n,q,\pm})$ are determined through the matching procedure. The function $S^\pm_m$ are particular solutions to

$$\begin{cases} -\Delta S^\pm_m = 0 & \text{in } \widehat{\Omega}^\pm, \\ S^\pm_m = 0 & \text{on } \partial\mathcal{K}^\pm, \\ \partial_n S^\pm_m = 0 & \text{on } \partial\widehat{\Omega}^\pm \setminus \partial\mathcal{K}^\pm, \end{cases} \qquad S^\pm_m \sim (R^\pm)^{\lambda_m} \sin(\frac{2m}{3}\theta^+) \quad \text{for large } R. \tag{1.13}$$

The proof of existence of $S^\pm_m$ (and their uniqueness adding some appropriate additional constraints) is based on variational arguments, see [48, Proposition 3.6]). However, in order to make the matching procedure, we need to exhibit their precise behavior as $R^\pm$ tends to infinity. In the present case, because of the presence of the thin layer of periodic holes this is far from being trivial. Indeed, there is no separation of variables. Additionally, because of the boundary layer appearing in the vicinity of the hoes, the method base on Mellin transform (and standard Weighted Sobolev spaces, see [162], [163, Chap. 5 and Chap. 6]) does not work directly here. Hopefully, the theory has ben adapted in [205] for our case.

Asymptotic blocks To understand these behavior, we shall introduce asymptotic blocks (we adopt this notion from [205]). For this let us consider a smooth cut-off function $\chi_{\text{macro},+}$ (see Fig. 1.6) that satisfies

$$\chi_{\text{macro},+}(X_1^+, X_2^+) = \begin{cases} \chi(X_2^+) & \text{for } X_1^+ < -1, \\ 1 & \text{for } X_1^+ > -\frac{1}{4}\ , \\ 1 & \text{for } X_1^+ > -1, |X_2^+| > 3\ , \end{cases} \tag{1.14}$$

and for $m \in \mathbb{Z} \setminus \{0\}$ the asymptotic block

$$\mathcal{U}_{m,p,+}(X_1^+, X_2^+) = \chi(R^+) \sum_{r=0}^{p} \Big(\chi_{\text{macro},+}(X_1^+, X_2^+)\, (R^+)^{\lambda_m - r}\, w_{m,r,+}(\ln R^+, \theta^+) + \chi_-(X_1^+)\, |X_1^+|^{\lambda_m - r} p_{m,r,+}(\ln |X_1^+|, X_1^+, X_2^+) \Big)\ , \tag{1.15}$$

where the cut-off function $\chi_-(X_2) = 1_{(-X_2>0)}\chi(X_2)$ and the function $w_{m,r,+}$ and $p_{m,r,+}$ are explicitly defined (Appendix A.2 and (3.32) Equation in [78]). There precise definition is not required but we have to make a few comments:

- Far from the periodic layer $\mathcal{U}_{m,p,+}$ is a sum of functions $(R^+)^{\lambda_m - r}\, w_{m,r,+}(\ln R^+, \theta^+)$. In particular, for large R^+, its leading asymptotic is $(R^+)^{\lambda_m} \sin(\lambda_m \theta^+)$.
- In the vicinity of it it, in order to satisfy Neumann boundary conditions on the set of holes, the previous sum is replaced with a sum of $|X_1^+|^{\lambda_m - r} p_{m,r,+}(\ln |X_1^+|, X_1^+, X_2^+)$, where the function $p_{m,r,+}$ are polynomial with respect to their first variable, periodic with respect to X_1^+ and exponentially decaying with respect to X_2^+.

The crucial point here is that, for large R^+,

$$\Delta \mathcal{U}_{m,p,+} \sim o((R^+)^{\lambda_m - p})$$

which means that, the Laplacian of the asymptotic block $\mathcal{U}_{m,p,+}$ becomes more and more decaying as $p \to \infty$.

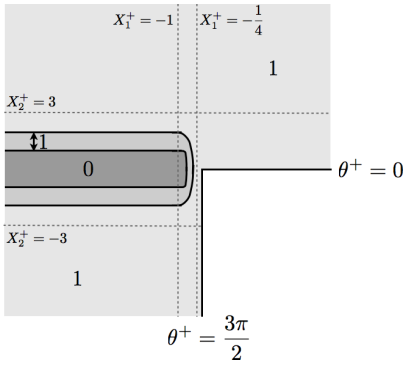

Figure 1.6: Schematic representation of the cut-off function $\chi_{\text{macro},+}$ defined in (1.14)

Remark 2. *In absence of holes, there is not need to introduce those asymptotic blocks: indeed, the function $(R^+)^{\lambda_n} \sin(\lambda_n \theta^+)$ is already harmonic.*

Asymptotic behavior of $S_m^\pm$ The asymptotic behavior of the functions S_m^+ can be expressed in terms of those asymptotic blocks: indeed, one has

$$S_m^+ = \mathcal{U}_{m,\lceil \frac{2(k+m)}{3} \rceil,+} + \sum_{n=1}^{k} \mathscr{L}_{-n}(S_m^+) \mathcal{U}_{-n,\lceil \frac{2(k-n)}{3} \rceil,+} + \mathcal{R}_{m,k}. \tag{1.16}$$

The most difficult part is to make a rigorous estimation of the remainder $\mathcal{R}_{m,k}$. Hopefully, [205] provides the appropriate family of weighted Sobolev spaces. For $\ell \in \mathbb{N}$, we introduce the space $\mathfrak{V}^{\ell}_{\beta,\gamma}(\widehat{\Omega}^+)$ defined as the completion of $C^{\infty}_c(\overline{\widehat{\Omega}^+})$ with respect to the norm

$$\|v\|_{\mathfrak{V}^{\ell}_{\beta,\gamma}(\widehat{\Omega}^+)} = \sum_{p=0}^{\ell} \left\| (1+R^+)^{\beta-\gamma-\delta_{p,0}} \rho^{\gamma-\ell+p+\delta_{p,0}} \nabla^p v \right\|_{L^2(\widehat{\Omega}^+)} \quad \rho = 1 + (1+R^+)|\theta^+ - \pi|. \tag{1.17}$$

The norm $\|\cdot\|_{\mathfrak{V}^2_{\beta,\gamma}(\widehat{\Omega}^+)}$ is a non-uniform weighted norm. The weight varies with the angle θ^+. Away from the periodic layer, i.e., for $|\theta^+ - \pi| \geq \varepsilon$ for some $\varepsilon > 0$ and R^+ sufficiently large, we recover the classical weighted Sobolev norm $V^2_{\beta}(\mathcal{K}^+)$ (cf. [163, Chap. 5 and Chap. 6]) :

$$\|v\|_{V^{\ell}_{\beta}(\mathcal{K}^+)} = \left(\sum_{p=0}^{\ell} \|(R^+)^{\beta-\ell+p} \nabla^p v\|^2_{L^2(\mathcal{K}^+)} \right)^{1/2}. \tag{1.18}$$

Indeed, in this part $\rho \sim 1 + R^+$ for $R^+ \to \infty$. In contrast, close to the layer, i.e., for $\theta^+ \to \pi$ for R^+ fixed, we have $\rho \to 1$, and the global weight in (1.17) becomes $(1+R^+)^{\beta-\gamma-\delta_{p,0}}$.

In the classical weighted Sobolev norm (1.18), the weight $(R^+)^{\beta-\ell+p}$ depends on the derivative ($p = 0$ or $p = 1$) under consideration. It increases by one at each derivative. This is linked to the fact that the gradient of a function of the form $(R^+)^{\lambda} g(\theta)$, which is given by $(R^+)^{\lambda-1}(\lambda g(\theta)\mathbf{e}_r + g'(\theta)\mathbf{e}_\theta)$, decays more rapidly than the function itself as R^+ tends to $+\infty$ (comparing $(R^+)^{\lambda-1}$ and $(R^+)^{\lambda}$). This property does not hold anymore for a function of the form $(X_1^+)^{\lambda} g(X_1^+, X_2^+)$ where $\mathbf{X}^+ = (X_1^+, X_2^+) = R^+(\cos\theta^+, \sin\theta^+)$ and $g \in \mathcal{V}^+(\mathcal{B})$ (g is periodic with respect to X_1^+ and exponentially decaying with respect to X_2^+). Indeed, in this case

$$\nabla\left((X_1^+)^{\lambda} g\right) = \left(\lambda (X_1^+)^{\lambda-1} g + (X_1^+)^{\lambda} \partial_{X_1^+} g\right) \mathrm{e}_1 + (X_1^+)^{\lambda} \partial_{X_2^+} g \, \mathrm{e}_2,$$

which does not decrease as $(X_1^+)^{\lambda-1}$. This remark gives a first intuition of the necessity to introduce a weighted space with a weight adjusted in the vicinity of the periodic layer, i.e., for $\theta^+ \to \pi$. The crucial argument to estimate $\mathcal{R}_{m,k}$ is that the standard Mellin analysis made in [163, Chap. 5 and Chap. 6] for domain with corners has been extended to our case in [205]:

Lemme 1. *Let $\beta^0 < 1 + \frac{2(k+1)}{3}$ such that, for any $n \in \mathbb{N}$ $\beta^0 - 1 \neq \lambda_n$ (β_0 is not a critical exponent). Then $\mathcal{R}_{m,k} \in \mathfrak{V}^2_{\beta^0,\gamma}(\widehat{\Omega}^+)$.*

1.2.3 Concluding remarks

First terms of the asymptotic A precise analysis shows that $u_{1,q} = 0$ for any integer q. As a result, far from the corners and the layers of holes (see Figure 1.7), we get

$$u^{\delta} = u_{0,0} + u_{0,1} + \delta^{\frac{4}{3}} u_{2,0} + O(\delta^2).$$

Because $u_{0,1}$ immediately derived from $u_{0,0}$, the first terms that encapsulate information about the corner is given in $u_{2,0}$ (which turns out to be independent of δ). In other words, the influence of the corner is of order $\delta^{\frac{4}{3}}$. In general (see [241]), in presence of a corner of angle α, its influence is of order $\delta^{\frac{2\pi}{\alpha}}$, which is always negligible with respect to δ^1 unless $\alpha = 2\pi$.

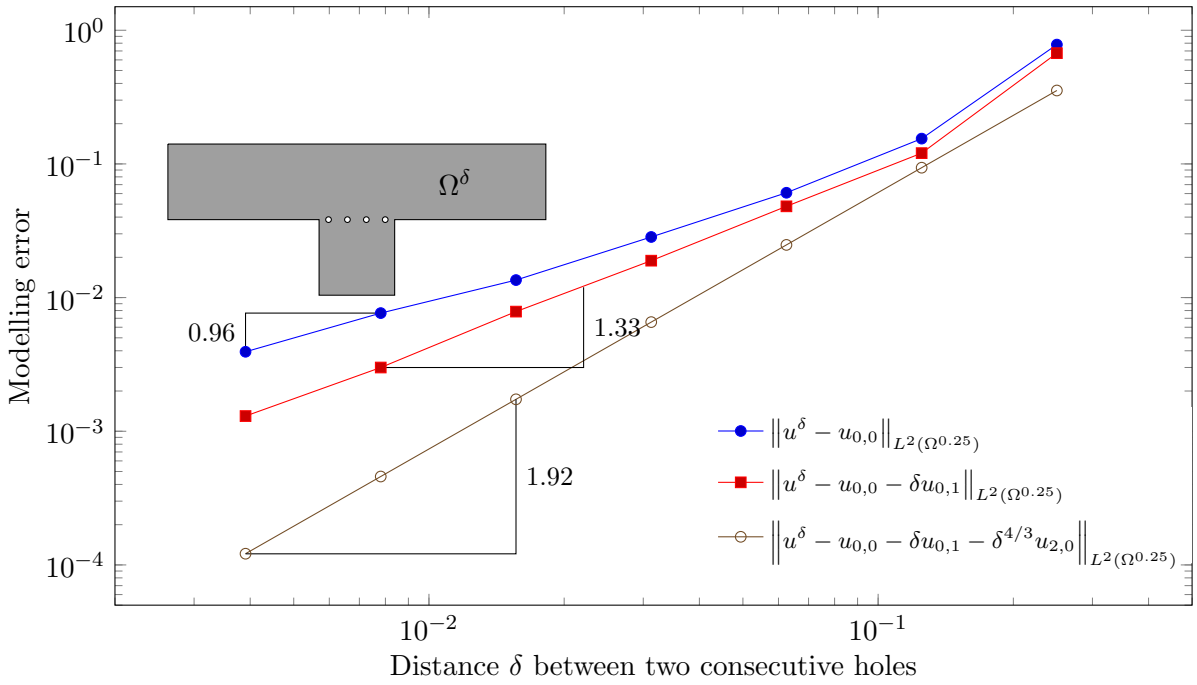

Figure 1.7: The numerically computed errors of macroscopic expansions truncated at different orders in dependence of δ. The computational domain Ω^δ is sketched for $\delta = 0.25$.

Extentions and open problems The method developed here has been extended (up to order δ^2) to the Helmholtz equation for any angle α. Using the functional framework of [205], the case of penetrable dielectric inclusions could be similarly investigated. *Formally*, the case of a periodic layer made of Dirichlet obstacles could be treated the same way. However, the justification is not obvious : the analysis made in [205] should be extended to the Dirichlet case, which is partially done in [202],[204].

To my knowledge, the building of approximate transmission conditions that can reproduce the effect of the corner is still an open problem. We highlight that our result proves that the use of first order approximate transmission condition (or boundary condition) (cf. [11],[3],[6],[74]) is still relevant but its approximation error deteriorates (from $O(\delta^2)$ to $O(\delta^{\frac{2\pi}{\alpha}})$) in presence of reentrant corners: indeed, the classical high order model cannot capture adequately the terms of order larger than one. We have tried to use the 'detached' asymptotic method (or self-adjoint extension) proposed in [212, 203, 155, 46] but we did not manage to produce a well design method (that could catch the macroscopic behavior induced by the corner in one shot, leading in fine to a profile correction method as in [67, 68, 13, 14]). Very interesting results can be found in [13, 14]: the authors propose to modify locally the approximate Robin boundary or to replace the Robin boundary condition by a Ventcel one. In each case, it permits to restore an optimal convergence rate for the L^2 norm.

1.3 Maxwell's equations: Faraday cage effect

This work has been done in collaboration with D.P. Hewett and corresponds to the item [12] of list of publications.

The ability of wire meshes to block electromagnetic waves (the celebrated "Faraday cage" effect) is well known to physicists and engineers. Experimental investigations into the phenomenon date back over 180 years to the pioneering work of Faraday [92], and the effect is routinely used to block or contain electromagnetic fields in countless practical applications. (An everyday example is the wire mesh in the door of a domestic microwave oven, which stops microwaves escaping, while letting shorter wavelength visible light pass through it.) But, somewhat remarkably, a rigorous mathematical analysis of the effect does not appear to be available in the literature.

The mathematical richness of the Faraday cage effect was highlighted in [58], where a number of different mathematical approaches were applied to the 2D electrostatic version of the problem. In particular it was shown in [58] how modern techniques of homogenization and asymptotic expansions could be used to derive effective interface conditions that accurately capture the shielding effect. These results were generalized to the 2D electromagnetic case (TE- and TM polarizations) in [139], and related approximations for similar problems have also been studied recently by other authors, e.g.[144, 186]. However, as far as we are aware, an analysis of the full 3D electromagnetic version of the problem with perfectly conducting scatterers has not previously been performed. We note that related approximations have been presented for thin layers of dielectric obstacles in [86, 87, 75, 70].

In this section, we consider full 3D electromagnetic scattering by a thin periodic layer of small, perfectly conducting obstacles. We derive leading-order homogenized interface conditions for three model configurations, namely where the periodic layer comprises (i) discrete obstacles, (ii) parallel wires, and (iii) a wire mesh. Our results verify that the effective behavior depends strongly on the topology of the periodic layer, with shielding of arbitrarily polarized waves occurring only in the case of a wire mesh. We note that analogous observations have been made in the related setting of volume homogenization in [240].

1.3.1 Statement of the problem

Our objective is to derive effective interface conditions for electromagnetic scattering by a thin periodic layer of equi-spaced perfectly-conducting obstacles on the interface $\Gamma = \{\mathbf{x} = (x_1, x_2, x_3) \in \mathbb{R}^3 : x_3 = 0\}$. Let $\hat{\Omega}_{\rm hole} \in \mathbb{R}^3$ be the canonical obstacle described by one of the following three cases (see Fig. 1.8):

1. $\hat{\Omega}_{\rm hole}$ is a simply connected Lipschitz domain whose closure is contained in $(0,1)^2 \times (-\frac{1}{2}, \frac{1}{2})$.
2. $\hat{\Omega}_{\rm hole} = [0,1] \times (\frac{3}{8}, \frac{5}{8}) \times (-\frac{1}{8}, \frac{1}{8})$, i.e. a wire (of square section) parallel to the direction $\mathbf{e}_1$.
3. $\hat{\Omega}_{\rm hole} = \{[0,1] \times (\frac{3}{8}, \frac{5}{8}) \times (-\frac{1}{8}, \frac{1}{8})\} \cup \{(\frac{3}{8}, \frac{5}{8}) \times [0,1] \times (-\frac{1}{8}, \frac{1}{8})\}$, i.e. a cross-shape domain made of the union of two perpendicular wires (one parallel to $\mathbf{e}_1$ and the other parallel to $\mathbf{e}_2$).

We construct the thin layer as a union of scaled and shifted versions of the canonical obstacle $\hat{\Omega}_{\rm hole}$. For $\delta > 0$ we define $\mathscr{L}^\delta \subset \mathbb{R}^2 \times [-\delta/2, \delta/2]$ by

$$\mathscr{L}^\delta = \text{int} \left(\bigcup_{(i,j) \in \mathbb{Z}^2} \delta \left\{ \overline{\hat{\Omega}_{\rm hole}} + i\mathbf{e}_1 + j\mathbf{e}_2 \right\} \right).$$

Our domain of interest is then $\Omega^\delta = \mathbb{R}^3 \setminus \overline{\mathscr{L}^\delta}$ (cf. Fig 1.9), and we define $\Gamma^\delta = \partial\Omega^\delta$.

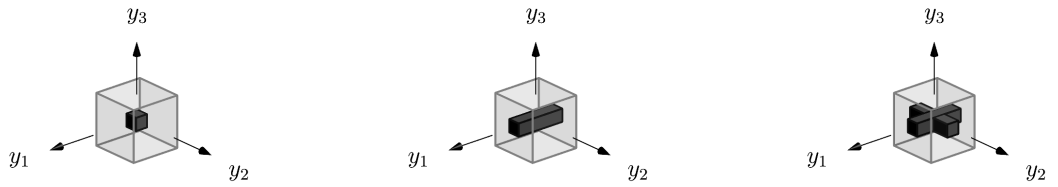

(a) Case (i) (b) Case (ii) (c) Case (iii)

Figure 1.8: The canonical obstacle $\hat{\Omega}_{\text{hole}}$ in the three cases under consideration.

Remark 3. *The precise geometry of the domains described above is not important (and the justification below is independent of their precise definition). The important point is that in (i) the periodic sheet is made of isolated domain, in case (ii) of a set of parallel wires and in (iii) of a mesh.*

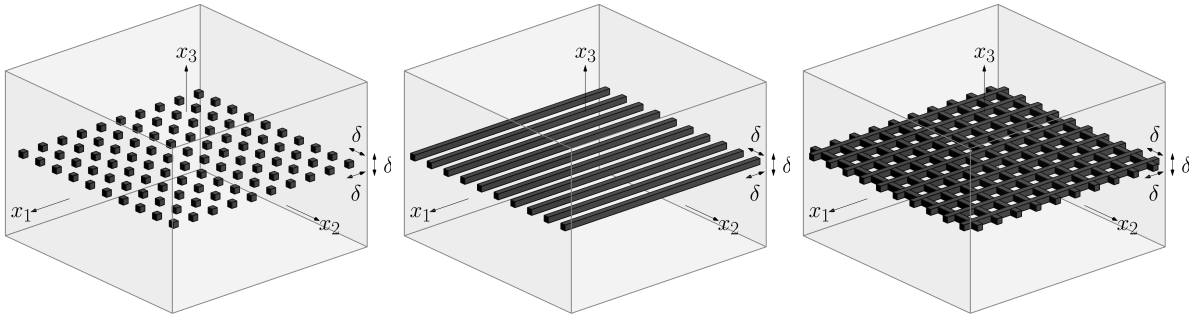

(a) Case (i) - discrete obstacles (b) Case (ii) - parallel wires (c) Case (iii) - wire mesh

Figure 1.9: The domain Ω^δ in the three cases under consideration.

On the domain Ω^δ we consider the solution $\mathbf{u}^\delta$ of the Maxwell equations

$$\text{curlcurl}\mathbf{u}^\delta - \omega^2\varepsilon\mathbf{u}^\delta = \mathbf{f} \quad \text{in } \Omega^\delta, \tag{1.19}$$

where $\omega \in \mathbb{C}$ and $\varepsilon \in \mathbb{C}$, subject to the perfectly conducting boundary condition

$$\mathbf{u}^\delta \times \mathbf{n} = 0 \quad \text{on} \quad \Gamma^\delta. \tag{1.20}$$

For analytical convenience we avoid any complications arising from far-field behavior by assuming that $\text{Re}[\varepsilon] > 0$ and $\text{Im}[\varepsilon] > 0$ (see Section1.5.3-2), and that the support of $\mathbf{f}$ does not intersect the interface Γ. Then, given $\mathbf{f} \in \left(L^2(\Omega^\delta)\right)^3$, the Lax-Milgram Lemma ensures that Problem (1.19)-(1.20) has a unique solution $\mathbf{u}^\delta$ in the standard function space

$$H(\text{curl};\Omega^\delta) = \left\{\mathbf{v} \in (L^2(\Omega^\delta))^3 : \text{curl}\mathbf{v} \in (L^2(\Omega^\delta))^3\right\}, \tag{1.21}$$

equipped with the usual graph norm $\|\mathbf{v}\|_{H(\text{curl};\Omega^\delta)} = \left(\|\mathbf{v}\|^2_{\left(L^2(\Omega^\delta)\right)^3} + \|\text{curl}\mathbf{v}\|^2_{\left(L^2(\Omega^\delta)\right)^3}\right)^{1/2}$. Moreover, one can prove that there exists $C > 0$, independent of δ, such that

$$\|\mathbf{u}^\delta\|_{H(\text{curl};\Omega^\delta)} \leq C\|\mathbf{f}\|_{\left(L^2(\Omega^\delta)\right)^3}, \qquad \text{for all } 0 < \delta < 1. \tag{1.22}$$

The objective of this work is to identify the limit $\mathbf{u}_0$ of $\mathbf{u}^\delta$ as δ tends to 0. This limit solution is defined in the union of two distinct domains $\Omega^\pm = \{\mathbf{x} \in \mathbb{R}^3 : \pm x_3 > 0\}$, whose common interface is Γ. Our main result is the following:

Theorem 2. *The limit solution* $\mathbf{u}^0$ *satisfies the Maxwell equations*

$$curlcurl\mathbf{u}^0 - \omega^2\varepsilon\mathbf{u}^0 = \mathbf{f} \quad \text{in } \Omega^+ \cup \Omega^-, \tag{1.23}$$

together with the following interface conditions on Γ*:*

Case (i): $[\mathbf{u}_0 \times \mathbf{e}_3]_\Gamma = \mathbf{0}$ *and* $[curl\mathbf{u}_0 \times \mathbf{e}_3]_\Gamma = 0$*.*

Case (ii): $\mathbf{u}_0 \cdot \mathbf{e}_1 = 0$ *on* Γ*,* $[\mathbf{u}_0 \cdot \mathbf{e}_2]_\Gamma = 0$*, and* $[(curl\mathbf{u}_0 \times \mathbf{e}_3) \cdot \mathbf{e}_2]_\Gamma = 0$*.*

Case (iii): $\mathbf{u}_0 \times \mathbf{e}_3 = \mathbf{0}$ *on* Γ*.*

As announced, we emphasize that the nature of the limit problem depends strongly on the topology of the thin layer of obstacles $\mathscr{L}^\delta$. In case (iii), where $\mathscr{L}^\delta$ comprises a wire mesh, we observe the "Faraday cage effect", where the effective interface Γ is a solid perfectly conducting sheet. Hence if the support of $\mathbf{f}$ lies in Ω^+ (above the layer $\mathscr{L}^\delta$), then $\mathbf{u}_0 = \mathbf{0}$ in Ω_-. In other words, despite the holes in its structure, the layer $\mathscr{L}^\delta$ shields the domain Ω^- from electromagnetic waves of all polarizations. At the opposite extreme, in case (i), where $\mathscr{L}^\delta$ comprises discrete obstacles, the interface is transparent and there is no shielding effect. In the intermediate case (ii), where $\mathscr{L}^\delta$ comprises an array of parallel wires, one observes polarization-dependent shielding. Fields polarized parallel to the wire axis are shielded, whereas those polarized perpendicular to the wire axis are not. Note that this case (ii) includes as a sub-case the simpler two-dimensional situation studied in [139, 144, 186] where the fields are invariant in the direction of the wire axis.

The proof of Theorem 2 is based on the construction of an asymptotic expansion of $\mathbf{u}^\delta$ using the method of matched asymptotic expansions (cf. [194]). To simplify the computation, we work with the first order formulation of (1.19), introducing the magnetic field $\mathbf{h}^\delta = \frac{1}{\mathrm{i}\omega}\mathrm{curl}\mathbf{u}^\delta$ (see e.g. [196]) and obtaining

$$\begin{cases} -\mathrm{i}\omega\mathbf{h}^\delta + \mathrm{curl}\mathbf{u}^\delta = 0 & \text{in } \Omega^\delta, \\ -\mathrm{i}\omega\mathbf{u}^\delta - \mathrm{curl}\mathbf{h}^\delta = -\frac{1}{\mathrm{i}\omega}\mathbf{f} & \text{in } \Omega^\delta, \end{cases} \quad \mathbf{u}^\delta \times \mathbf{n} = 0 \text{ and } \mathbf{h}^\delta \cdot \mathbf{n} = 0 \text{ on } \Gamma^\delta. \tag{1.24}$$

Far from the periodic layer $\mathscr{L}^\delta$, we construct an expansion of $\mathbf{h}^\delta$ and $\mathbf{u}^\delta$ of the form

$$\mathbf{h}^\delta = \mathbf{h}_0(\mathbf{x}) + \delta\mathbf{h}_1(\mathbf{x}) + \cdots, \quad \mathbf{u}^\delta = \mathbf{u}_0(\mathbf{x}) + \delta\mathbf{u}_1(\mathbf{x}) + \cdots, \quad \mathbf{x} = (x_1, x_2, x_3), \tag{1.25}$$

and, in the vicinity of $\mathscr{L}^\delta$,

$$\mathbf{h}^\delta = \mathbf{H}_0(x_1, x_2, \frac{\mathbf{x}}{\delta}) + \delta\mathbf{H}_1(x_1, x_2, \frac{\mathbf{x}}{\delta}) + \cdots, \quad \mathbf{u}^\delta = \mathbf{U}_0(x_1, x_2, \frac{\mathbf{x}}{\delta}) + \delta\mathbf{U}_1(x_1, x_2, \frac{\mathbf{x}}{\delta}) + \cdots, \tag{1.26}$$

where, for $i \in \{0, 1\}$, $\mathbf{H}_i(x_1, x_2, y_1, y_2, y_3)$ and $\mathbf{U}_i(x_1, x_2, y_1, y_2, y_3)$ are assumed to be 1-periodic in both y_1 and y_2. Near and far field expansions communicate through so-called matching conditions, which ensure that the far and near field expansions coincide in some intermediate areas. Since we are only interested in the leading order terms, it is sufficient to consider only the $O(1)$ matching conditions, namely

$$\lim_{x_3 \to 0^\pm} \mathbf{h}_0 = \lim_{y_3 \to \pm\infty} \mathbf{H}_0 \quad \text{and} \quad \lim_{x_3 \to 0^\pm} \mathbf{u}_0 = \lim_{y_3 \to \pm\infty} \mathbf{U}_0. \tag{1.27}$$

Inserting (1.3) into (1.19) and separating the different powers of δ directly gives (1.23). To obtain the interface conditions, we have to study the problems satisfied by $\mathbf{U}_0$ and $\mathbf{H}_0$:

$$\begin{cases} \mathrm{curl}_y\mathbf{U}_0 = 0 & \text{in } \mathscr{B}_\infty, \\ \mathrm{div}_y\mathbf{U}_0 = 0 & \text{in } \mathscr{B}_\infty, \\ \mathbf{U}_0 \times \mathbf{n} = 0 & \text{on } \partial\mathscr{B}_\infty, \end{cases} \quad \begin{cases} \mathrm{curl}_y\mathbf{H}_0 = 0 & \text{in } \mathscr{B}_\infty, \\ \mathrm{div}_y\mathbf{H}_0 = 0 & \text{in } \mathscr{B}_\infty, \\ \mathbf{H}_0 \cdot \mathbf{n} = 0 & \text{on } \partial\mathscr{B}_\infty, \end{cases} \quad \mathscr{B}_\infty = \Omega^1 = \mathbb{R}^3 \setminus \overline{\mathscr{L}^1}. \tag{1.28}$$

1.3.2 The spaces $K_N(\mathscr{B}_\infty)$ and $K_T(\mathscr{B}_\infty)$

Denoting by $\mathscr{B}$ the restriction of $\mathscr{B}_\infty$ to the strip $(0,1)^2 \times (-\infty,\infty)$, we introduce the spaces

$$\mathscr{H}_N(\mathscr{B}_\infty) = \{\mathbf{u} \in H_{\rm loc}({\rm curl};\mathscr{B}_\infty) \cap H_{\rm loc}({\rm div};\mathscr{B}_\infty) :\ \mathbf{u} \text{ is 1-periodic in } y_1 \text{ and } y_2,$$
$$\frac{\mathbf{u}_{|\mathscr{B}}}{\sqrt{1+(y_3)^2}} \in (L^2(\mathscr{B}))^3, \quad {\rm curl}\mathbf{u}_{|\mathscr{B}} \in (L^2(\mathscr{B}))^3, \quad {\rm div}\,\mathbf{u}_{|\mathscr{B}} \in L^2(\mathscr{B}), \quad \mathbf{u}\times\mathbf{n} = 0 \text{ on } \partial\mathscr{B}_\infty\big\}, \quad (1.29)$$

$$\mathscr{H}_T(\mathscr{B}_\infty) = \{\mathbf{h} \in H_{\rm loc}({\rm curl};\mathscr{B}_\infty) \cap H_{\rm loc}({\rm div};\mathscr{B}_\infty) :\ \mathbf{h} \text{ is 1-periodic in } y_1 \text{ and } y_2,$$
$$\frac{\mathbf{h}_{|\mathscr{B}}}{\sqrt{1+(y_3)^2}} \in (L^2(\mathscr{B}))^3, \quad {\rm curl}\mathbf{h}_{|\mathscr{B}} \in (L^2(\mathscr{B}))^3, \quad {\rm div}\,\mathbf{h}_{|\mathscr{B}} \in L^2(\mathscr{B}), \quad \mathbf{h}\cdot\mathbf{n} = 0 \text{ on } \partial\mathscr{B}_\infty\big\}, \quad (1.30)$$

both of which include periodic vector fields in $H_{\rm loc}({\rm curl};\mathscr{B}_\infty) \cap H_{\rm loc}({\rm div};\mathscr{B}_\infty)$ that tend to a constant vector as $|y_3| \to \infty$. Investigation of (1.28) requires the characterization of the so-called normal and tangential cohomology spaces $K_N(\mathscr{B}_\infty)$ and $K_T(\mathscr{B}_\infty)$ defined by (see [9])

$$K_N(\mathscr{B}_\infty) = \{\mathbf{u} \in \mathscr{H}_N(\mathscr{B}_\infty), {\rm curl}\mathbf{u} = 0, {\rm div}\mathbf{u} = 0\}\,,\ K_T(\mathscr{B}_\infty) = \{\mathbf{h} \in \mathscr{H}_T(\mathscr{B}_\infty), {\rm curl}\mathbf{h} = 0, {\rm div}\mathbf{h} = 0\}\,. \quad (1.31)$$

This characterization involves the representation of elements of $K_N(\mathscr{B}_\infty)$ and $K_T(\mathscr{B}_\infty)$ as gradients of harmonic scalar potentials, constructed by solving certain variational problems in the space

$$\mathcal{W}_1(\mathscr{B}_\infty) = \big\{p \in H^1_{\rm loc}(\mathscr{B}_\infty) :\ p \text{ is 1-periodic in } y_1 \text{ and } y_2, \frac{p_{|\mathscr{B}}}{\sqrt{1+(y_3)^2}} \in L^2(\mathscr{B}), \nabla p_{|\mathscr{B}} \in L^2(\mathscr{B})\big\}, \quad (1.32)$$

and variants of it. In each case the existence and uniqueness of the potential follows from the Lax-Milgram Lemma. While we do not reproduce the proofs here, we remark that the unbounded nature of the domain $\mathscr{B}$ requires us, when verifying coercivity of the requisite bilinear forms, to appeal to the inequality

$$\left\| \frac{p}{\sqrt{1+(y_3)^2}} \right\|_{L^2(\mathscr{B}_+)} \le 2\|\nabla p\|_{L^2(\mathscr{B}_+)}, \qquad \mathscr{B}_+ = \mathscr{B} \cap \{y_3 > 0\}, \quad (1.33)$$

valid if $p \in C^\infty(\overline{\mathscr{B}_+})$, $p/\sqrt{1+(y_3)^2} \in L^2(\mathscr{B}_+)$, $\nabla p \in L^2(\mathscr{B}_+)$ and $p = 0$ in a neighborhood of $\{y_3 = 0\}$, which is an elementary consequence of the Hardy inequality [214, Lemma 2.5.7]

$$\int_0^\infty t^{-2}|\varphi(t)|^2\,{\rm d}t \le 4\int_0^\infty |\varphi'(t)|^2\,{\rm d}t, \qquad \varphi \in C_0^\infty((0,\infty)). \quad (1.34)$$

Characterization of $K_N(\mathscr{B}_\infty)$

To characterize $K_N(\mathscr{B}_\infty)$ we first define two functions $p_3^\pm \in H^1_{\rm loc}(\mathscr{B}_\infty)$, 1-periodic in y_1 and y_2, such that

$$\begin{cases} -\Delta p_3^\pm = 0 & \text{in } \mathscr{B}_\infty, \\ p_3^\pm = 0 & \text{on } \partial\mathscr{B}_\infty, \end{cases} \quad \lim_{y_3\to\pm\infty} \nabla p_3^\pm = \mathbf{e}_3, \quad \lim_{y_3\to\mp\infty} \nabla p_3^\pm = 0.$$

Then, in case (i) we introduce the functions $\tilde{p}_1 \in \mathcal{W}_1(\mathscr{B}_\infty)$ and $p_1 \in H^1_{\rm loc}(\mathscr{B}_\infty)$, such that

$$\begin{cases} -\Delta\tilde{p}_1 = 0 & \text{in } \mathscr{B}_\infty, \\ \tilde{p}_1 = -\mathscr{P}\mathscr{R}y_1 & \text{on } \partial\mathscr{B}_\infty, \end{cases} \quad \text{and} \quad p_1 = \tilde{p}_1 + y_1.$$

Here, for any function $u \in L^2_{\rm loc}(\mathscr{B}_\infty)$, $\mathscr{R}u$ denotes its restriction to $\mathscr{B}$, while for any function $u \in L^2_{\rm loc}(\mathscr{B})$, $\mathscr{P}u$ denotes its periodic extension to $\mathscr{B}_\infty$. Similarly, in cases (i) and (ii) we introduce the functions $\tilde{p}_2 \in \mathcal{W}_1(\mathscr{B}_\infty)$ and $p_2 \in H^1_{\rm loc}(\mathscr{B}_\infty)$, such that

$$\begin{cases} -\Delta\tilde{p}_2 = 0 & \text{in } \mathscr{B}_\infty, \\ \tilde{p}_2 = -\mathscr{P}\mathscr{R}y_2 & \text{on } \partial\mathscr{B}_\infty, \end{cases} \quad \text{and} \quad p_2 = \tilde{p}_2 + y_2.$$

We emphasize that it is not possible to construct $\tilde{p}_1$ in cases (ii) and (iii), and it is not possible to construct $\tilde{p}_2$ in case (iii). An adaptation of the proof of [9, Proposition 3.18] leads to the following result:

Proposition 1.

Case (i): K_N is the space of dimension 4 given by $K_N(\mathscr{B}_\infty) = \mathrm{span}\left\{\nabla p_1, \nabla p_2, \nabla p_3^-, \nabla p_3^+\right\}$.

Case (ii): K_N is the space of dimension 3 given by $K_N(\mathscr{B}_\infty) = \mathrm{span}\left\{\nabla p_2, \nabla p_3^-, \nabla p_3^+\right\}$.

Case (iii): K_N is the space of dimension 2 given by $K_N(\mathscr{B}_\infty) = \mathrm{span}\left\{\nabla p_3^-, \nabla p_3^+\right\}$.

Sketch of the proof in case (ii). First, one can verify directly that the family $\left\{\nabla p_2, \nabla p_3^-, \nabla p_3^+\right\}$ is linearly independent (using the limit of ∇p_2 and $\nabla p_3^\pm$ as y_3 tends to $\pm\infty$). Moreover, it is clear that ∇p_2 and $\nabla p_3^\pm$ belong to $K_N(\mathscr{B}_\infty)$. Now, let $\mathbf{u} \in K_N(\mathscr{B}_\infty)$. Since $\mathscr{B}_\infty$ is connected, there exists $p \in H^1_{\mathrm{loc}}(\mathscr{B}_\infty)$, unique up to the addition of a constant, such that $\mathbf{u} = \nabla p$. (This follows e.g. from applying [196, Theorem 3.37] on an increasing sequence of nested subsets of $\mathscr{B}_\infty$ after extension of $\mathbf{u}$ by zero inside $\mathbb{R}^3 \setminus \overline{\mathscr{B}_\infty}$.) Moreover, ∇p is periodic and there exists a real sequence $(c_j)_{j\in\mathbb{Z}}$ such that

$$-\Delta p = 0 \text{ in } \mathscr{B}_\infty, \quad p = c_j \text{ on } \partial\mathscr{B}_{\infty,j} = \partial\mathscr{B}_\infty \cap \{j < y_2 < (j+1)\}.$$

Because ∇p is periodic and $\frac{\mathbf{u}_{|\mathscr{B}}}{\sqrt{1+(y_3)^2}} \in (L^2(\mathscr{B}))^3$, there exists four constants α_1, α_2, $\alpha_3^\pm$ such that

$$\tilde{p} = p - \alpha_1 y_1 - \alpha_2 y_2 - \sum_{\pm} \alpha_3^\pm p_3^\pm \in \mathcal{W}_1(\mathscr{B}_\infty).$$

Since $\tilde{p} = c_j - \alpha_1 y_1 - \alpha_2 y_2$ on $\partial\mathscr{B}_{\infty,j}$, the periodicity of $\tilde{p}$ in y_1 implies that $\alpha_1 = 0$, while its periodicity in y_2 leads to $c_j = c_0 + \alpha_2 j$. As a result,

$$\tilde{p} = c_0 - \alpha_2(y_2 - j) \quad \text{ on } \partial\mathscr{B}_{\infty,j}.$$

Since $\tilde{p}$ is harmonic, we deduce that $\tilde{p} = c_0 + \alpha_2\tilde{p}_2$, and hence that $p = c_0 + \alpha_2 p_2 + \sum_\pm \alpha_3^\pm p_3^\pm$, which completes the proof. Cases (i) and (iii) follow similarly. □

Characterization of $K_T(\mathscr{B}_\infty)$

First, let us define $q_3 \in H^1_{\mathrm{loc}}(\mathscr{B}_\infty)$ as the unique function such that

$$\begin{cases} -\Delta q_3 = 0 & \text{in } \mathscr{B}_\infty, \\ \partial_{\mathbf{n}} q_3 = 0 & \text{on } \partial\mathscr{B}_\infty, \end{cases} \quad \lim_{y_3\to\pm\infty} \nabla q_3 = \mathbf{e}_3, \quad \lim_{y_3\to+\infty} q_3 - y_3 = 0.$$

Then for $i \in \{1, 2\}$ we introduce the functions $\tilde{q}_i \in \mathcal{W}_1(\mathscr{B}_\infty)$ and $q_i \in H^1_{\mathrm{loc}}(\mathscr{B}_\infty)$ such that

$$\begin{cases} -\Delta\tilde{q}_i = 0 & \text{in } \mathscr{B}_\infty, \\ \partial_{\mathbf{n}}\tilde{q}_i = -\mathbf{e}_i \cdot \mathbf{n} & \text{on } \partial\mathscr{B}_\infty, \end{cases} \quad \lim_{y_3\to+\infty} \tilde{q}_i = 0, \quad \text{and} \quad q_i = \tilde{q}_i + y_i.$$

In case (ii) we introduce a set of 'cuts' Σ defined by

$$\Sigma = \bigcup_{j\in\mathbb{Z}} \Sigma_j, \quad \text{where} \quad \Sigma_j = \Sigma_0 + j\mathbf{e}_2, \quad \Sigma_0 = (-\infty, \infty) \times (-\tfrac{3}{8}, \tfrac{3}{8}) \times \{0\}.$$

Similarly, in case (iii) we introduce the cuts

$$\Sigma = \bigcup_{(i,j)\in\mathbb{Z}^2} \Sigma_{ij}, \quad \text{where} \quad \Sigma_{ij} = \Sigma_{00} + i\mathbf{e}_1 + j\mathbf{e}_2, \quad \Sigma_{00} = (-\tfrac{3}{8}, \tfrac{3}{8})^2 \times \{0\}.$$

In both cases, $\mathscr{B}_\infty\backslash\Sigma$ is then the union of the two simply connected domains $\mathscr{B}^\pm_\infty = (\mathscr{B}_\infty \setminus \Sigma)\cap\{\pm y_3 > 0\}$. We denote by $\mathcal{W}_1(\mathscr{B}^\pm_\infty)$ the space defined by formula (1.32) replacing $\mathscr{B}_\infty$ with $\mathscr{B}^\pm_\infty$. In case (ii) we let $q^\pm_{2,p} = \Big((q^\pm_{2,p})_+, (q^\pm_{2,p})_-\Big) \in \mathcal{W}_1(\mathscr{B}^+_\infty) \times \mathcal{W}_1(\mathscr{B}^-_\infty)$ be the unique solutions to

$$\begin{cases} -\Delta q^\pm_{2,p} = 0 & \text{in } \mathscr{B}_\infty \setminus \Sigma, \\ \partial_{\mathbf{n}} q^\pm_{2,p} = -\mathbf{e}_2\cdot\mathbf{n} & \text{on } \partial\mathscr{B}^\pm_\infty \cap \partial\mathscr{B}_\infty, \\ \partial_{\mathbf{n}} q^\pm_{2,p} = 0 & \text{on } \partial\mathscr{B}^\mp_\infty \cap \partial\mathscr{B}_\infty, \end{cases} \quad \begin{cases} [q^\pm_{2,p}]_{\Sigma_j} = \pm(j - y_2), \\ [\partial_{y_3} q^\pm_{2,p}]_{\Sigma_j} = 0, \end{cases} \quad \lim_{y_3\to+\infty} q^\pm_{2,p} = 0, \tag{1.35}$$

and we define $q^\pm_2 = q^\pm_{2,p} + y_2 1_{\mathscr{B}^\pm_\infty}$, $1_{\mathscr{B}^\pm_\infty}$ being the indicator function of $\mathscr{B}^\pm_\infty$. In case (iii) the functions $q^\pm_2$ are defined similarly, except that we replace Σ_j by Σ_{ij} in the jump conditions. In case (iii) we additionally introduce the functions $q^\pm_{1,p} = \Big((q^\pm_{1,p})_+, (q^\pm_{1,p})_-\Big) \in \mathcal{W}_1(\mathscr{B}^+_\infty) \times \mathcal{W}_1(\mathscr{B}^-_\infty)$ as the unique solutions to

$$\begin{cases} -\Delta q^\pm_{1,p} = 0 & \text{in } \mathscr{B}_\infty \setminus \Sigma, \\ \partial_{\mathbf{n}} q^\pm_{1,p} = -\mathbf{e}_1\cdot\mathbf{n} & \text{on } \partial\mathscr{B}^\pm_\infty \cap \partial\mathscr{B}_\infty, \\ \partial_{\mathbf{n}} q^\pm_{1,p} = 0 & \text{on } \partial\mathscr{B}^\mp_\infty \cap \partial\mathscr{B}_\infty, \end{cases} \quad \begin{cases} [q^\pm_{1,p}]_{\Sigma_{ij}} = \pm(i - y_1), \\ [\partial_{y_3} q^\pm_{1,p}]_{\Sigma_{ij}} = 0, \end{cases} \quad \lim_{y_3\to+\infty} q^\pm_{1,p} = 0, \tag{1.36}$$

and we define $q^\pm_1 = q^\pm_{1,p} + y_1 1_{\mathscr{B}^\pm_\infty}$. Then, adapting the proof of [9, Proposition 3.14] one obtains the following result:

Proposition 2.

Case (i): K_T is the space of dimension 3 given by $K_T(\mathscr{B}_\infty) = span\{\nabla q_1, \nabla q_2, \nabla q_3\}$.

Case (ii): K_T is the space of dimension 4 given by $K_T(\mathscr{B}_\infty) = span\{\nabla q_1, \nabla q^+_2, \nabla q^-_2, \nabla q_3\}$.

Case (iii): K_T is the space of dimension 5 given by $K_T(\mathscr{B}_\infty) = span\{\nabla q^+_1, \nabla q^-_1, \nabla q^+_2, \nabla q^-_2, \nabla q_3\}$.

1.3.3 Formal proof of Theorem 2

We treat the three cases separately. In case (i), using Propositions 1-2, we have

$$\mathbf{U}_0 = \sum_{i=1}^{2} a_i(x_1,x_2)\nabla p_i + \sum_{\pm} a^\pm_3 \nabla p^\pm_3 \quad \text{and} \quad \mathbf{H}_0 = \sum_{i=1}^{3} b_i(x_1,x_2)\nabla q_i.$$

The behavior at infinity of the functions p_i and q_i and the matching conditions (1.27) then imply

$$a_i = (\mathbf{u}_0)^\pm_i(x_1,x_2,0) \quad b_i = (\mathbf{h}_0)^\pm_i(x_1,x_2,0) \quad \forall i \in \{1,2\},$$

and, consequently (by (1.24)), that $[\mathbf{u}_0\times\mathbf{e}_3]_\Gamma = 0$ and $[\mathrm{curl}\mathbf{u}_0\times\mathbf{e}_3]_\Gamma = 0$. In case (ii) we have

$$\mathbf{U}_0 = a_2(x_1,x_2)\nabla p_2 + \sum_{\pm} a^\pm_3\nabla p^\pm_3 \quad \text{and} \quad \mathbf{H}_0 = b_1(x_1,x_2)\nabla q_1 + \sum_{\pm} b^\pm_2(x_1,x_2)\nabla q^\pm_2 + b_3(x_1,x_2)\nabla q_3,$$

which, together with the matching conditions (1.27), leads to $(\mathbf{u}_0)^\pm_1(x_1,x_2) = 0$, $[(\mathbf{u}_0)_2]_\Gamma = 0$, $[(\mathbf{h}_0)_1]_\Gamma = 0$. Finally, in case (iii) we have $\mathbf{U}_0 = \sum_\pm a^\pm_3\nabla p^\pm_3$, which implies that $(\mathbf{u}_0)^\pm_i(x_1,x_2) = 0$ for $i = 1$ or 2.

Remark 4. *We point out that our formal proof can be made entirely rigorous by justifying the asymptotic expansions* (1.3)-(1.8)*. This can be done a posteriori by constructing an approximation of $\mathbf{u}^\delta$ on Ω^δ (based on the truncated series* (1.3)-(1.8)*) and using the stability estimate* (1.22) *(see [194]).*

1.4 Asymptotic models for resonances

This part is a joint work with E.- Luneville, J.J-Marigo, A. Maurel, J.-F. Mercier, K. Pham (item [14] in the list of publications).

This section addresses the question of the validity of high-order asymptotic models in the vicinity of resonances. We investigate a toy-problem where we formally prove that the asymptotic model of order 1 remains accurate in presence of resonances. Similarly to Section 1.2, we consider a domain Ω^δ (Figure 1.10) consisting of a rectangular domain $\Omega = (-L, L) \times (-d, d)$ which excludes a set of similar small obstacles $\Omega^\delta_{\text{hole}}$ equi-spaced along the line

$$\Gamma = \{(x_1, 0) \in \mathbb{R}^2, x_1 \in (-L, L)\}.$$

Again, the size of the holes and the period are of the same order of magnitude δ (see [139] where different asymptotic regimes have been studied). In addition, to simplify the limit model (and the associated computations), we assume that the 'holes' are symmetric with respect to $x_2 = 0$. As δ goes to 0, the domain Ω^δ shrinks to the domains $\Omega^+ \cup \Omega^-$, with

$$\Omega^+ = (-L, L) \times (0, d) \quad \text{and } \Omega^- = (-L, L) \times (-d, 0),$$

that share the common interface Γ. Let $\omega > 0$, $f \in L^2(\Omega^\delta_{\text{hole}})$ compactly supported in Ω^+.

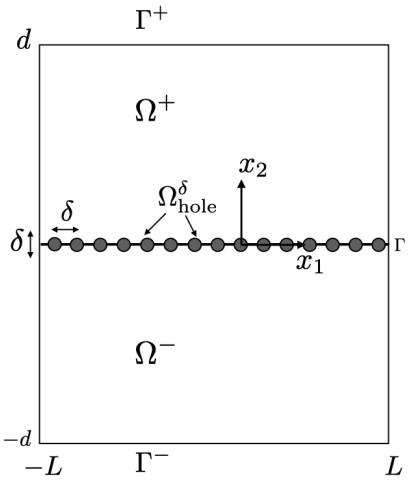

Figure 1.10: The domain Ω^δ. Away from resonance frequencies, the sheet $\Omega^\delta_{\text{hole}}$ shields the domain Ω^-.

We consider the following problem on the domain Ω^δ: find $u^\delta \in H^1(\Omega^\delta)$, $2L$-periodic w.r.t. x_1 such that

$$\begin{cases} -\Delta u^\delta - \omega^2 u^\delta = f & \text{in } \Omega^\delta, \\ u^\delta = 0 & \text{on } \partial\Omega^\delta_{\text{hole}} \cap \Gamma^-, \\ \partial_n u^\delta = \imath\omega u^\delta & \text{on } \Gamma^+. \end{cases} \tag{1.37}$$

As δ goes to 0, the formal limit u_0 (defined in $\Omega^+ \cup \Omega^-$) of this problem (see [58, 139, 186]) is given by

$$\begin{cases} -\Delta u_0 - \omega^2 u_0 = f & \text{in } \Omega^+, \\ u_0 = 0 & \text{on } \Gamma, \\ \partial_n u_0 = \imath\omega u_0 & \text{on } \Gamma^+. \end{cases} \quad \begin{cases} -\Delta u_0 - \omega^2 u_0 = 0 & \text{in } \Omega^-, \\ u_0 = 0 & \text{on } \Gamma^- \cup \Gamma, \end{cases} \tag{1.38}$$

and it turns out that the limit problem uncouples the behavior of u^δ below and above Γ. As soon as ω^2 is not an eigenvalue of the Dirichlet-Laplace operator in Ω^-, u^0 vanishes in Ω^- (supp $f \subset \Omega^+$): the set of obstacles $\Omega^\delta_{\text{hole}}$ shields Ω^-, this is the Faraday cage effect (see [58, 190]).

By contrast, if ω^2 is an eigenvalue of the Dirichlet-Laplace operator in Ω^-, then the limit problem is ill-posed. It reflects the presence of resonances for the initial problem (1.37) having a real part close to ω^2 and a small imaginary part (see [111] for the proof in the case of a circular sheet of perforated conducting plates). In that case, the structure does not shield anymore and behaves like a Helmholtz resonator (see [229, 140, 110, 88]).

Away from this set of resonance frequencies, it is known that is it possible to capture the macroscopic effect (of the periodic layer) up to order 1 with respect to δ, by solving the following unified problem (see e.g.[186]):

$$\begin{cases} -\Delta u^{1,\delta} - \omega^2 u^{1,\delta} = f \quad \text{in } \Omega^+ \cup \Omega^-, \\ u^{1,\delta} = 0 \quad \text{on } \Gamma^-, \\ \partial_n u^{1,\delta} = \imath\omega u^{1,\delta} \quad \text{on } \Gamma^+, \\ u^{1,\delta}(x_1, 0^+) = \delta\mathcal{B}\partial_{x_2} u^{1,\delta}(x_1, 0^+) - \delta\mathcal{A}\partial_{x_2} u^{1,\delta}(x_1, 0^-), \\ u^{1,\delta}(x_1, 0^-) = \delta\mathcal{A}\partial_{x_2} u^{1,\delta}(x_1, 0^+) - \delta\mathcal{B}\partial_{x_2} u^{1,\delta}(x_1, 0^-), \end{cases} \tag{1.39}$$

where, as usual, the constant $\mathcal{A}$ and $\mathcal{B}$ are obtained by solving periodic cell-problems. But unlike Problem (1.38), Problem (1.39) appears to be always well-posed for any frequency ω. We **formally** proved that it also provides a good approximation of u^δ for any frequency as stated below:

Formal Result 1. *For any $\Lambda = \omega^2$, u^δ and $u^{1,\delta}$ have the same-leading order asymptotic expansion.*

formal proof. Let $\Lambda_n = \omega_n^2$ be any eigenvalue of the Dirichlet-Laplace operator in Ω^- and let us denote by p_n a given (real) $L^2(\Omega^-)$-normalized corresponding eigenvector. Following [139], we consider three different regims of frequencies Λ, where we verify that the behavior of u^δ inside the cavity are different.

1. The *off resonance case*: $|\Lambda_n - \Lambda| = O(1)$. In that case (far from the resonances), u^δ is order $O(\delta)$ inside the cavity Ω^- and the validity of (1.39) is known [186, 139].

2. The *on resonance case*: If
$$\Lambda = \Lambda_n + \delta\tilde{\Lambda} + O(\delta^2),$$
with $\tilde{\Lambda} = -\mathcal{B}\int_\Gamma \partial_{x_2} p_n^2(x_1, 0)dx_1$, then u^δ blows up in the cavity, namely there exists $c_R \in \mathbb{C}^*$ such that
$$u^\delta \sim \frac{c_R}{\delta}\, p_n \text{ in } \Omega^-.$$

3. The *near resonance case*: If
$$\Lambda = \Lambda_n + \delta\Lambda_1 + O(\delta^2) \quad \text{with } \Lambda_1 \neq \tilde{\Lambda},$$
then u^δ is of order 1 in the cavity: there exists $c_{NR} \in \mathbb{C}^*$ such that
$$u^\delta \sim c_{NR}\, p_n \text{ in } \Omega^-.$$

In each of those three cases, the proof of Result 1 consists in constructing the leading order of the **formal** asymptotic expansions of u^δ and $u^{1,\delta}$ and to show that they indeed coincide. □

Numerical study On Figure 1.11, we represent the 'exact' field u^δ and the 'approximate' one $u^{1,\delta}$ for three different frequencies corresponding to the three cases described above. The source term is a plane wave of incident angle $\pi/4$ and the inclusion are small equi-spaced squares (period 1) of length side $e = 0.1$. The numerical results for the direct problems are obtained using a multi-modal approach [187]. The agreement between u^δ and $u^{\delta,1}$ is qualitatively good. The validity of the approximate model is further illustrated in Figure 1.12, where we have plotted the maximum of the evolution of absolute value of u^δ (resp. $u^{1,\delta}$) with respect to the frequency for three different values of $e \in \{0.01, 0.1, 1\}$. The reader might also find in [77] numerical tests of the model in the transient regime.

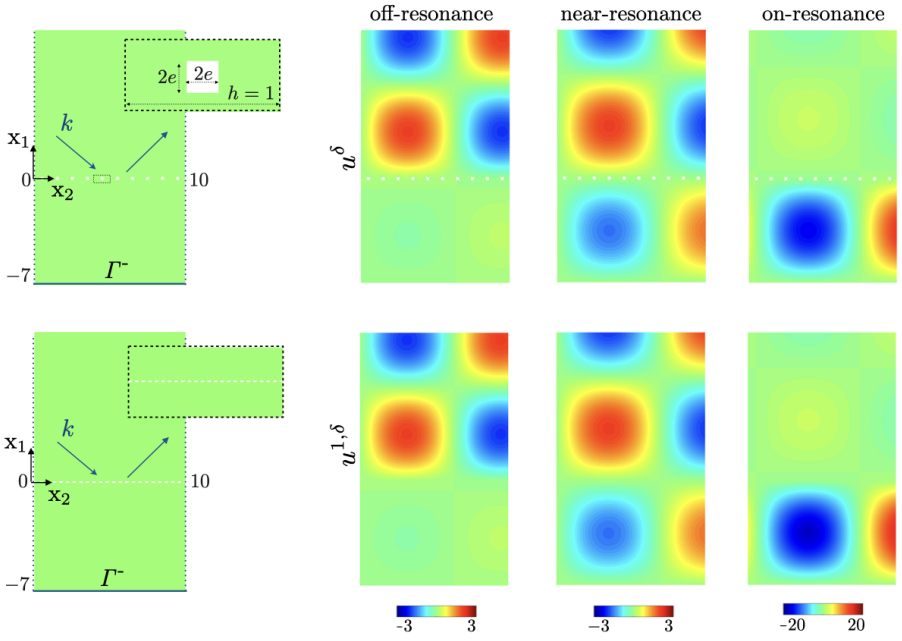

Figure 1.11: 'Exact' and 'Approximate' fields in the three different regimes

Remark 5. *In presence of the curvature, the model fails to be completely accurate. However, the model still predicts the resonance location.*

1.5 Perspectives and open problems

1.5.1 About the asymptotic models for thin periodic structures

The modeling of meta-surfaces using asymptotic methods has been a quite-active topic of research this last decade. High order transmission conditions have been derived for several problems : non exhaustively, electromagnetic grating [231, 198] (solar cell design), extension to general 3D geometrical configurations [55] array of resonant inclusions (planar and Anti planar-shear waves) [188, 189], array of Helmholtz resonators [191, 192], Maxwell's equation [177], Fano/Fabry-Perot resonnances [264], application to inverse problem [219]. Their adaptation to transient regime (together with numerical experiments) can be found in [183, 247] (and references therein). We point out that the stabilization technique described in [73, Section 5.2] appears to be important for time domain simulation in order to preserve an energy

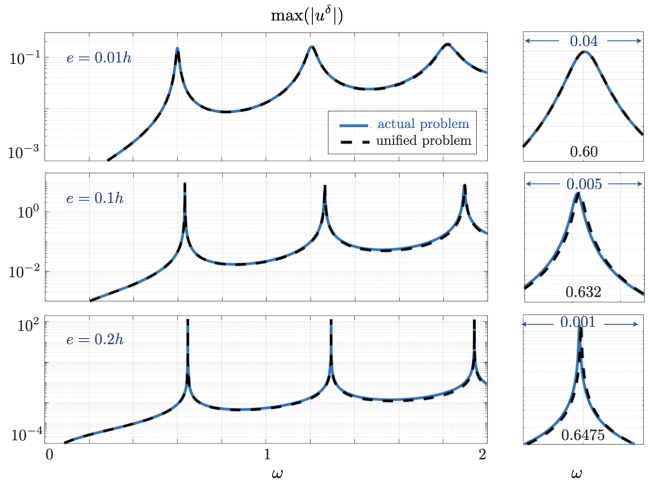

Figure 1.12: 'Maximum field inside the cavity Ω^- w.r.t ω: Direct numeric (plain blue line), appr. model (dashed black lines). Right-panel: zoom on the first resonance

(another stabilization technique can be found in [26]). The mathematical investigation (based on the Unfolding method [61]) of thin periodic sheet of very-closed Neumann obstacles (three scales) might me found in [81]. High order transmission for an interface between a periodic material and a homogeneous one can be found in the PhD dissertations [255] and [26]. Finally, the case of a thin random layer covering a conductor may be found in [40] (and forthcoming publications to appear).

1.5.2 Finite meta-surface

To complete the work developed in Section 1.2 (with a numerical purpose), it would be interesting to develop a method to resolve accurately the near field problems (1.11). Those problems are posed in the unbounded domain $\widehat{\Omega}^+$, and thus require to be truncated for the numerical resolution. To be more specific, let $f \in L^2(\widehat{\Omega}^+)$ be a compactly supported function and consider the following (well-posed) problem: find $u \in H^1_{\rm loc}(\widehat{\Omega}^+)$

$$\left\{\begin{array}{rcl} -\Delta u = & f & \text{in } \widehat{\Omega}^+, \\ u = & 0 & \text{on } \partial\mathcal{K}^+, \\ \partial_n u = & 0 & \text{on } \partial\widehat{\Omega}^\pm_{\rm hole} = \partial\widehat{\Omega}^+ \setminus \partial\mathcal{K}^+, \\ \lim\limits_{r\to+\infty} u = & 0. & \end{array}\right. \tag{1.40}$$

1. As a first investigation, we could truncate the domain at

$$\Gamma_R = \{(R\cos(\theta), R\sin(\theta)), \theta \in [0, \frac{3\pi}{2}]\},$$

and solve the problem with either homogeneous Dirichlet condition or homogeneous Neumann boundary condition (see Figure 1.13):

$$u_D = 0 \text{ on } \Gamma_R \quad \text{or} \quad u_N = 0 \text{ on } \Gamma_R.$$

Then, we could try to prove that, for any compact set Ω

$$\lim_{R\to+\infty} \|u - u_D\|_{H^1(\Omega)} = 0 \qquad \lim_{R\to+\infty} \|u - u_N\|_{H^1(\Omega)} = 0$$

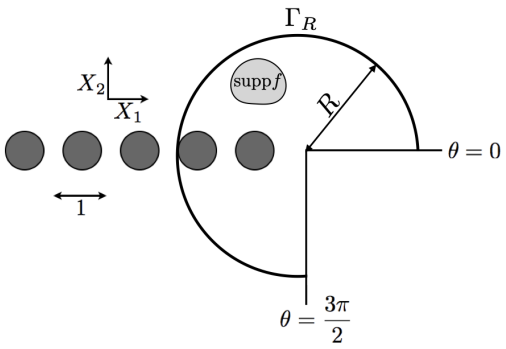

Figure 1.13: artificial truncation at Γ_R

and, if so, can we quantify the decay as R goes to ∞.

Naturally, we could presumably improve the truncation process by using the decomposition in asymptotic block described in Section 1.2.2, constructing so a more sophisticated approximation of the Dirichlet to Neumann map on Γ_R.

2. Another approach, adapted to the Helmholtz equation as well (but more prospective) could consist in using a cartesian truncation as represented in Figure 1.14. The idea would be to use the so called 'half-space' matching method (see e.g [37, 35, 36]). In that case, the problem posed in the truncated bounded domain is coupled with additional unknowns living on the infinite lines Γ_l, Γ_r, Γ_t and Γ_b. The main difficulty here is the representation on Γ_l, since the half space is periodic (one might use special methods dedicated to periodic media [106, 109]). Alternatively, the use of perfectly matched layers (PML) might be considered (see [30, 2, 22, 21, 151]) at the top and the bottom of the structure could also be considered (see Figure 1.15), as done in [**?**] for homogeneous open-waveguides. We emphasize that an important amount of bibliographical work is needed for that part: far from being exhaustive, rough and periodic surfaces [57, 10, 56, 262], radiation conditions for periodic structure [211, 142, 107, 160, 159], periodic waveguides [108, 239, 263], locally perturbed periodic problems [178, 261]...

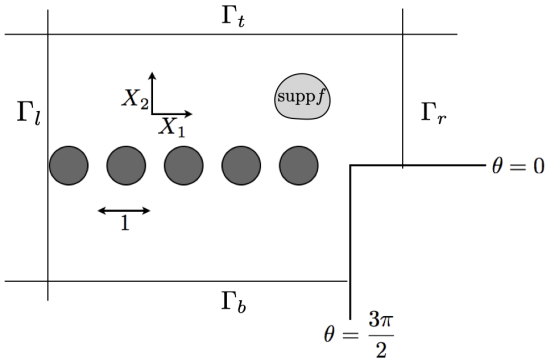

Figure 1.14: artificial cartesian truncation for the Half Space Matching Method

1.5.3 About the Faraday cage effect

The presented study could be naturally completed in the three following directions:

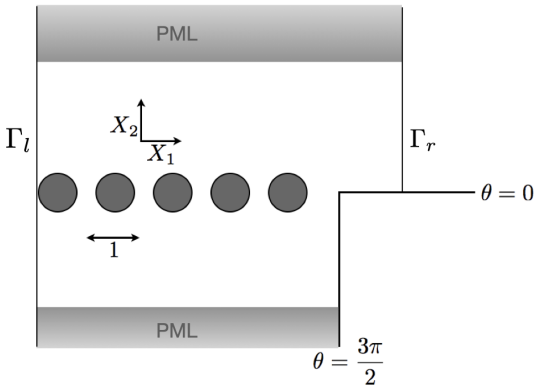

Figure 1.15: Artifical truncation with PML

1. Numerical simulations: to start with, it should be very nice to have numerical illustrations of Theorem 2. First computations has been done during the master's thesis of Doan Tran Nguyen Tung (Apr-June 2019) with the help of Marcella Bonazzoli ([248, 33]) and are reported on Fig. 1.16-1.17. An infinite grating (located at the mid-height of the structure) is illuminated under normal incidence by a plane wave (leading to a quasi-periodic problem posed in only one periodicity cell [193, 158]). The bottom of the structure is perfectly conducting. The first two components of the electric field are displayed in three configurations (corresponding to the three cases of Theorem 2). In configuration (i) (cubic obstacle), the two components of the electric field go through the grating, while in the case (iii) (cross-shape obstacle) the electric field is entirely blocked by the grating. Partial shielding is observed for configuration (ii) (square section wire), the first component being blocked by the grating while the second goes through. The simulations are done in FreeFem++ [135] together with H-curl Nedelec finite elements ([197, Chap.7]-[213]), see also [176] and the associated webpage for Freefem examples applied to Time Harmonic Maxwell's equations. Those computations turn out to be extremely costly (basically due to the three dimensional vectorial structure of Maxwell's equations). The use of parallel computation is mandatory for solving more realistic configurations (not only the grating case), including more sophisticated geometries, smaller parameter δ and higher frequencies. The use of integral equations/boundary element methods ([65, 214]) and/or domain decompositions methods for parallelization may be considered. We point out that this project necessitates an important time investment.

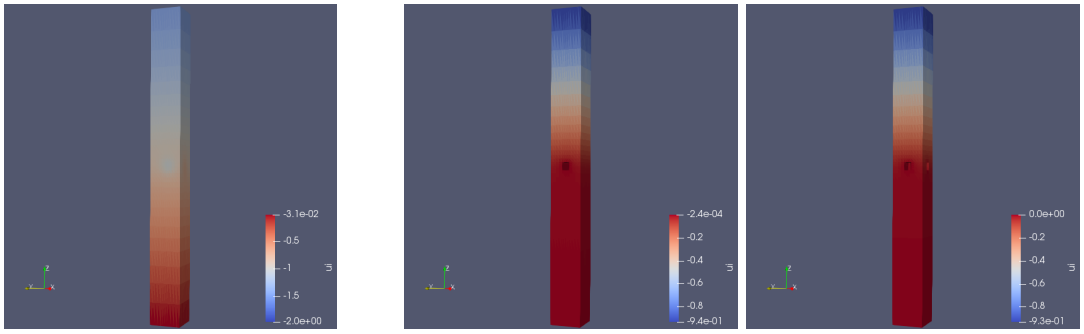

(a) Case (i) (b) Case (ii). (c) Case (iii)

Figure 1.16: First component of the electric field

2. The problem without absorption. In the investigation of Section 1.3, we made the assumption that $\mathrm{Im}[\varepsilon] > 0$. This is due to the fact that we are not able to prove the stability estimate (1.22) (uniform

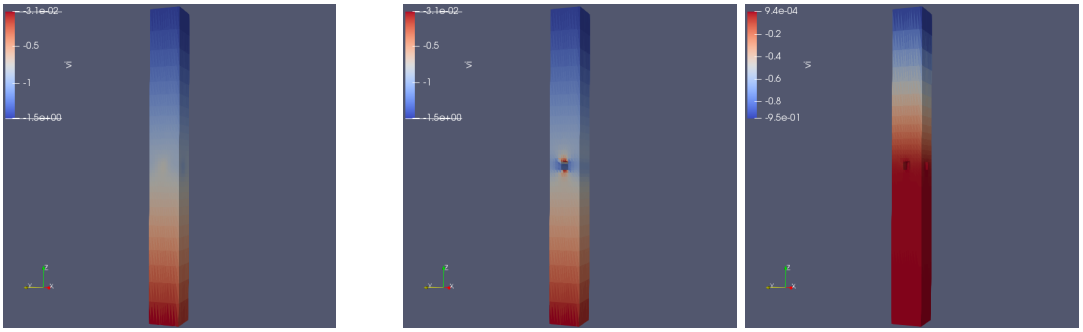

(a) Case (i) (b) Case (ii). (c) Case (iii)

Figure 1.17: Second component of the electric field

with respect to δ) in the case $Im[\varepsilon] = 0$ (we do not succeed in writing a proof by contradiction as in [70, Prop. 2.2]). As a result, we are not able to prove convergence of the asymptotic expansion without absorption, although the formal asymptotic remains exactly the same. Besides, the proofs proposed in [228] (see also [218, 217]) seem not directly extendable to Maxwell's Equations.

To tackle this problem, one possibility could be to try to prove a limiting absorption principle. Because we need uniformity with respect to δ, it seems not easy. To start with, I would rather suggest to consider the Maxwell eigenvalue problem (operator curlcurl together with free divergence condition) in a box domain (as represented in Figure 1.9) with periodic condition on the lateral boundaries and perfectly conducting boundary conditions (1.20) on the heterogeneities and on the top and bottom boundary (to avoid difficulties coming from radiation condition or absorbing condition). Because the operator is self-adjoint with compact resolvent (free divergence condition), we may use the method of quasi-modes (see the method and references described in Section 2.2) to construct and justify asymptotic expansion of its eigenvalues. It would then provide well-posedness (uniformly w.r.t δ) result for the associated Maxwell's problem without dissipation for any frequency away from those eigenvalues.

3. Finally, it would be interesting to extend the work of [139] to the 3D Maxwell's case by varying the size of the periodic obstacles (compared to the period), introducing so a new scale. It should conduct to different asymptotic regimes, yielding possibly to non trivial limit problems (with for instance Robin boundary conditions). Note that, due the introduction of the new scale, a rigorous analysis is not entirely trivial (periodicity cell problems depending of δ). The investigation of more general geometries could also reinforces the work (note that the classification of differents geometries is not totally obvious).

1.5.4 Asymptotic models for resonances

Section 1.4 could be advantageously completed by a rigorous proof of existence of resonance (which extended the result [111] to more general configuration). Unfortunately we cannot mimic directly the method of quasi-modes (presented in Section 2.2, which is appropriate to locate the spectrum self-adjoint operators) for complex resonances. As a first strategy, we could try to extend the method [111, 110] (based on an integral representation) or use general methods derived in [140]. But, we could also try to use the formal asymptotic we are able to construct to use the strategy of quasi-resonances developed in [246] (roughly speaking, quasi-resonances implies resonance). More specifically, we aim to base our work on the proofs of [17].

Chapter 2

Guided waves in periodic 'graph-like' domains

2.1 Context

Photonic crystals, also known as electromagnetic bandgap metamaterials, are 2D or 3D periodic media designed to control the light propagation. Indeed, the multiple scattering resulting from the periodicity of the material can give rise to destructive interferences at some range of frequencies. It follows that there might exist intervals of frequencies (called gaps) wherein the monochromatic waves cannot propagate. At the same time, a local perturbation of the crystal can produce defect mid-gap modes, that is to say solutions to the homogeneous time-harmonic wave equation, at a fixed frequency located inside one gap, that remains strongly localized in the vicinity of the perturbation. Those phenomena are of particular interest for a variety of promising applications in optics, for instance the design of highly efficient waveguides [149, 150] (see [129] for a concret application to the reduction of noise pollution).

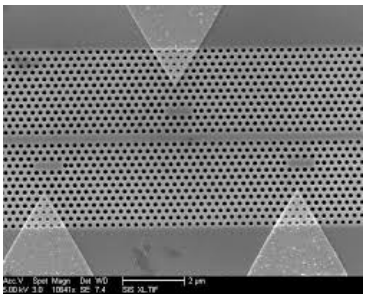

(a) Crystal perturbed on a line ([1])

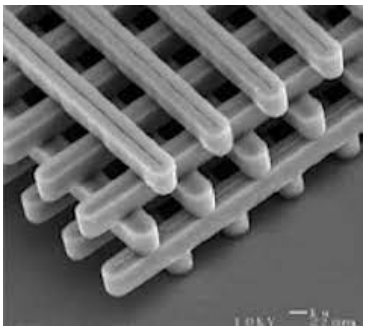

(b) 3D. crystal ([244])

Figure 2.1: Exemples de cristaux photoniques

From a mathematical point of view, the presence of gaps is theoretically explained by the band-gap structure of the spectrum of the periodic partial differential operator associated with the wave propagation in such materials (Floquet-Bloch theory, see for instance [89, 165], [230, Vol 4, Chap. XIII, Section 16] for a 1D). In turn, the localization effect is directly linked to the possible presence of discrete spectrum appearing when perturbing the perfectly periodic operator. A thorough mathematical description of photonic crystals can be found in [170]. Without being exhaustive, let us remind the reader about a few important results on the topic. In the one dimensional case, it is well-known [39] that a periodic material has infinitely many gaps unless it is constant. By contrast, in 2D and 3D, a periodic medium might or might not have gaps. Nevertheless, several configurations where at least one gap do exist can be found in [103, 104, 143, 206, 208, 16, 156, 157] and references therein. Numerical evidence can also be found

in [150, 125]. In any case, except in dimension one, the number of gaps is expected to be finite. This statement, known as the Bethe Sommerfeld conjecture is fully demonstrated in t [221, 222] for the periodic Schrödinger operator but is still partially open for Maxwell equations (see [256]). For the localization effect, several papers exhibit situations where a compact (resp. lineic) perturbation of a periodic medium give rise to localized (resp. guided) modes [101, 102, 99, 8, 168, 169, 210, 43, 44]. They all are based on some asymptotic arguments.

Among the periodic media, the ones having the honeycomb symmetry (or hexagonal symmetry) have been widely investigated those last two decades, supported by the remarquable properties of graphene (periodic medium made of an hexagonal arrangement of atoms, synthesized in 2004, cf. Figure 2.2). Mathematically, the study of the associated operator reveals the presence of Dirac points in their dispersion surfaces. There existence, first proved for discrete models (knowns as 'tight binding models', cf e.g. the seminal works [257, 53]), quantum graphs [171] and then extended to the Schrödinger and waves operators [94, 179, 51, 260], is due to the presence of three invariants:

- Rotation of angle $\pm 2\pi/3$,
- Central symmetry,
- Complex conjugation (time reversal symmetry).

Furthermore, the Dirac point might disappear when perturbing the structure by breaking one of those symmetries, leading to the creation of a spectral gap. Adding then a lineic (or localized) perturbation might create guided modes in the gap, which turn out to be very stable with respect to perturbations. This incredible stability is referred to as topological stability or *bulk edge correspondance* and may be linked to topological properties of the eigenspaces associated with dispersion relation : see (for instance) [128, 79, 258, 242] for physical oriented literature and [93, 96, 83, 85, 84, 127, 180] for the more mathematical one.

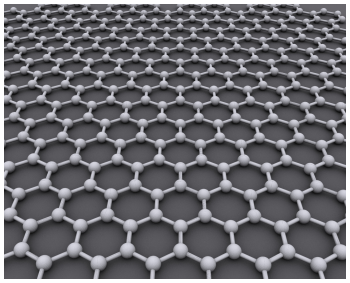

Figure 2.2: Schematic representation of [7]

In that context, our contribution to that topic relies on the investigation of particular two dimensional configurations consisting of graph-like periodic structures (see Figure 2.3 in the case of a square lattice). As the thickness of the rungs (proportional to a small parameter δ) tends to zeros, the domain shrinks to an (infinite) periodic graph. More precisely, the spectrum of the operator posed on the 2D domain tends to the spectrum of a self-adjoint operator posed on the limit graph ([232, 172, 235, 227, 220]). This limit operator consists of the second order derivative operator on each edge of the graph together with transmission conditions (called Kirchhoff conditions) at its vertices ([223, 50, 172]). As opposed to the initial operator, the spectrum of the limit operator can be explicitly determined using a finite difference scheme ([15, 91]). Computing explicitly the spectral properties of the limit operator, we are able to transfer them for δ sufficiently small to the 2D configurations.

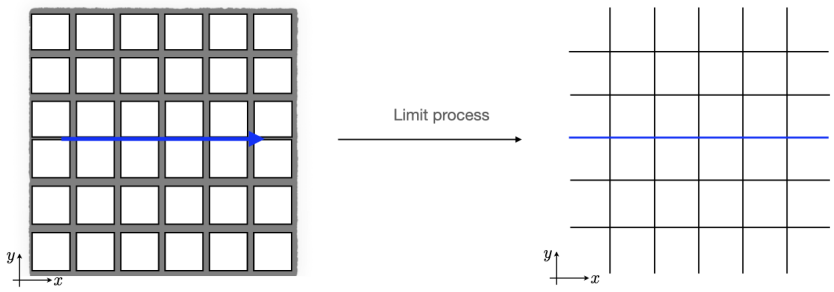

Figure 2.3: Perturbed periodic Graph Like domain

2.2 Square graph-like domains

The work described in the next section, corresponding to items [7], [8] and [11] in the list of publications, have been made during the PhD thesis of E. Vasilevskaya (LAGA, 2012-2016) under the supervision of P. Joly in strong collaboration with S. Fliss.

2.2.1 Main results

We present the methodology in a simple geometrical configuration. Let $\delta > 0$ (supposed to be small) and $\mu > 0$. We consider the comb-shape domain Ω_δ^μ presented on Figure 2.4: it consists of a periodic domain locally perturbed on one rode (the thickness of all the rods is equal to δ except for the central one whose thickness is $\mu\delta$). On that domain, we investigate the spectral properties of the self-adjoint and positive operator $A^{\delta,\mu}$:

$$A_\delta^\mu u = -\Delta u, \qquad D(A_\delta^\mu) = \left\{ u \in H^1(\Omega_\delta^\mu), \Delta u \in L^2(\Omega_\delta^\mu), \quad \partial_n u|_{\partial\Omega_\delta^\mu} = 0 \right\},$$

and we prove the following result:

Theorem 3. *For any $m_0 > 0$, there exists δ_0 such that, if $\delta < \delta_0$ the essential spectrum of A_δ^μ has at least m_0 gaps. Moreover, for $\mu < 1$, the operator $A^{\delta,\mu}$ has at least one eigenvalue in each of those gaps.*

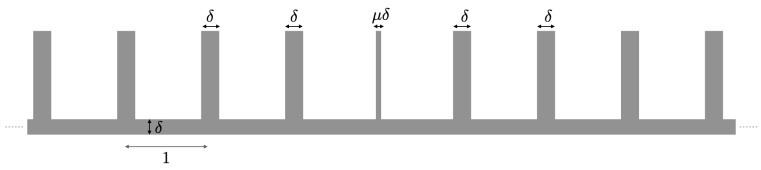

Figure 2.4: Periodic graph-like comb shape domain perturbed one vertical rod

The proof of the previous result relies on the following three steps:

1. **Formal limit:** as $\delta \to 0$, the domain Ω_δ^μ tends to the periodic graph $\mathcal{G}$ represented on Figure 2.5.

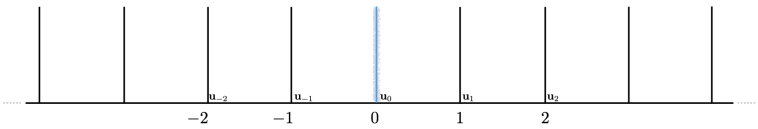

Figure 2.5: Limit comb Graph $\mathcal{G}$ ('perturbed' central edge in blue)

Let

$$L_2^\mu(\mathcal{G}) = \left\{ u \,/\, u \in L_2(e) \text{ on each edge } e \text{ of } \mathcal{G}; \quad \|u\|^2_{L_2^\mu(\mathcal{G})} = \sum_{e\in\mathcal{E}} w^\mu(e)\,\|u\|^2_{L_2(e)} < \infty \right\}, \tag{2.1}$$

the function w^μ being a weighted function that encapsulates the perturbation: it is equal to μ on the *perturbed* edge (in blue on the Figure 2.5, although note that geometrically speaking there is no 'perturbed' edge) and to one everywhere else. Then, the operator A_δ^μ tends to the operator $\mathcal{A}^\mu$ defined on the space

$$(\mathcal{A}^\mu u)_e = -u_e'', \qquad \text{on each edge } e \text{ of } \mathcal{G}, \tag{2.2}$$

$$D(\mathcal{A}^\mu) = \big\{ u \in H^2(\mathcal{G}), \sum_{e\in\mathcal{E}(M)} w^\mu(e) u_e'(M) = 0 \text{ at each vertex } M \big\}, \tag{2.3}$$

where the space $H^2(\mathcal{G})$ consists of the continuous functions on the graph that are H^2 on each edge, and such that

$$\sum_{e\in\mathcal{G}} \|u\|^2_{H^2(e)} < \infty.$$

Here, we abusively use $e \in \mathcal{G}$ to sum over all the edges of the graph. The conditions

$$\sum_{e\in\mathcal{E}(M)} w^\mu(e) u_e'(M) = 0$$

are known as Kirchhoff conditions [172, 223, 50] (note that high-order models with improved Kirchhoff conditions can be also obtained, see [152]). The operator $\mathcal{A}^\mu$ is positive self-adjoint [167]. Its spectrum can be decomposed into an essential part and a discrete one ([230, Vol. 1 Chap. VII]-[141]).

2. **Investigation of the spectrum of $\mathcal{A}^\mu$.** The essentiel spectrum of $\mathcal{A}^\mu$ coincides with the spectrum of the purely periodic operator $\mathcal{A}^1$ (Theorem 4, Chapter 9 in [32]) and can be explicitly determined using the Floquet-Bloch Theory [89, 166]. More specifically, we can prove that the essential spectrum operator $\mathcal{A}$ has infinitely many gaps whose ends tend to infinity. Denoting by $\mathbf{u}_j$ the value of a localized mode at the vertex j (see Fig. 2.5), the discrete spectrum can be computed explicitly remarking that the sequence $(\mathbf{u}_j)_{j\in\mathbb{Z}}$ satisfies a collection of finite difference equations:

$$\mathbf{u}_{j+1} + 2\,g(\omega)\,\mathbf{u}_j + \mathbf{u}_{j-1} = 0, \qquad j \in \mathbb{Z}^*, \tag{2.4}$$

$$\mathbf{u}_1 + 2\,g_\mu(\omega)\,\mathbf{u}_0 + \mathbf{u}_{-1} = 0, \tag{2.5}$$

with

$$\begin{cases} g(\omega) = -\cos\omega + \dfrac{\sin\omega}{\phi(\omega)}, \\ g^\mu(\omega) = -\cos\omega + \mu\dfrac{\sin\omega}{\phi(\omega)} \end{cases} \qquad \phi(\omega) := \frac{2}{\tan(\omega)}. \tag{2.6}$$

By a direct study of those equations, we show the following result:

- For $\mu \geq 1$,the discrete spectrum of $\mathcal{A}^\mu$ is empty.
- For $0 < \mu < 1$, the discrete spectrum of $\mathcal{A}^\mu$ contains at least one eigenvalue in each gap of its essential spectrum.

3. **Justification of the asymptotic, proof of convergence:** for $\mu < 1$, we deduce the existence of eigenvalues of A^μ_δ close to the ones of $\mathcal{A}^\mu$ as soon as δ is small enough. To do so, we could definitely (and directly) use the general results by O. Post [227][Theorem 3.4, Theorem 3.5], which extend the ones of [232, 233, 172]). Broadly speaking, it proves that the spectrum of A^μ_δ converges to the spectrum of $\mathcal{A}^\mu$. We choose a more constructive approach, based on a quasi-mode method (a kind of approximation of the eigenmodes): we construct a function $u_\delta \in H^1(\Omega^\mu_\delta)$ such that for any $v \in H^1(\Omega^\mu_\delta)$

$$\left| \int_{\Omega^\mu_\delta} (\nabla u_\delta \nabla v - \lambda u_\delta v)\, d\mathbf{x} \right| \leqslant C\sqrt{\delta}\, \|u_\delta\|_{H^1(\Omega^\mu_\delta)} \|v\|_{H^1(\Omega^\mu_\delta)}. \tag{2.7}$$

By adapting the Lemma 4 for [207] (see Appendix A in [71]) the existence of such a function provides an estimate of the distance from λ to the spectrum of A^μ_δ, namely

$$dist(\sigma(A^\mu_\delta), \lambda) \leqslant \widetilde{C}\sqrt{\delta}, \tag{2.8}$$

with some constant $\widetilde{C}$ that does not depend on δ, but depends on λ. The construction of u_δ is based on a simple extrapolation of the eigenmode u_0 defined on the graph $\mathcal{G}$ to the 'fattened' graph-like domain Ω^μ_δ: essentially u_δ is equal to u_0 on the rods of Ω^μ_δ and constant on the junctions.

Remark 6. *We point out that imposing Dirichlet conditions leads to an entirely different asymptotic analysis because the limit model is not the same: indeed, Dirichlet boundary conditions impose that the solution cannot be approximatively constant in the transverse direction of the rod. The Dirichlet 'ladder' is investigated in [209]-[210]: as in our case, changing the size of one or several rungs of the ladder can create eigenvalues inside the first gap ([210, Theorem 8.1]). We refer the reader to [130, 31] for the study of different types of boundary conditions.*

Remark 7. *In the case $\mu > 1$, we are not able to prove that the discrete spectrum of A^μ_δ is empty (although the one of $\mathcal{A}^\mu$ is). This comes from the fact that we cannot exclude the presence of eigenvalues located in a small neighborhood of the essential spectrum. We do not understand how to make the distinction between discrete and essential spectrum in that case.*

2.2.2 Extensions

- Imitating the above approach, we found a sufficient condition that ensures the existence of guided modes in a ladder-like open periodic waveguides (see Fig 2.3)([252, Chap. 4]): for δ small enough, and a perturbed periodic domain presented in Fig. 2.3 (the lineic perturbation consists of diminishing the distance between two consecutive columns of obstacles), there exists a guided mode for any wave number (quasi-moment) β.

- Together with the theoretical approach, we made numerical illustrations: to approximate the discrete spectrum, we have to solve eigenvalue problems posed on an unbounded domain. To address this difficulty, we have used the method in [106], based on the construction of Dirichlet-to-Neumann operators in periodic waveguides (Fig. 2.6-2.7) (Note that the supercell-approach [49] could also be used). E. Vasilvsekaya also made time-domain simulations, using the code and the method in [64],

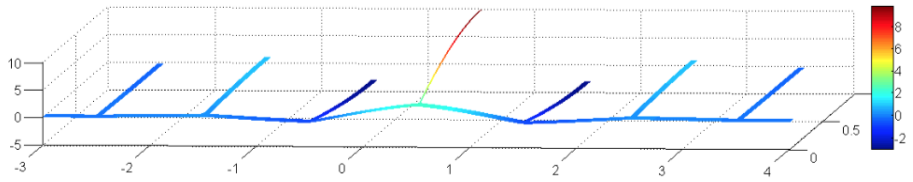

Figure 2.6: Eigenfunction corresponding to the first eigenvalue of A_δ^μ for $\delta = 0.06$ and $\mu = 0.25$.

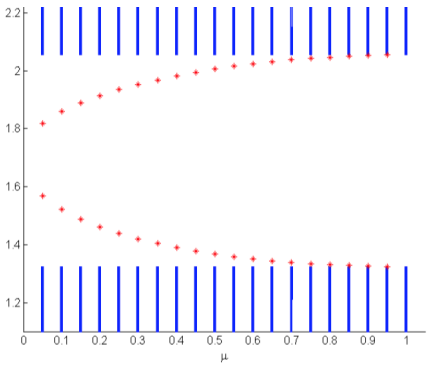

Figure 2.7: Example of eigenvalues (in the first gap) and their dependance w.r.t. μ for $\delta = 0.1$ (essential spectrum in blue and discrete one in red)

where we could visualise guided modes travelling along the defect as $\mu < 1$ (Fig. 2.8).

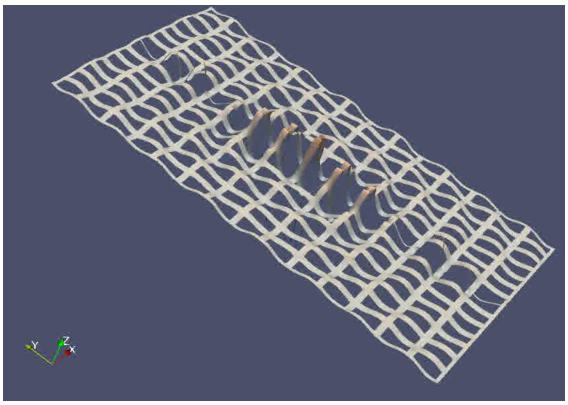

Figure 2.8: Snapshot of the time domain simulation at time $T = 0.17$, $\mu = 0.25$, $\delta = 0.2$

- In [72], we constructed high order asymptotic expansions of the eigenvalues using (again) the method of matched asymptotic expansion [251, 194, 147]. This also provides an alternative constructive method to compute the eigenvalues. On Figure 2.9, we have represented the first eigenvalue of A_δ^μ

in the case $L = 2$ and $\mu = 0.25$. In the left part, we compute the evolution of

$$\lambda^{\delta,n} = \sum_{k=0}^{n} \delta^k \lambda^{(k)} \tag{2.9}$$

with respect to δ for n varying between 1 and 5 and δ between 0.02 and 0.6.

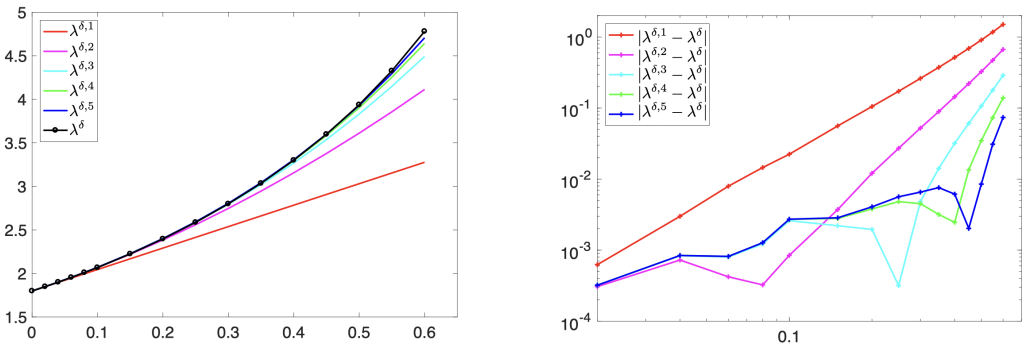

Figure 2.9: Results for the first eigenvalue of A_δ^μ, for $\mu = 0.25$: λ^δ w.r.t δ (left), Error w.r.t δ (right).

This computation requires to solve near field problems defined in some unbounded junctions. To do so, we use a first order approximation of the Dirichlet-to-Neumann operator (to bound the junction) and we use standard P_1-finite elements. Examples of such numerical solutions are printed on Figure 2.10.

We compare $\lambda^{\delta,n}$ with a reference value of λ^δ obtained by computing numerically the first eigenvalue of the full two dimensional operator A_δ^μ using the method [106] mentioned above. To verify the accuracy of our asymptotic expansion, we represent on Figure 2.9 the evolution of the errors $e_n = |\lambda^{\delta,n} - \lambda^\delta|$ with respect to δ. For the first two orders, the experimental convergence rates (2.1 for e_1 and 2.9 for e_2) coïncide with the theoretical ones. Unfortunately, this is not the case for the higher order ones. It might be due to the fact that the 'exact' solution λ^δ is computed with a limited precision of 10^{-3}. From a computational point of view, the main advantage of the asymptotic method is that it suffices to make one computation in order to obtain an approximation of λ^δ for an arbitrary value δ. Moreover, the approximation is highly-accurate when δ is small (the accuracy depending on the numerical error made in the computation of the near field terms).

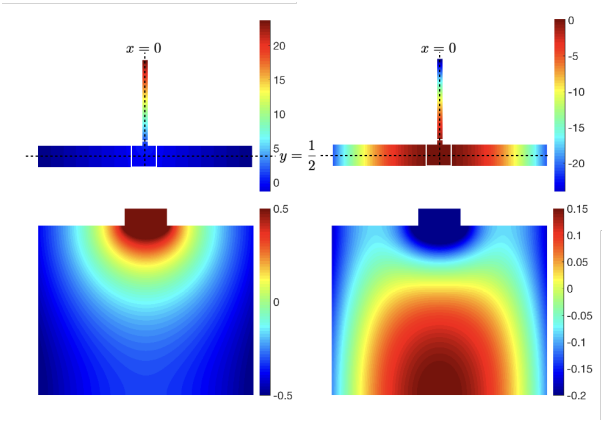

Figure 2.10: Example of near field profile functions defined in the unit junctions. (Bottom picture: zoom inside the white rectangle)

- The method has been extended in [76] to a 3D configurations presented in Figure 2.11. The main technical difference is that the 3D finite different equation (3D equivalent of (2.6)) is studied through discrete Fourier transform.

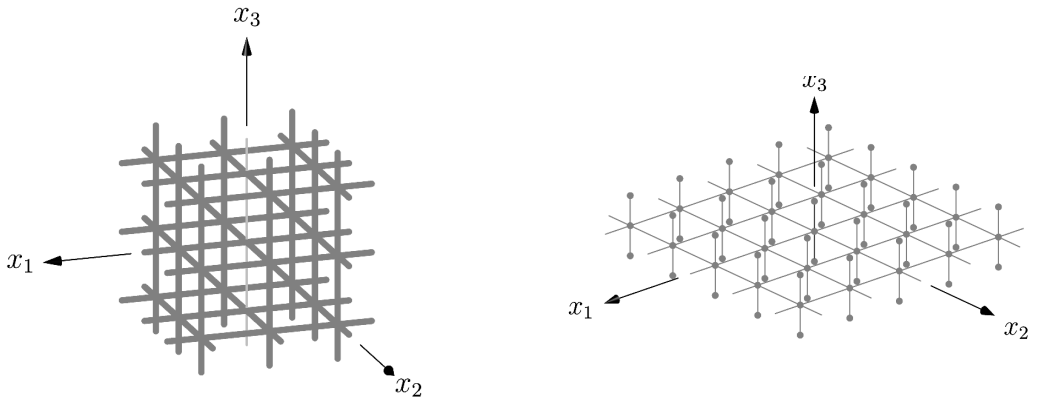

(a) The perturbed domain Ω_δ^μ (b) The associated graph $\mathcal{G}$.

Figure 2.11: Illustration of the 3D configuration.

2.3 Hexagonal graph-like domain

The following work is in collaboration with S. Fliss.

2.3.1 Fully periodic setting: existence of Dirac points

We start our investigation by studying the spectrum of the Laplace-Neumann operator A_δ (2.2.1) on the (unperturbed) periodic hexagonal graph-like domain Ω_δ presented on Figure 2.12. The domain Ω_δ (and

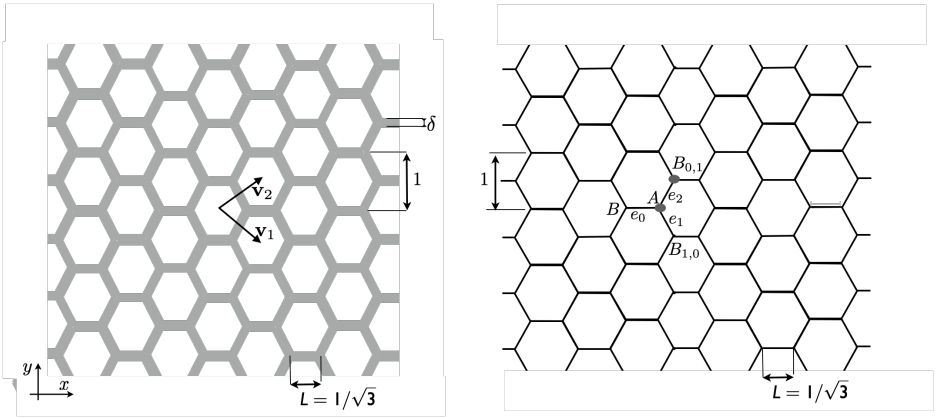

Figure 2.12: The hexagonal periodic medium Ω_δ (left figure), the associated quantum graph $\mathcal{G}$ (right figure)

the underlying operator A_δ) has the honeycomb symmetry: it is periodic with respect to translation of vector $\mathbf{v}_1$, $\mathbf{v}_2$ (triangular lattice $\Lambda = m\mathbf{v}_1 + n\mathbf{v}_2, (m,n) \in \mathbb{Z}^2$), invariant with respect to rotation R (resp. R^*) centered at the origin of angle $2\pi/3$ (resp. $-2\pi/3$), and it is symmetric with respect to the origin.

We use again the Bloch-Floquet theory [89, 166] to investigate the spectrum of A_δ. For a fixed $\mathbf{k} = (k_x, k_y) \in \mathbb{R}^2$ (named quasi-momentum), let us define the sets $L^2_{\mathbf{k}}(\Omega_\delta)$ (resp. $H^1_{\mathbf{k}}(\Omega_\delta)$) of $\mathbf{k}$ quasi-periodic locally L^2 (resp. H^1) functions:

$$L^2_{\mathbf{k}}(\Omega_\delta) = \left\{ f \in L^2_{loc}(\Omega_\delta) \text{ s.t. } f(\cdot + \mathbf{v}) = f e^{2\imath\pi \mathbf{k}\cdot\mathbf{v}} \text{ for any } \mathbf{v} \in \Lambda \right\}. \tag{2.10}$$

and

$$H^1_{\mathbf{k}}(\Omega_\delta) = \left\{ f \in L^2_{\mathbf{k}}(\Omega_\delta) \text{ s.t. } \nabla f \in L^2_{\mathbf{k}}(\Omega_\delta)^2 \right\}.$$

We then consider the collection of 'quasi-periodic' operators $A_\delta(\mathbf{k})$:

$$A_\delta(\mathbf{k}) = -\Delta, \quad D(A_\delta(\mathbf{k})) = \left\{ v \in H^1_{\mathbf{k}}(\Omega_\delta) \text{ s.t. } \Delta v \in L^2_{\mathbf{k}}(\Omega_\delta), \partial_n v = 0 \text{ on } \partial\Omega_\delta \right\}. \tag{2.11}$$

For any $\mathbf{k} \in \mathbb{R}^2$, the operator $A_\delta(\mathbf{k})$ is self-adjoint (non negative) with compact resolvent. As a result, its spectrum corresponds to a sequence of eigenvalues $\lambda_{n,\delta}(\mathbf{k})$ that goes to $+\infty$. The Floquet Theorem states that the spectrum of A_δ is the union over all $\mathbf{k} \in \mathbb{R}^2$ of the spectra of $A_\delta(\mathbf{k})$:

$$\sigma(A_\delta) = \bigcup_{\mathbf{k}\in\mathbb{R}^2} \sigma(A_\delta(\mathbf{k})) = \bigcup_{\mathbf{k}\in\mathbb{R}^2} \bigcup_{n\in\mathbb{N}} \lambda_{n,\delta}(\mathbf{k}).$$

The mappings $\mathbf{k} \mapsto \lambda_n(\mathbf{k})$ are called dispersion surfaces (Fig. 2.14). A priori, the quasi-momentum $\mathbf{k}$ has to be taken over $\mathbb{R}^2$, but examining the quasi-periodicity conditions (2.10), we see that it suffices to consider it on the so-called 'Brillouin' area. In the case of a triangular lattice, the Brillouin zone is the hexagon represented on Figure 2.13.

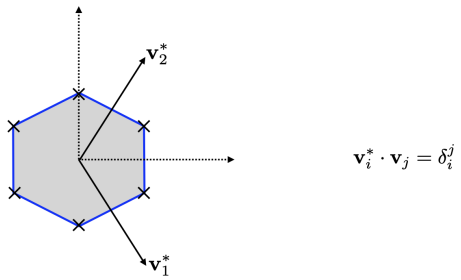

Figure 2.13: Brillouin zone (dual lattice $\Lambda = m\mathbf{v}_1^* + n\mathbf{v}_2^*, (m,n) \in \mathbb{Z}^2$, $\mathbf{v}_i^* \cdot \mathbf{v}_j = \delta_i^j$)

Let us now remind the mathematical definition of a Dirac point (see Fig. 2.14), notion that plays a central role in the study of operators with honeycomb symmetry (it is known that the presence of a Dirac point modifies the dynamic of wave packets whose frequency is localized around it, see Remark 5 in [179] and [97]).

Definition 1 (Dirac points)**.** *We say that the pair $(\mathbf{k}^*, \lambda^*) \in \mathbb{R}^2 \times \mathbb{R}^+$ is a Dirac point if the dispersion surfaces are locally conical around $(\mathbf{k}^*, \lambda^*)$: there exists $n \in \mathbb{N}$ such that $\mathbf{k} \mapsto \lambda_{n,\delta}(\mathbf{k})$ and $\mathbf{k} \mapsto \lambda_{n+1,\delta}(\mathbf{k})$ satisfies*

- *$\lambda^* = \lambda_{n,\delta}(\mathbf{k}^*) = \lambda_{n+1,\delta}(\mathbf{k}^*)$ is an eigenvalue of multiplicity 2 of $A_\delta(\mathbf{k}^*)$;*
- *there exists a constant $\alpha^* > 0$ such that*

$$\left| \begin{array}{l} \lambda_{n,\delta}(\mathbf{k}) = \lambda^* - \alpha^*|\mathbf{k} - \mathbf{k}^*| + o(\|\mathbf{k} - \mathbf{k}^*\|), \\ \lambda_{n+1,\delta}(\mathbf{k}) = \lambda^* + \alpha^*|\mathbf{k} - \mathbf{k}^*| + o(\|\mathbf{k} - \mathbf{k}^*\|). \end{array} \right. \tag{2.12}$$

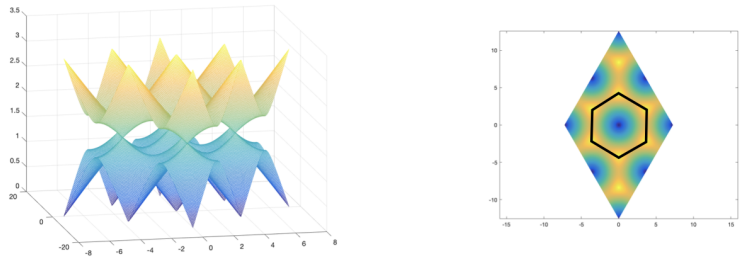

Figure 2.14: Dispersion surface for the graph model: presence of Dirac points at the vertices of the Brillouin area

The existence of Dirac point has first been demonstrated for 'tight binding models' [53], quantum-graph [171], before being to two dimensional Schrödinger and wave models [94, 179, 51] (see also [54] for a recent extension to the periodic Hartree-Fock model): the following result *completes* the results mentioned above by proving the existence of Dirac points for A_δ:

Theorem 4. *For δ small enough, the spectrum of the operator A_δ contains $N_\delta > 0$ Dirac points located at the vertices of the Brillouin area;*

Sketch of the proof. The proof exactly follows the demonstration of Theorem 2 in [179]. It is mainly based on symmetry arguments and asymptotic analysis. Let $\mathbf{K}$ be a vertex of the Brillouin area and define, $\forall s \in \{0, 1, 2\}$,

$$L^2_{\mathbf{K},s}(\Omega_\delta) := \{u \in L^2_{\mathbf{K}}(\Omega_\delta),\ u(R^*\mathbf{x}) = e^{\imath s \frac{2\pi}{3}} u(\mathbf{x})\}.$$

As a milestone of the proof, we have the following orthogonal decomposition of $L^2_{\mathbf{K}}(\Omega_\delta)$ (and the associated operators)

$$L^2_{\mathbf{K}}(\Omega_\delta) = L^2_{\mathbf{K},0}(\Omega_\delta) \oplus L^2_{\mathbf{K},1}(\Omega_\delta) \oplus L^2_{\mathbf{K},2}(\Omega_\delta), \quad A_{\delta,s}(\mathbf{K}) := A_\delta(\mathbf{K})\big|_{L^2_{\mathbf{K},s}(\Omega_\delta)}, \tag{2.13}$$

and the additional observation (strongly based on the honeycomb symmetry) that if $(u(\mathbf{x}), \lambda)$ is an eigenpair for $A_{\delta,1}(\mathbf{K})$), then $(\overline{u}(-\mathbf{x}), \lambda)$ is an eigenpair for $A_{\delta,2}(\mathbf{K})$.

Then, by the standard asymptotic analysis tools explained in Section 2.2 (based on explicite computations on the corresponding graph), it is easy to see that

(1) the operator $A_{\delta,1}(\mathbf{K})$ (and so $A_{\delta,2}(\mathbf{K})$) has a simple eigenvalue for a frequency λ_δ close to $\left(\frac{\pi}{2L} + \ell\pi\right)^2$.

(2) the number λ_δ is not an eigenvalue of $A_{\delta,0}(\mathbf{K})$.

As a result the 'full' operator $A_\delta(\mathbf{K})$ has double eigenvalues any of those frequencies. Finally, it remains to prove that they are not degenerated, namely that the number α^* in Definition 1 does not vanish. Because α^* can be expressed in term of the corresponding eigenvectors ([179, Theorem 2], this part is again demonstrated using asymptotic analysis.

□

Remark 8. *We can prove the persistence of this Dirac points when using a discretization (by finite-elements) of the operator A_δ that preserves the honeycomb symmetry.*

2.3.2 ZigZag perturbed domain

We perturbed our domain by truncated it along the so-called zig-zag direction $\mathbf{v}_z = \mathbf{v}_2 - \mathbf{v}_1$ as represented on Figure 2.15. By doing so, we break the hexagonal symmetry, the truncated domain remaining periodic with respect to $\mathbf{v}_z$ though.

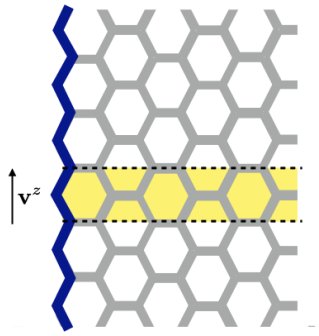

Figure 2.15: The perturbed domain Ω_δ^c. In yellow, the domain Ω_δ^0 (bounded in the $\mathbf{v}_z$ direction)

On that domain, we interrogate the presence of guided modes along the zig zag edges, that is to say the existence of a non empty discret spectrum for the operator A_δ^β (see [252, p.5]) defined for any $\beta \in [-\pi, \pi]$ by

$$A_\delta^\beta u = -\Delta u \quad D(A_\delta^\beta) = \left\{ u \in H^1_\beta(\Omega_\delta^c), \Delta u \in L^2_\beta(\Omega_\delta^c), \quad \partial_n u|_{\partial\Omega_\delta^t} = 0 \right\},$$

with

$$L^2_\beta(\Omega_\delta^c) = \{u \in L^2_{\text{loc}}(\Omega_\delta^c), u \in (L^2(\Omega_\delta^0))^2 \text{ and. } u(\mathbf{x} + \mathbf{v}_z) = e^{\imath\beta} u(\mathbf{x})\},$$

and

$$H^1_\beta(\Omega_\delta^c) = \{u \in L^2_\beta(\Omega_\delta^c), \nabla u \in L^2_\beta(\Omega_\delta^c)\}.$$

The essential spectrum of A_δ^β can be deduced form the spectrum A_δ: to be more specific,

$$\sigma_{\text{ess}}(A_\delta^\beta) = \bigcup_{k_1 \in \mathbb{R}} \sigma\left(A_\delta\left(k_1 \mathbf{v}_1^* + (k_1 + \beta)\mathbf{v}_2^*\right)\right).$$

Geometrically, it corresponds to make 'horizontal' cuts in the dispersion surfaces of A_δ^β. We consequently deduce that, for any $\beta \neq \frac{2\pi}{3}$, for δ sufficiently small there is a gap $G_\ell^{\beta,\delta}$ around the any Dirac point frequency of the limit operator $\lambda_\ell = \left(\frac{\pi}{2L} + \ell\pi\right)^2$. Then, by similar asymptotic arguments than previously, we prove that A_δ^β has eigenvalues that are almost independent of β :

Theorem 5. *For any δ sufficiently small, there exists $\varepsilon > 0$ such that, for any $\beta \in (\frac{2\pi}{3} + \varepsilon, \pi)$, the operator A_δ^β has an eigenvalues $\lambda_{\ell,\delta}(\beta)$ satisfying*

$$\lim_{\delta \to 0} \lambda_{\ell,\delta}(\beta) = \lambda_\ell.$$

The previous theorem, illustrated in Figure 2.16, says that the curve $\beta \mapsto \lambda_{\ell,\delta}(\beta)$ are almost flat. This is directly due to the well-known fact that the underlying graph model has a flat eigenvalue at any Dirac frequency for any $\beta \in (\frac{2\pi}{3}, \pi]$(see e.g. [200, 161, 98]).

Remark 9. *We remark that Theorem 5 remains true if we modify the thickness of the Zig Zag edge (in blue on Fig. 2.15) from δ to $\mu\delta$ for any positive parameter μ.*

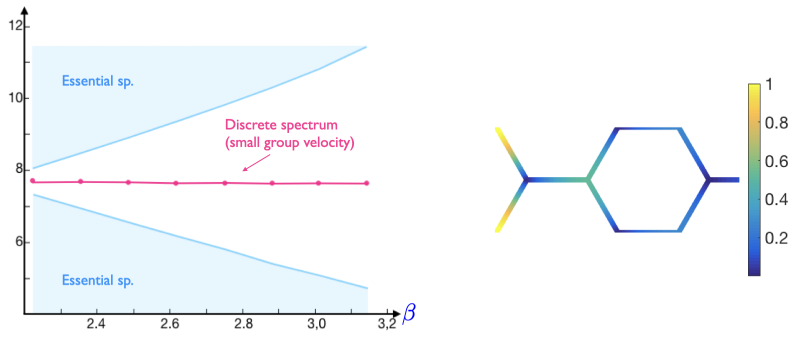

Figure 2.16: (left) Spectrum of A_δ^β w.r.t. β for $\delta = 0.05$ (in blue the essential spectrum, in pink the eigenvalue). (right) Modulus of an associated eigenmode for $\beta = \frac{5\pi}{6}$.

The previous result deserves a few comments:

1. For the graph model, the previous result is often explained by a change appearing in the Zak phase as $\beta = \frac{2\pi}{3}$ (see .e.g. the Su-Schrieffer-Heeger model [245]) : indeed, in the graph case, our operator reduces to a two by two hermitian matrix (it suffices to know the value of u at the nodes A and B of the graph to know it everywhere). More specifically, we can see that $\lambda \in \sigma_{\text{ess}}(A_\delta^\beta)$ if there exists $\theta \in (0, \pi)$ such that the matrix M_θ^β, defined by

$$M_\theta^\beta = \begin{bmatrix} 3\cos(\sqrt{\lambda}L) & a_\beta(\theta) \\ \overline{a_\beta(\theta)} & 3\cos(\sqrt{\lambda}L) \end{bmatrix} \quad \text{with } a_\beta(\theta) = 1 + e^{-i\theta} + e^{-i(\theta+\beta)},$$

is singular. The eigenvalues of M_θ^β are the solutions to the dispersion relation

$$3\cos(\sqrt{\lambda}L) = \pm|a_\beta(\theta)|,$$

and their associated eigenvector is proportional to

$$\begin{bmatrix} 1 \\ \varphi(\theta) \end{bmatrix} \text{ with } \quad \varphi^\pm(\theta) = \mp\frac{a_\beta(\theta)}{|a_\beta(\theta)|}.$$

We note that $\varphi^\pm(\theta)$ belongs to the unit circle centered at the origin. The Zak phase (also called geometrical phase) is then defined by

$$\phi_{Zak}^\pm = \frac{1}{i\pi}\int_{-\pi}^{\pi} \partial_\theta\varphi^\pm(\theta)\overline{\varphi^\pm(\theta)}d\theta.$$

In the present context, it exactly corresponds to the winding number (see [127], section 2.1) of the function $\varphi^\pm$, namely the number of loops of $\varphi^\pm$ around the origin as the quasi-momentum θ varies from $-\pi$ to π. Thus, it is an integer (and a topological number).

In addition, looking at the arguments a_β (which describes the circle of center 1 and of radius $2\cos(\beta/2)$, we can see that

$$\phi_{Zak}^\pm = \begin{cases} 1 & \text{if } 0 \le \beta < \frac{2\pi}{3}, \\ 0 & \text{if } \frac{2\pi}{3} < \beta \le \pi. \end{cases}$$

This 'brutal' change of phase (through a conical degeneracy) seems to be responsable of the appearing of the eigenvalues of Theorem 5 (see [66] and reference therein for a complete description). This is one model example of *bulk edge correspondance* and topology stability related to the SSH model (see [79]), which is however discussed in [243]. The notion of Zak phase is also extended for the one-dimensional e.d.o, see e.g [258, 180, 131]: It is proven that this number remains an integer when the periodicity cell is symmetric, but might not be integer (thus topological) in general [131].

To the author understanding it is not clear how to extend that notion to the two dimensional EDP system ([243, 83] might help to answer however). Methods to compute Zak phase (and its two dimensional version named the Berry phase) can be find in [131].

2. On the graph model, we have extended our study by varying horizontally the location where we cut our domain along the zigzag direction (see Figure 2.17). We thus introduce a new 'dislocation' parameter $t \in [0, 2L]$ to indicate the abscissa of location of the cut and obtain a corresponding operator $\mathcal{A}_t^\beta$, which is $2L$ periodic. This model corresponds to a 'graph' generalization of the study [127] made for the one dimensional schrödinger periodic operator.

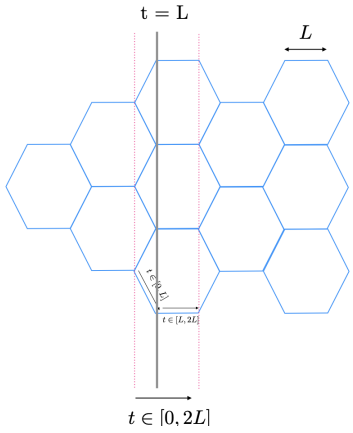

Figure 2.17: Variation of the location of the cut along the horizontal direction

For any frequency λ in the gap G_ℓ^β, we denote by $N_\ell(\lambda)$ the number of points $t \in [0, 2L]$ such that λ belongs to $\sigma_d(\mathcal{A}_t^\beta)$. Our result is the following:

Proposition 3. *For any $\beta \in [0, \frac{2\pi}{3}[\cup]\frac{2\pi}{3}, \pi[$, for any $\lambda \in G_\ell^\beta$, $N_\ell(\lambda)$ is constant equal to $2\ell+1$: there exist exactly $2\ell+1$ values $t_{\ell,q} \in (0, 2L)$ such that $\lambda \in \sigma_d(\mathcal{A}_t^\beta)$. Moreover, the curves $\omega \mapsto t_{\ell,q}(\omega)$ are strictly increasing.*

The previous proposition is illustrated by the Figures 2.18 ($\beta \in [0, \frac{2\pi}{3}[$) and 2.19 ($\beta \in]\frac{2\pi}{3}, \pi[$). The blue crosses represents the eigenvalues inside the gaps G_ℓ^β: we see the existence of $2\ell + 1$ spectral flows through the gap G_ℓ^β. The blue points materialize values of $t_{\ell,q}$ that are independent of β, leading to flat eigenvalues when β is varying. For instance, in the case $\ell = 0$, this invariant corresponds to $t = L$ (bearded configuration) for $\beta \in [0, \frac{2\pi}{3}[$ and to $t = 0$ for $\beta \in]\frac{2\pi}{3}, \pi[$ (classical zig-zag configuration). We demonstrate that there are exactly $2\ell+1$ invariants in the gap G_ℓ^β. Those invariants are not present for tight binding models (that have only one gap).

However, by contrast to [127], we cannot not make any link with topological properties since our model lacks of continuity at $t = 0$ and $t = L$ (Kirchhoff conditions of the graph model).

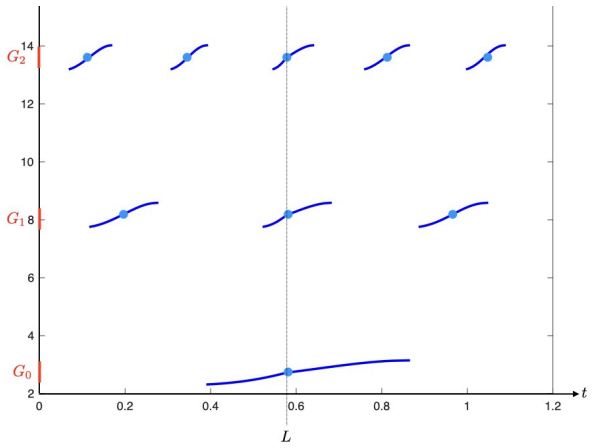

Figure 2.18: Representation of the function $t \mapsto \omega(t) = \sqrt{\lambda(t)}$ in G_0, G_1 and G_2 for $\beta = \frac{\pi}{3}$. The blue points stand for eigenvalues independent of β

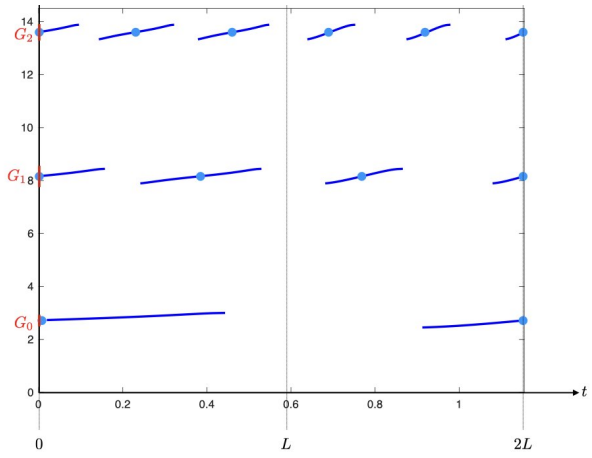

Figure 2.19: Representation of the function $t \mapsto \omega(t) = \sqrt{\lambda(t)}$ in G_0, G_1 and G_2 for $\beta = \frac{5\pi}{6}$. The blue points stand for eigenvalues independent of β

2.4 Future work

We conclude this part be a few directions that might be interesting to explore:

1. A first natural extension of our work consists in investigating the existence of guide modes for different cut direction (well-known direction are 'zigzag' and 'armchair', which exhibit very different behavior). The question is answered in [95] for tight binding models, we aim to extend it to graph-models. At first step, the rational directions are easier to investigate since the medium remains periodic in one direction. Naturally, non rational directions are much difficult to handle (the definition of guided mode is even not clear).

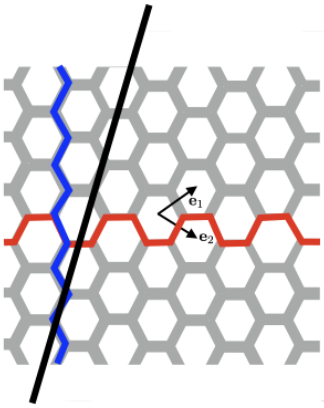

Figure 2.20: Several cut directions (in blue, the 'zigzag' direction, in red the 'armchair' one)

2. As a more prospective possibility, we aim to find configuration that breaks the Dirac point (this is starting point for constructing topologically protected states [179]), open ing up a gap for the complete operator. This is traditionally done by breaking some symmetries: for instance, in the discrete model of Haldane [133] (that enriches the SSH one), the time reversal symmetry is broken by adding a second neighbor magnetic coupling while in [179, 83] a magnetic potential is added. Can we find two dimensional configurations (based on graph like geometry) whose limit model has a gap? We might for instance try to find a two dimensional model that collapses to the Haldane model as the thickness of the structure goes to 0. Note that we already saw that adding naively a magnetic potential in our operator does not help since it just make a translation in the dispersion curve at the limit. One possibility would be to consider high order asymptotic models (with enriched Kirchhoff conditions, see [152, 72]): for instance, the 'brick wall' tight binding model is equivalent to the graphene honeycomb model, but what about its thickened version (Figure 2.21). Since the honeycomb symmetry is not satisfied anymore, does it break the Dirac point? Studying the higher order asymptotic as in [72] could answer this question. We finally mention that numerical simulations can also help us to find suitable models and are therefore needed to make progress in this project. Last, once those models will be defined, studying the existence of guided modes and their stability is of course a wide subject to consider.

3. As a last technical question (disconnected from the honeycomb symmetry problematic though), we would like to raise is the pertinence of the graph and fattened graph like models for waves. More specifically, does those models can be obtained using composite high-contrast material (see for instance [100, 105, 138])? To avoid first the difficulty due to the presence of the junction, we could start by studying first a thin linear a 'tube'.

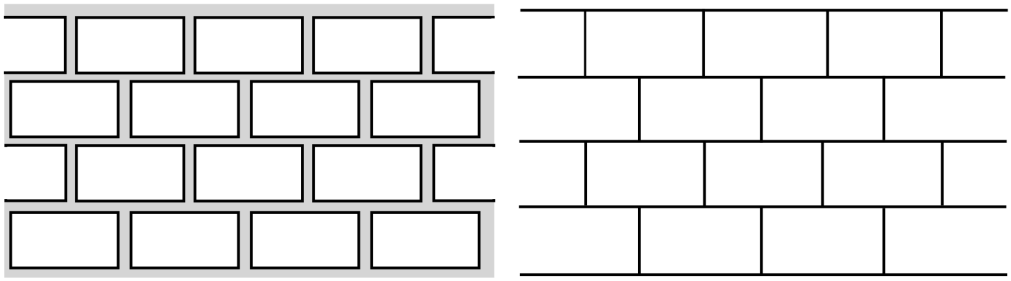

Figure 2.21: Brick wall graph like domain (left) and brick wall graph (right)

Chapter 3

Optimized Schwarz method for control problems

This chapter, less long as the two first ones, presents some pieces of work made in the context of the ANR project named ALLOWAP (ALgorithms for Large-scale optimisation of WAve Propagation) dedicated to the design, mathematical and numerical study of space-time parallel algorithms for optimisation problems that arise when modeling wave phenomena.

Such problems occur in geophysical applications such as seismic inversion, data assimilation, medical applications. To make the optimisation tractable, parallel computers must be used to cope with the large amounts of data and intensive computation inherent to these problems. In the last decade, parallel-in-time methods have made a lot of progress: for parabolic problems, a near-optimal scaling with respect to the number of processors has been achieved (scalability). For wave propagation, there has been no such success. The objective of this project is to try to make improvement in that direction following three mains axis: (1) Space-time parallelism for wave propagation problems, (2) Space-time parallelism for optimal control problems, (3) Time parallelization of assimilation and identification procedures. My contribution in this project focus on to the second point, and more specifically on optimized Schwarz methods for control problems.

Since I have been investigating the topics of optimisation, control and domain decomposition more recently, the results presented below are less documented than those in the previous two chapters.

3.1 An optimized Schwarz method of an elliptic optimal control problems

The next results are a joint work with L. Halpern (number [9] and [15] in the list of publications).

Description of the algorithm and theoretical results

optimized Schwarz algorithms are powerful tools for domain decomposition methods in view of parallelization. They have been introduced by P.L. Lions [52]. B. Després in his thesis used radiation transmission conditions [20] on the interface for Helmholtz equation [80]. T. Hagström and collaborators presented in [132] the first numerical experiments with "optimal" transmission conditions. The principle at the root of optimized Robin-Schwarz methods is to find the coefficients in the Robin transmission conditions which optimise the convergence factor of the algorithm. This is achieved in the most simple case of two half-spaces or rectangular subdomains by using a Fourier transform or Fourier series in the direction of the interface. F. Nataf and co-authors gave an extended analysis of the optimal transmission conditions, see [201]. Since then, optimized transmission conditions have been designed, starting in C. Japhet's thesis, see e.g. [148, 116], see [112] for the elliptic case, [123] for the Helmholtz equation in [134] for the

Schrödinger equation.

In that context, our aim is to analyse such a method for a complex coercive equation in view of its application to elliptic control problem. Consider the 1D dissipative (coercive) Helmholtz equation with a complex coefficient $\eta \in \mathbb{C} \setminus \mathbb{R}_-$ on the domain $\mathbb{R}^2$:

$$-\Delta w + \eta w = g \text{ in } \Omega, \qquad \eta = \alpha + 2i\mu,\ \alpha \in \mathbb{R} \text{ and } \mu > 0. \tag{3.1}$$

We split the domain Ω into two subdomains $\Omega_1 = (-\infty, L) \times \mathbb{R}$ and $\Omega_2 = (L, +\infty) \times \mathbb{R}$, where the so called overlapping L parameter is non negative: the alternate Robin-Schwarz algorithm introduced by P.L. Lions in [52] works as follows. An initial guess w_2^0 is given in Ω_2. The algorithm computes alternatively in the subdomains Ω_j: for $j \in \{1, 2\}$, for $n \geq 1$,

$$\begin{cases} -\Delta w_1^n + \eta w_1^n = g \text{ in } \Omega_1, \\ (w_1^n)'(L) + \ell w_1^n(L) = (w_2^{n-1})'(L) + \ell w_2^{n-1}(L), \end{cases}$$
$$\begin{cases} -\Delta w_2^n + \eta w_2^n = g \text{ in } \Omega_2, \\ -(w_2^n)'(0) + \ell w_2^n(0) = -(w_1^n)'(0) + \ell w_1^n(0). \end{cases} \tag{3.2}$$

The parameter ℓ is a complex number that will be searched so as to optimise the convergence factor of the algorithm. If ℓ belongs to the quarter of plane $\mathcal{Q} = \{z \in \mathbb{C}, \arg z \in]0, \frac{\pi}{2}[\}$, then for $j = 1, 2$ the problem defining w_j^n is well-posed in $H^1(\Omega_j)$ and the Robin-Schwarz algorithm is convergent.

The errors after n iterations $e_j^n = w_j^n - w$, follow the same algorithm with vanishing righthand side. By doing a Fourier transform in the second variable, we see that

$$-(\hat{e}_j^n)_{xx} + (k^2 + \eta)\hat{e}_j^n = 0.$$

where k is the 'frequency' variable in the Fourier space.Since the errors are in $H^1(\Omega_j)$, their Fourier coefficients cannot be exponentially increasing in x, therefore

$$\hat{e}_1^n(x, k) = a_1^n(k)\, e^{\omega(k)\, x},\ \hat{e}_2^n(x, k) = a_2^n(k)\, e^{-\omega(k)\, x}, \quad \omega(k) = \sqrt{k^2 + \eta}. \tag{3.3}$$

For $\mathrm{Im} z > 0$, $\sqrt{z}$ is the usual principal branch of the square root of z, and since $\mathrm{Im}\eta \neq 0$, the complex square root ω is perfectly defined in $\mathcal{Q}$. Then the interface conditions leads to the following recursion relation

$$a_j^{n+1}(k) = \left(\frac{\omega(k) - \ell}{\omega(k) + \ell}(k) e^{-\omega(k)\, L}\right)^2 a_j^n = \left(\frac{\omega(k) - \ell}{\omega(k) + \ell} e^{-\omega(k)\, L}\right)^{2n} a_j^1(k).$$

The convergence factor is then naturally defined by

$$\delta_L(\ell, k) = \left|\frac{\omega(k) - \ell}{\omega(k) + \ell}\, e^{-L\omega(k)}\right|, \tag{3.4}$$

To accelerate the convergence of the DD algorithm, we want to optimise the convergence factor (3.4) over an interval $K = [k_{\min}, k_{\max}]$. It leads to consider (and solve) the 'min-max' non linear problem:

$$\min_{\ell \in \mathcal{Q}} \max_{k \in K} \delta_L(\ell, k) \tag{3.5}$$

Remark 10. *Problem* (3.5) *is a best approximation problem by a polynomial of degree* 0 *(see e.g. [195]). Historically, those have been investigated for the problem*

$$\inf_{P \in \mathbb{P}_n(\mathbb{C})} \sup_{z \in K} \zeta(P, z), \qquad \zeta(P, z) = |f(z) - P(z)|.$$

It has then been extended in [28, 27] (with applications in optimized Schwarz methods) for the following weighted homographic approximation best problem

$$\inf_{P\in\mathbb{P}_n(\mathbb{C})}\sup_{z\in K}\zeta(P,z),\qquad \zeta(P,z)=\left|\frac{f(z)-P(z)}{f(z)+P(z)}e^{-Lf(z)}\right|. \tag{3.6}$$

In computations, the frequency interval K in (3.5) depends on the geometry of the domain and the size of the discretization h: typically, for a Dirichlet problem on a segment $[0,1]$ (in the second variable) we take $k_{\min}=\pi$ and $k_{\max}=\frac{\pi}{h}$ (For a Neumann one, we would take $k_{\min}=0$). In the analysis we sometimes consider also the case $k_{\max}=+\infty$, which is only relevant in the overlapping case $L>0$. Indeed, $\lim_{k\to+\infty}\delta_0(\ell,k)=1$. We prove the following results:

Theorem 6. *Problem* (3.5) *has a unique solution* (ℓ_L^*,δ_L^*)*:*

1. *In the non overlapping case,* ρ_L^* *admits the following asymptotic:*

$$\delta_0^*\sim 1-c_\rho k_{\max}^{-1/2}\qquad \ell_0^*\sim c_\ell k_{\max}^{1/2}.$$

2. *In the overlapping case, for* $k_{\max}$ *large enough*

$$\delta_L^*\sim 1-C\sqrt{L\ell_L^*},\qquad \ell_L^*\sim\begin{cases} c_\ell & arg(\omega_{\min})\le\frac{\pi}{3}\\ c_\ell L^{-1/3} & otherwise.\end{cases}$$

where, if $\theta_{\min}=arg(\omega_{\min})\le\frac{\pi}{3}$ $\ell_L^*\sim$ *is of order 1 while for* $\theta_{\min}>\frac{\pi}{3}$, $\ell_L^*\sim c_\ell L^{-1/3}$.

Main lines of the proof.

1. Well-posedness and equi-oscillation properties: following the methodology of [28] we prove that for any $L>0$ and $k_{\max}\in\overline{\mathbb{R}}$, Problem (3.5) has a unique solution (δ_L^*,ℓ_L^*). Furthermore there are at least two equi-oscillation points for ℓ_L^*: there are k_1 and k_2 distinct in K such that

$$\delta_L^*=\delta_L(\ell_L^*,k_1)=\delta_L(\ell_L^*,k_2). \tag{3.7}$$

   Note that the previous equi-oscillation property is rather standard for best approximation problems.

2. Alternation property: since ℓ is allowed to be complex (and in opposition to the real case), the equi-oscillation property (3.7) does not uniquely define ℓ_L^*: there is a complex curve of equi-oscillation points ℓ and we have to find the 'best' one among them. This is characterized by the following 'alternation' property: Let $\hat\ell\in\mathbb{C}$ such that there are two **alternating** points k_j in K, that is

$$\delta_L(\hat\ell,k_1)=\delta_L(\hat\ell,k_2)=\sup_{k\in K}\delta_L(\hat\ell,k),$$
$$\exists p\in\mathbb{R}_+^*,\ \nabla_\ell\delta_L(\hat\ell,k_2)+p\nabla_\ell\delta_L(\hat\ell,k_1)=0.$$

   Then $\hat\ell=\ell_L^*$.

3. We prove the asymptotic formula for ρ_L^* and ℓ_L^*.

We point out that the steps two and three are interlocked, since we need asymptotic analysis to find (and prove the existence) of an alternation point. □

Remark 11. *In the non overlapping case and for* $arg(\omega_{\min})\le\frac{\pi}{3}$*, we recover the well-known closed form obtained in [112] (for equation* (3.1) *with real positive parameter* $\eta>0$*):*

$$\ell_0^*=\sqrt{\omega_{\min}\omega_{\max}},\quad \delta_0^*=\left|\frac{\sqrt{\omega_{\max}}-\sqrt{\omega_{\min}}}{\sqrt{\omega_{\max}}+\sqrt{\omega_{\min}}}\right|. \tag{3.8}$$

Application to an optimal control problem

We illustrate our result by considering an elliptic optimal control problem described: consider a conductive body occupying a domain $\Omega \subset \mathbb{R}^d$. The temperature is fixed on the boundary, heat sources are represented by a function $f \in L^2(\Omega)$, and a control may be provided in a part $\underline{\Omega}$ of Ω , defined by $v \in L^2(\underline{\Omega})$. The state of the system is the temperature field y, defined by the Poisson equation

$$\begin{cases} -\Delta y = f + v & \text{in } \Omega, \\ y = 0 & \text{on } \partial\Omega. \end{cases} \tag{3.9}$$

For a given v, the equation above has a unique solution in $H_0^1(\Omega)$, that will be called $y(v)$ to stress the dependency in v. Let y_d be a given temperature profile target, the optimal control problem is defined as the minimization of the cost function

$$J(v) = \frac{1}{2}\int_\Omega (y(v) - y_d)^2 dx + \frac{\nu}{2}\int_{\underline{\Omega}} v^2 dx. \tag{3.10}$$

The first term measures the distance to the desired profile y_d, and the second term the energy consumption. The weight parameter ν is defined by the user, corresponding to what effect is to be privileged: a small coefficient ν means that the user wants to approach the desired state without caring about the cost in energy, while large ν means to reduce the cost in energy. The functional J is strictly convex and classical optimisation results show that for any $\nu > 0$, there is a unique control u. The optimal control u and the optimal state y can be computed by introducing the dual state $p \in H_0^1(\Omega)$, see [181]. In the simplest case of distributed control, that is $\underline{\Omega} = \Omega$, with controls in $H_0^1(\Omega)$, the optimal control u, the optimal state y and the adjoint state p are related by

$$\begin{cases} -\Delta y = f + u, \ y|_{\partial\Omega} = 0, \\ -\Delta p = y - y_d, \ p|_{\partial\Omega} = 0, \quad p = -\nu u. \end{cases} \tag{3.11}$$

Domain decomposition algorithms for this problem have received much attention, see [29, 137, 19, 182, 175, 119, 238]. More particularly Benamou in [23] used the newly established non-overlapping domain decomposition algorithm written by Després in [24] for the Helmholtz equation to design a new algorithm for (3.11).

The particular case of distributed control allows for a clever trick, see [23]. Introducing the new unknown $w = y - \frac{i}{\sqrt{\nu}}p$, Problem (3.11) is equivalent to the complex problem: find $w \in H_0^1(\Omega)$ such that

$$-\Delta w + \frac{i}{\sqrt{\nu}} w = g \text{ in } \Omega \qquad \text{with } \ g = f + \frac{i}{\sqrt{\nu}} y_d. \tag{3.12}$$

This is a Helmholtz equation with a complex coefficient $\eta = \frac{i}{\sqrt{\nu}} \in i\mathbb{R}$, to which the analysis above applies. In [23], the author proves convergence of the non-overlapping algorithm, and shows that each iterate corresponds to optimal control problems in the subdomains.

Remark 12. *We point out that general class of optimized Schwarz methods has been investigated in [259] (with formal justifications for the optimal parameters).*

Numerical results We consider here the Helmholtz equation (3.12) in $\Omega = (0, 2) \times (0, 1)$, discretized with the usual centered second order finite difference scheme. The domain decomposition scripts are adapted from those described in [115].

In a first stage, we analyze the performance of the operational parameter for two subdomains. To do so we solve the homogeneous equation, that is no internal source g nor boundary source, thus computing the

error. The mesh size is the same in the x and y direction, equal to $h = 0.01$. Two subdomains of equal size are considered without overlap, or with an overlap of one grid point, that is $L = h$. A numerically best parameter ℓ_L^{num} is computed by a Nelder-Mead Simplex Method (`Matlab fminsearch`) minimizing the solution after 20 iterations, with a uniformly random initial guess. Then the domain decomposition algorithm is run with a uniformly random initial guess. Figure 3.1 displays in the semi-log scale the L^∞ error on the interface of the first subdomain, as a function of the iteration number n, comparing the convergence behavior over 20 iterations for the classical algorithm and the Robin algorithm, with and without overlap, together with the theoretically expected behavior in dash. As it is well-known in the domain decomposition community, the overlapping Robin-Schwarz outperforms the non-overlapping Robin-Schwarz which outperforms the classical Schwarz. In addition, these plots show that the asymptotic regime for the computation of the coefficients is attained quite rapidly. In the overlapping case for instance, with $L = 0.01$, the first term in the asymptotic in $L^{\frac{1}{3}}$ is sufficient to fit the theoretical convergence behavior. Furthermore we see that the convergence properties do not deteriorate when the coefficient ν decreases.

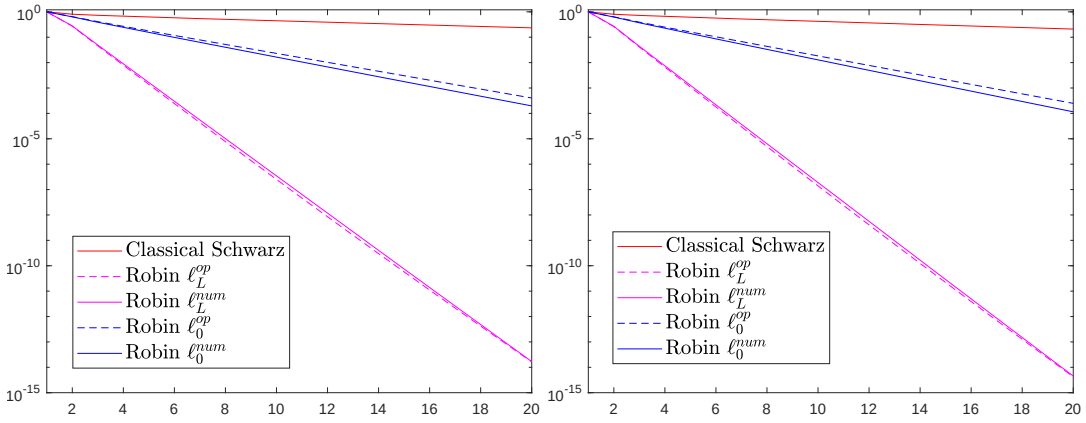

(a) $\nu = 1$ (b) $\nu = 0.01$

Figure 3.1: Convergence history for Classical Schwarz and optimized Robin algorithms

In a second stage, we compute the control of the heat in a room with various physical boundary conditions, using the parallel algorithm, with three subdomains.The room has a fixed temperature on three walls, the western wall communicates with another heated room through a door, and the eastern wall is insulated. This example of room has been presented before, for instance in [115]. The radiant floor heating is represented by a distributed control u and $f = 0$. The temperature profile target is constant equal to $y_d = 1$. The discretization of the solution y and the control u are represented on Figure 3.2 for values of ν in the range (1, 0.01, 0.001, 0.0001). As expected, when ν decreases, the control u becomes more expansive, but the approximation of the desired solution is better. Furthermore, the control becomes more concentrated along the Dirichlet walls. We display in Figure 3.3 the iterates 1, 2, 5 and 10 of y for the overlapping and non-overlapping Robin-Schwarz with the operational parameters described in the analysis. The overlap is kept constant equal to 1 grid points and there are three subdomains of equal size. As expected, the order of performances described before is respected, the best performance is reached by overlapping optimized Robin.

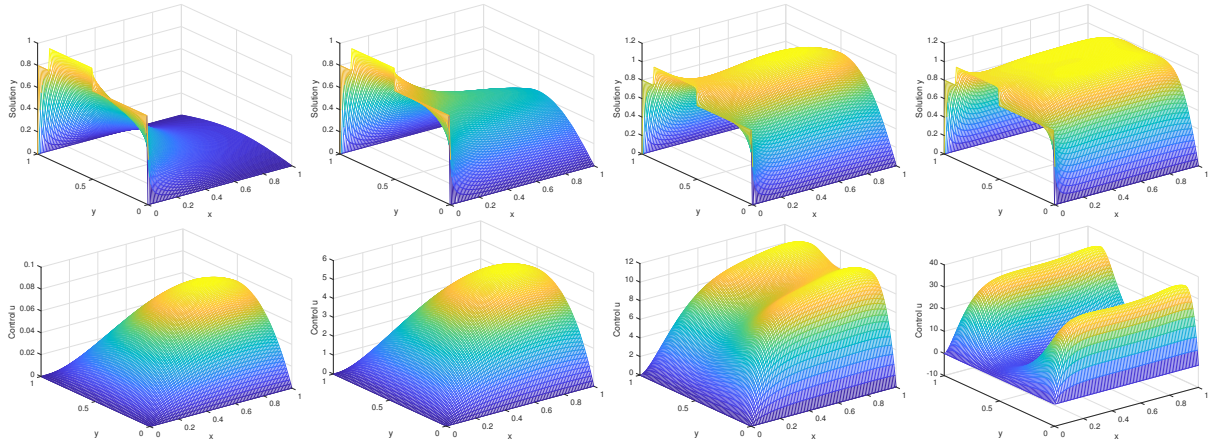

Figure 3.2: Solution (top) and control (bottom) for four values of the parameter $\nu \in \{1, 0.01, 0.001, 0.0001\}$ starting from $\nu = 1$ on the left

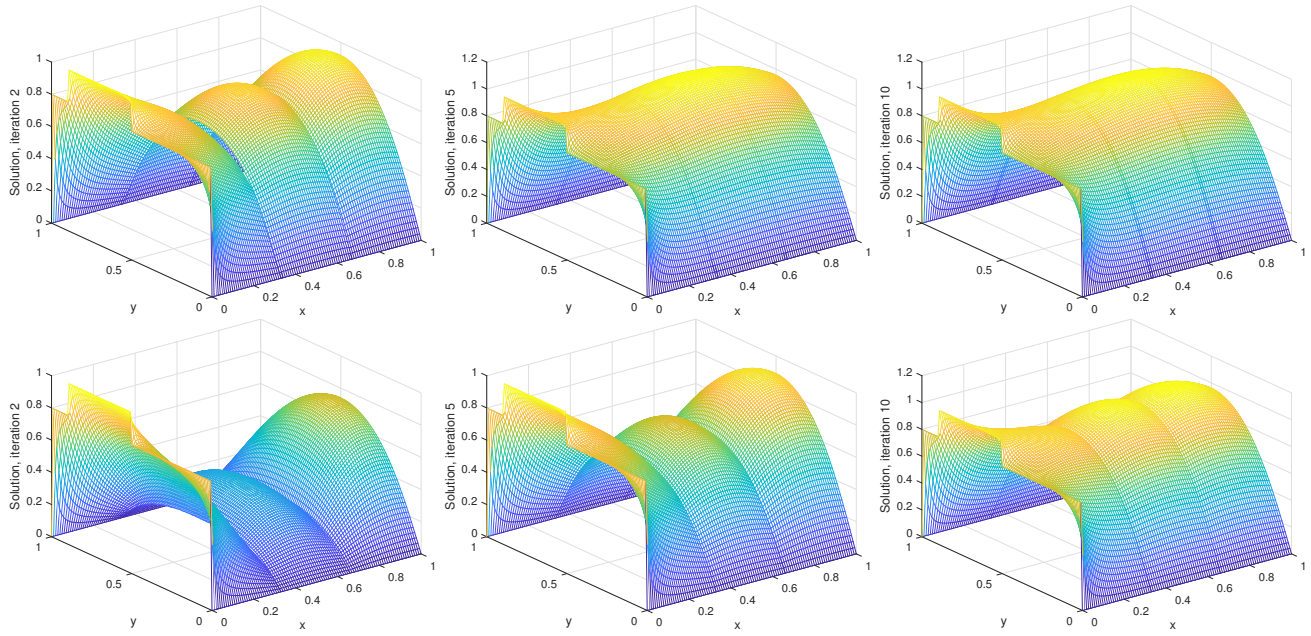

(a) Solution Iteration 2 (b) Solution Iteration 5 (c) Solution Iteration 10

Figure 3.3: Iterates of the solution y for Overlapping Robin Schwarz (first row), Non-overlapping Robin Schwarz (third row). $\nu = 0.001$.

3.2 On going work: time domain decomposition for wave and transport control problems

This work are a joint work with Laurence Halpern, Felix Kwok, Bui Duc Quang and Dang Thanh Vuong.

In this section, we aspire to design *time domain* decomposition methods for optimal control wave problems. To be more specific, our aim is to build D.D. algorithms for the following (well-posed) model problem: let Ω be a bounded domain in $\mathbb{R}^2$, $T > 0$, $\hat{y} \in L^2(\Omega\times]0,T[)$, $\hat{z} \in L^2(\Omega\times]0,T[)$. We consider the minimization problem

$$\min_{v\in L^2(\Omega)} J(v), \quad J(v) = \frac{\gamma}{2}\|y(\cdot,T) - \hat{y}\|^2_{L^2(\Omega)} + \frac{1}{2}\|v\|^2_{L^2(\Omega\times]0,T[)}, \tag{3.13}$$

with $\gamma > 0$ and y the solution to

$$\begin{cases} \partial_{tt} y - \Delta y = v & \text{in } \Omega\times]0,T[, \\ y(\cdot,t) = 0 & \text{on } \partial\Omega\times]0,T[, \\ y(\cdot,0) = y^0 & \text{at } t = 0, \\ \partial_t y(\cdot,0) = y^1 & \text{at } t = 0. \end{cases} \tag{3.14}$$

The initial datas (y^0, y^1) are supposed to be regular (for instance in $H^1_0(\Omega)^2$).

Remark 13. *Problem* (3.13) *is an 'approximate control problem', where the parameter γ in J makes a balance between the cost of the control and the difference between $y(\cdot,T)$ and the target $\hat{y}$ (measured in $L^2(\Omega)$-norm). In fact, we are also interesting in computing an exact control, where we impose*

$$y(\cdot,T) = \hat{y}.$$

However, it is a well-known fact that this problem is difficult to solve numerically. Indeed, the discretization produces high frequencies that are almost impossible to control (see [265]). Several cures have been proposed: non exhaustively, Fourier Filtering, Tickhonov regularization, Big-grid methdods (see non e.g. [215, 90, 199, 47])...

The optimal control u (solution to (3.13)) can be computed by solving the associated problem that couples the state y and its adjoint λ (associated Euler equations, see e.g. [126, 250, 120]).

$$\begin{cases} \partial_{tt} y - \Delta y = \lambda & \text{in } \Omega\times]0,T[, \\ y(\cdot,t) = 0 & \text{on } \partial\Omega\times]0,T[, \\ y(\cdot,0) = y^0 & \text{at } t = 0, \\ \partial_t y(\cdot,0) = y^1 & \text{at } t = 0, \end{cases} \qquad \begin{cases} \partial_{tt} \lambda - \Delta \lambda = 0 & \text{in } \Omega\times]0,T[, \\ \lambda(\cdot,t) = 0 & \text{on } \partial\Omega\times]0,T[, \\ \gamma(y(\cdot,T) - \hat{z}) - \partial_t \lambda(\cdot,T) = 0 & \text{at } t = T. \end{cases} \tag{3.15}$$

Once (3.15) is solved, the optimal control u is equal to λ. Note that problem (3.15) is very costly to solve numerically since it requires to solve a non triangular linear system (sparse though) of the size $2 \times N \times M$ (with M and N the number of grid points in time and space). Alternatively, a gradient type method can be directly apply to the minimization problem, but the computation of the gradient requires to solve one forward and one backward equation at each iteration. That explains why efficient parallelization methods are required to be able to tackle real applicative problems. We shall focus on the parallelization in time (although parallelization in space is also essential, see e.g [117, 249, 60]); Following the seminal approach in [174] and (see also [136, 118, 18] for different strategies), our aim is to developed *optimized* Schwarz in time methods for solving this problem.

Optimized Schwarz time domain decomposition for transport problems

To start with a very simple ('toy') hyperbolic problem, we consider the following 1 dimensional exact control of transport equation:

$$\min_{v\in L^2(\Omega)} J(v), \quad J(v) = \frac{1}{2}\|v\|^2_{L^2(\mathbb{R}\times]0,T[)}, \tag{3.16}$$

and y the solution to

$$\begin{cases} \partial_t y - \partial_x y = v & \text{in } \mathbb{R}\times]0,T[, \\ y(\cdot,0) = y_{\text{ini}} & \text{at } t=0, \end{cases} \tag{3.17}$$

and subject to the constraint

$$y(\cdot,T) = y_{\text{tar}}. \tag{3.18}$$

For sake of simplicity, we can for instance consider y_{tar} and y_{ini} to be periodic in space. The Euler coupled system associated with (3.16) is given by

$$\begin{cases} \partial_t y + \partial_x y = \lambda & \text{in } \mathbb{R}\times]0,T[, \\ \partial_t \lambda + \partial_x \lambda = 0 & \text{in } \mathbb{R}\times]0,T[, \end{cases} \quad y(\cdot,T) = y_{\text{tar}} \quad y(\cdot,0) = y_{\text{ini}}. \tag{3.19}$$

Problem (3.19) is not an evolution problem. In fact, it corresponds to an 'elliptic degenerated' system: indeed, introducing the change of variable

$$s = x + t \quad r = x - t \quad \hat{y}(r,s) = y(x,t),$$

we can see that

$$\begin{cases} \partial_s^2 \hat{y}(s,r) = 0, s \in [r, r+T], \\ \hat{y}(s=r,r) = y_{\text{ini}}(r), \\ \hat{y}(s=r+2T,r) = y_{\text{tar}}(r+T). \end{cases} \tag{3.20}$$

In other words, for each r, $\hat{y}(r,\cdot)$ satisfies a Dirichlet Laplace problem for $s \in [r, r+T]$: it means that we have a natural parallelization in r, r appearing only as a parameter of the equation. Note also that any discretization following the characteristic lines would be suitable for solving numerically this system.

This remark motivates us to investigate optimized Schwarz method for this problem, since we know that those methods are well-adapted for elliptic problems. Let us decompose our time interval $[0,T]$ into two subdomains (without overlap) of equal-size $\Delta T = T/2$ and consider the following set of transmission conditions: for any $(p,q) \in (\mathbb{R}^+)^2$

$$\begin{cases} \hat{q}\, y_1^k(x,\Delta T), + \lambda_1^k(x,\Delta T) = \hat{q}\, y_2^{k-1}(x,\Delta T) + \lambda_2^{k-1}(x,\Delta T), \\ -\hat{p}\, y_2^k(x,\Delta T), + \lambda_2^k(x,\Delta T) = -\hat{p}\, y_1^k(x,\Delta T) + \lambda_1^k(x,\Delta T). \end{cases} \tag{3.21}$$

The next results is immediate (through a Fourier transport in space).

Theorem 7. *The previous algorithm is well-posed for any pair of positive numbers $\hat{p}$ and $\hat{q}$. Moreover, choosing $\hat{p} = \hat{q} = \Delta T$ leads to its convergence in 2 iterations.*

Remark 14. *For $\hat{p} = \hat{q}$, a convergence analysis based on energy technics can be found in [164]. We can extend this result to the case of N subdomains, obtaining convergence after N iterations.*

To go further, we study the discretization of (3.16) (together with (3.21)). To discretize our problem, we consider a spatial discretization based on the upwind scheme with N uniform nodes and a mesh size of $\Delta x = 1/N$. We denote by $\mathcal{A}_{\Delta x} \in \mathcal{M}_N(\mathbb{R})$ the corresponding matrix: its diagonal terms are Δx^{-1}, its lower sub-diagonal ones are equal to $-\Delta x^{-1}$, and $[\mathcal{A}_{\Delta x}]_{1,N} = -\Delta x^{-1}$ (to take into account the periodicity). The time discretization is made using the semi-implicit Euler scheme (explicit in y and implicit in v), using $M+1$ uniform nodes on $[0,T]$ and a mesh size of $\Delta t = \frac{T}{M}$. We denote by $\mathbf{y}_{\rm ini}$, $\mathbf{y}_{\rm tar}$ (vectors of $\mathbb{R}^N$), the discretization of $y_{\rm ini}$ and $y_{\rm tar}$. We mimic the continuous minimization problem (3.16)-(3.17)-(3.18) by considering the following discrete one:

$$\min_{\mathbf{v}=(\mathbf{v}_i^n)\in\mathbb{R}^{N\times M}} J(\mathbf{v}) = \frac{1}{2}\Delta t\,\Delta x\,\|\mathbf{v}\|^2, \tag{3.22}$$

where the control $\mathbf{v} = (\mathbf{v}^1, \dots, \mathbf{v}^M)$ is such that $\mathbf{y} = (\mathbf{y}^0, \dots, \mathbf{y}^M) \in (\mathbb{R}^N)^{M+1}$ satisfies

$$\begin{cases} \dfrac{\mathbf{y}^m - \mathbf{y}^{m-1}}{\Delta t} + \mathcal{A}_{\Delta x}\mathbf{y}^{m-1} = \mathbf{v}^m \quad m = 1, \dots, M, \\ \mathbf{y}^0 = \mathbf{y}_{\rm ini}, \end{cases} \tag{3.23}$$

as well as the target constraint

$$\mathbf{y}^M = \mathbf{y}_{\rm tar}. \tag{3.24}$$

In the problem (3.22), $\|\cdot\|$ denotes the usual Euclidean norm on $\mathbb{R}^{N\times M}$. Problem (3.22)-(3.23)-(3.24) admits a unique solution $\mathbf{v}_*^m = \boldsymbol{\lambda}^m$, where $(\mathbf{y}^m, \boldsymbol{\lambda}^m)$ is the solution of the following optimality system

$$\begin{cases} \mathbf{y}^m - (\mathcal{I} - \Delta t\ \mathcal{A}_{\Delta x})\mathbf{y}^{m-1} = \Delta t\boldsymbol{\lambda}^m & m = 1, \dots, M, \\ \boldsymbol{\lambda}^{m-1} - (\mathcal{I} - \Delta t\ \mathcal{A}_{\Delta x}^t)\boldsymbol{\lambda}^m = 0 & m = 1, \dots, M, \\ \mathbf{y}^0 = \mathbf{y}_{\rm ini}, \\ \mathbf{y}^M = \mathbf{y}_{\rm tar}. \end{cases} \tag{3.25}$$

in order to guarantee the convergence of the scheme, we shall consider the standard relation between Δt and Δx given by

$$\frac{\Delta t}{\Delta x} = r, \tag{3.26}$$

where r is a given real parameter in $]0,1[$. We apply the DD strategy (3.21) to the discrete problem. For its analysis, we use the Discrete Fourier Transform. As in Section 3.1, it leads (also it is not completely direct) to consider the min-max problem

$$\min_{p,q>0}\left(\max_{0\le z\le z_{{\rm r},\Delta t}} |\rho_{\Delta t}(p,q,z)|\right) \quad \text{with} \quad \rho_{\Delta t}(p,q,z) = \frac{\varphi_{\Delta t}(z) - p}{\varphi_{\Delta t}(z) + q}\cdot\frac{\psi_{\Delta t}(z) - q}{\psi_{\Delta t}(z) + p}, \tag{3.27}$$

$p = \hat{p}\Delta T$, $q = \hat{q}\Delta T$, $z_{{\rm r},\Delta t} = \dfrac{4r(1-r)\Delta T}{\Delta t}$,

$$\varphi_{\Delta t}(z) = \frac{\Delta T}{\gamma_{\Delta t}(z)}, \quad \gamma_{\Delta t}(z) = \Delta t\sum_{m=0}^{L-1}\left(1 - \frac{\Delta t}{\Delta T}\cdot z\right)^m,$$

and

$$\psi_{\Delta t}(z) = \frac{|\beta_{\Delta t}(z)|^2\Delta T}{\gamma_{\Delta t}(z)} \quad |\beta_{\Delta t}(z)|^2 = \left(1 - \frac{\Delta t}{\Delta T}\cdot z\right)^L.$$

.

We first investigate the one-sided case (correponding to $p = q$):

Theorem 8. *Assume that $p = q$. Problem (3.27) has a unique minimizer $(p^*_{\Delta t}, \rho^*_{\Delta t})$, which as the following asymptotic as Δt goes to 0:*

$$p^*_{\Delta t} \sim c_\ell(\Delta t)^{-1/2} \qquad \rho^*_{\Delta t} \sim 1 - c_\delta\sqrt{\Delta t}.$$

Let us comment the previous result. First, it is remarquable to see that $p_{\Delta t^*}$ does not converge to 1, the optimized parameter for the continuous problem (see Theo.7). Mathematically, this is due to the fact that the numerical convergence factor does not converge uniformly (in z) to the continuous convergence factor as Δt goes to 0. Note that we can show that taking $\Delta t = \Delta x^s$ with $s > 2$ permits to recover the continuous case at the limit, but this has no practical interest. It is not clear to us weither changing our discretization scheme could help to recover the continuous case under the classical CFL condition. Naturally, using a scheme following the characteristic lines (solving the collection of Problem (3.20)) would be suitable (but not generalizable to higher dimension). Besides, generally speaking, the result is a bit disappointed since the convergence factor deteriorates as Δt goes to 0.

Hopefully, the two sided algorithm ($p \neq q$) is much more efficient:

Theorem 9. *For any $\Delta t > 0$, Problem (3.27) has at least one global solution $(p^*_{\Delta t}, q^*_{\Delta t})$ that 'equioscillates' at three points: there exists $z^*_{\Delta t} \in]0, z_{\mathrm{r},\Delta t}[$ such that*

$$|\rho_{\Delta t}(p^*_{\Delta t}, q^*_{\Delta t}, z = 0)| = |\rho_{\Delta t}(p^*_{\Delta t}, q^*_{\Delta t}, z = z^*_{\Delta t})| = |\rho_{\Delta t}(p^*_{\Delta t}, q^*_{\Delta t}, z = z_{\mathrm{r},\Delta t})|. \tag{3.28}$$

Moreover, there exists $\Delta t_0 > 0$, such that for any $\Delta t < \Delta t_0$, Problem (3.27) has a unique solution. In addition, there exist $(p^*, q^*) \in \mathbb{R}^2$ and $\rho^* \in]0, 1[$ such that

$$p^*_{\Delta t} = p^* + o(1), \quad q^*_{\Delta t} = q^* + o(1) \max_{0 \leq z \leq z_{\mathrm{r},\Delta t}} |\rho_{\Delta t}(p^*_{\Delta t}, q^*_{\Delta t}, z)| = \rho^* + o(1). \tag{3.29}$$

In the previous theorem p^* is solution to a non linear 'limit' equation. Solving numerically this equation leads to

$$p^* \simeq 1.1993, \quad q^* \simeq 0.0906 \text{ and, } \rho^* \simeq 0.0755. \tag{3.30}$$

Here again, as in the one-sided algorithm ($p = q$), we do not recover the continuous case. However, the convergence of the algorithm is much better since it goes to a fixed rate ρ^*, which is not 0 but small, as Δt goes to 0. Note that a convergence factor independent of the discretization parameter is also obtained for optimized Schwarz method [118, 173] applied to parabolic optimal control problems.

We illustrate the previous results in the case $T = 1$. On Figure 3.4a, we consider the one sided algorithm and we plot $1 - \rho^*_{\Delta t}$ with respect to Δt (in logarithmic scale) for three different values of r. In each case, the optimized parameter $p^*_{\Delta t}$ is computed using `fminsearch` in Matlab. As expected, whatever the choice of $r \in]0, 1[$, we obtain straight lines with slope equal to that of the curve $y = \sqrt{\Delta t}$.

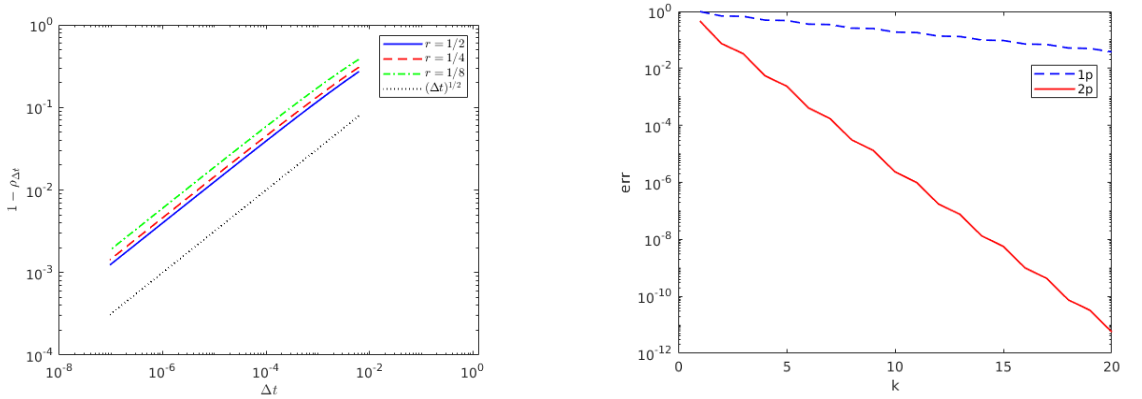

(a) Asymptotic behaviour of $\rho^*_{\Delta t}$

(b) performance of $p^*_{\Delta t}$ for $\Delta t = 1/160, r = 1/2$.

Figure 3.4: Illustration of the performances of algorithm 3.21

Next, we test the performance of our domain decomposition-in-time algorithm. For the simulation, we take $\Delta t = 1/160$, $r = 1/2$, $y_{\text{ini}} = y_{\text{tar}} = 0$, and we start from a random initial guess (i.e. we compute the zero solution). On Figure 3.4b, we display in blue the evolution of the error with respect to the number of iterations; in the present case, it just consists of computing the maximum of the L^2 norm of the Robin interface data. The performance is as predicted by the theory. On the other hand, the convergence rate is drastically improved by using the two-sided algorithm. The `fminsearch` function provides us with two optimized parameters $(p^*_{\Delta t}, q^*_{\Delta t}) = (1.1831, 8.5024 \times 10^{-2})$ (remarkably closed to the predicted limit 3.30), leading to a convergence factor of 7.0728×10^{-2}. The performance of the two-sided algorithm for this value is displayed in red, and appears to be much better than the optimized one-sided one.

Future directions of work

We are currently continuing the work in the following directions:

1. A first natural extension of our work (it should not be out of reach) consists in studying the convergence properties of the overlapping algorithm. We are currently investigating the behavior of the DD algorithm for more than 2 subdomains. We expect to observe a deterioration of the convergence properties as the number of subdomain increase. A coarse grid strategy could then be used (and analyzed) to overcome this difficulty.

2. We are looking into a second strategy of time-domain decomposition method based on the the ParaOpt algorithm developed in [121]. This method is an extension of the Parareal algorithm [184, 113, 114] to optimal control problems. It works very well for in the parabolic case. Unfortunately we have proved that its direct application for transport equation leads to a divergent algorithm (one eigenvalue of the iteration matrix is larger than one for large frequencies). In addition, numerical experiments suggest that the use of GMRES on the interfaced preconditioned equation would not help. I do not understand if this lack of convergence is related to the poor convergence property of Parareal for hyperbolic equations [234] and if the possible cures suggested [124, 216] could be applied.

3. We are currently working on the adaptation of the results to the wave equations: it leads to bi-laplacian-like equations on the characteristic lines and thus make the computations (and the analysis) heavier. At the continuous level, we can prove that the classical Dirichlet-Neumann algorithm converges as for as the final time is not too large (see also. [122] for different proposition of Dirichlet-Neumann algorithm bi-laplacian operators). Again, we can try to speed up our algorithm by adding a relaxation parameter or modifying the transmission condition.

Bibliography

[1] Perturbed periodic medium. `https://www.nisenet.org/catalog/scientific-image-photonic-crystal`. Accessed: 2022-08-22.

[2] S. Abarbanel and D. Gottlieb. A mathematical analysis of the pml method. *Journal of Computational Physics*, 134(2):357–363, 1997.

[3] T. Abboud and H. Ammari. Diffraction at a curved grating: TM and TE cases, homogenization. *J. Math. Anal. Appl.*, 202(3):995–1026, 1996.

[4] Y. Achdou. Etude de la réflexion d'une onde électromagnétique par un métal recouvert d'un revêtement métallisé. Technical report, INRIA, 1989.

[5] Y. Achdou. Effect of a thin letallized coating on the reflexion of a thin mettallized coating on the reflection of an electromagnetic wave. *Comptes rendus de l'académie des sciences Série I-Mathématique*, 314(3):217–222, Jan 30 1992.

[6] Y. Achdou, O. Pironneau, and F. Valentin. Effective boundary conditions for laminar flows over periodic rough boundaries. *J. Comput. Phys.*, 147(1):187–218, 1998.

[7] A. Aius. Representation of the graphen. `https://www.photoniques.com/articles/photon/pdf/2018/02/photon2018S3p50.pdf`. Accessed: 2022-08-22.

[8] H. Ammari and F. Santosa. Guided waves in a photonic bandgap structure with a line defect. *SIAM J. Appl. Math.*, 64(6):2018–2033 (electronic), 2004.

[9] C. Amrouche, C. Bernardi, M. Dauge, and V. Girault. Vector potentials in three-dimensional non-smooth domains. *Math. Methods Appl. Sci.*, 21(9):823–864, 1998.

[10] T. Arens, S.-N. Chandler-Wilde, and J.-A. DeSanto. On integral equation and least squares methods for scaterring by diffraction gratings. *Commun. Comput. Phys.*, 1(6):1010–1042, December 2006.

[11] M. Artola and M. Cessenat. Diffraction d'une onde électromagnétique par une couche composite mince accolée à un corps conducteur épais. I. Cas des inclusions fortement conductrices. *C. R. Acad. Sci. Paris Sér. I Math.*, 313(5):231–236, 1991.

[12] M. Artola and M. Cessenat. Scattering of an electromagnetic wave by a slender composite slab in contact with a thick perfect conductor. II. Inclusions (or coated material) with high conductivity and high permeability. *CR Acad. Sci. Paris Sér. I Math*, 313(6):381–385, 1991.

[13] Alexis Auvray and Grégory Vial. Asymptotic expansions and effective boundary conditions: a short review for smooth and nonsmooth geometries with thin layers. *ESAIM: Proceedings and Surveys*, 61:38–54, 2018.

[14] Alexis Auvray and Grégory Vial. Improved impedance conditions for a thin layer problem in a nonsmooth domain. *Mathematical Methods in the Applied Sciences*, 42(5):1432–1448, 2019.

[15] Y. Avishai and J.-M. Luck. Quantum percolation and ballistic conductance on a lattice of wires. *Physical Review B*, 45(3):1074, 1992.

[16] F.-L. Bakharev, S.-A. Nazarov, and K.-M. Ruotsalainen. A gap in the spectrum of the Neumann-Laplacian on a periodic waveguide. *Appl. Anal.*, 92(9):1889–1915, 2013.

[17] S. Balac, M. Dauge, and Z. Moitier. Asymptotics for 2d whispering gallery modes in optical microdisks with radially varying index. *IMA Journal of Applied Mathematics*, pages 1212–1265, 2021.

[18] Andrew T Barker and Martin Stoll. Domain decomposition in time for pde-constrained optimization. *Computer Physics Communications*, 197:136–143, 2015.

[19] R.-A. Bartlett, M. Heinkenschloss, D. Ridzal, and B.-G. van Bloemen Waanders. Domain decomposition methods for advection dominated linear-quadratic elliptic optimal control problems. *Comput. Methods Appl. Mech. Engrg.*, 195(44-47):6428–6447, 2006.

[20] A. Bayliss and E Turkel. Radiation boundary conditions for wave-like equations. *Comm. Pure and Appl. Math.*, 33(6):707–725, 1980.

[21] E. Bécache, S. Fauqueux, and P. Joly. Stability of perfectly matched layers, group velocities and anisotropic waves. *Journal of Computational Physics*, 188(2):399–433, 2003.

[22] E. Bécache and P. Joly. On the analysis of bérenger's perfectly matched layers for maxwell's equations. *ESAIM: Mathematical Modelling and Numerical Analysis*, 36(1):87–119, 2002.

[23] J.-D. Benamou. A domain decomposition method with coupled transmission conditions for the optimal control of systems governed by elliptic partial differential equations. *SIAM J. Numer. Anal.*, 33(6):2401–2416, 1996.

[24] J.-D. Benamou and B. Després. A domain decomposition method for the Helmholtz equation and related optimal control problems. *J. Comput. Phys.*, 136(1):68–82, 1997.

[25] A. Bendali, A. Makhlouf, and S. Tordeux. Field behavior near the edge of a microstrip antenna by the method of matched asymptotic expansions. *Quart. Appl. Math.*, 69(4):691–721, 2011.

[26] C. Beneteau. *Modèles homogénéisés enrichis en présence de bords: Analyse et traitement numérique*. PhD thesis, Institut polytechnique de Paris, 2021.

[27] D. Bennequin, M. Gander, L. Gouarin, and L. Halpern. Optimized Schwarz waveform relaxation for advection reaction diffusion equations in two dimensions. *Numer. Math.*, 73:167–195, 2016.

[28] D. Bennequin, M.-J. Gander, and L. Halpern. A homographic best approximation problem with application to optimized Schwarz waveform relaxation. *Mathematics of Computation*, 78(265):185–223, 2009.

[29] A. Bensoussan, R. Glowinski, and J.-L. Lions. Méthode de décomposition appliquée au contrôle optimal de systèmes distribués. In *IFIP Technical Conference on Optimization Techniques*, pages 141–151. Springer, 1973.

[30] J.-P. Berenger. A perfectly matched layer for the absorption of electromagnetic waves. *J. Comput. Phys.*, 114(2):185–200, 1994.

[31] L. Berlyand, G. Cardone, Y. Gorb, and G.-P. Panasenko. Asymptotic analysis of an array of closely spaced absolutely conductive inclusions. *Netw. Heterog. Media*, 1(3):353–377, 2006.

[32] M.-Sh. Birman and M.-Z. Solomjak. *Spectral theory of selfadjoint operators in Hilbert space*. Mathematics and its Applications (Soviet Series). D. Reidel Publishing Co., Dordrecht, 1987. Translated from the 1980 Russian original by S. Khrushchëv and V. Peller.

[33] M. Bonazzoli, V. Dolean, F.c Hecht, and F. Rapetti. An example of explicit implementation strategy and preconditioning for the high order edge finite elements applied to the time-harmonic maxwell's equations. *Computers & Mathematics with Applications*, 75(5):1498–1514, 2018.

[34] V. Bonnaillie-Noël, M. Dambrine, S. Tordeux, and G. Vial. Interactions between moderately close inclusions for the Laplace equation. *Math. Models Methods Appl. Sci.*, 19(10):1853–1882, 2009.

[35] A.-S. Bonnet-Ben Dhia, S.-N. Chandler-Wilde, and S. Fliss. On the half-space matching method for real wavenumber. *SIAM Journal on Applied Mathematics*, 82(4):1287–1311, 2022.

[36] A.-S. Bonnet-Ben Dhia, S.-N Chandler-Wilde, S. Fliss, C. Hazard, K.-M. Perfekt, and Y. Tjandrawidjaja. The complex-scaled half-space matching method. *SIAM Journal on Mathematical Analysis*, 54(1):512–557, 2022.

[37] A.-S. Bonnet-Ben Dhia, S. Fliss, and A. Tonnoir. The halfspace matching method: A new method to solve scattering problems in infinite media. *Journal of Computational and Applied Mathematics*, 338:44–68, 2018.

[38] A.S. Bonnet-Ben Dhia, D. Drissi, and N. Gmati. Mathematical analysis of the acoustic diffraction by a muffler containing perforated ducts. *Mathematical Models and Methods in Applied Sciences*, 15(07):1059–1090, 2005.

[39] G. Borg. Eine Umkehrung der Sturm-Liouvilleschen Eigenwertaufgabe. Bestimmung der Differentialgleichung durch die Eigenwerte. *Acta Math.*, 78:1–96, 1946.

[40] A. Boucart, S. Fliss, L. Giovangigli, and B. Stupfel. Modélisation de la diffraction par une couche mince de nanoparticules disposées aléatoirement.

[41] I. Brener, S. Liu, I. Staude, J. Valentine, and C.-L. Holloway. *Dielectric metamaterials: fundamentals, designs and applications*. Woodhead publishing, 2019.

[42] D. Bresch and V. Milisic. High order multi-scale wall-laws, Part I: the periodic case. *Quart. Appl. Math.*, 68(2):229–253, 2010.

[43] B.-M. Brown, V. Hoang, M. Plum, and I. Wood. Spectrum created by line defects in periodic structures. *Math. Nachr.*, 287(17-18):1972–1985, 2014.

[44] B.-M. Brown, V. Hoang, M. Plum, and I. Wood. On the spectrum of waveguides in planar photonic bandgap structures. *Proc. A.*, 471(2176):20140673, 20, 2015.

[45] S.-S Bukhari, J.-Y. Vardaxoglou, and W. Whittow. A metasurfaces review: Definitions and applications. *Applied Sciences*, 9(13):2727, 2019.

[46] R. Bunoiu, G. Cardone, and S.-A. Nazarov. Scalar problems in junctions of rods and a plate-ii. self-adjoint extensions and simulation models. *ESAIM: Mathematical Modelling and Numerical Analysis*, 52(2):481–508, 2018.

[47] E. Burman, A. Feizmohammadi, and L. Oksanen. A fully discrete numerical control method for the wave equation. *SIAM Journal on Control and Optimization*, 58(3):1519–1546, 2020.

[48] G. Caloz, M. Costabel, M. Dauge, and G. Vial. Asymptotic expansion of the solution of an interface problem in a polygonal domain with thin layer. *Asymptot. Anal.*, 50(1-2):121–173, 2006.

[49] Eric Cancès, Virginie Ehrlacher, and Yvon Maday. Periodic schrödinger operators with local defects and spectral pollution. *SIAM Journal on Numerical Analysis*, 50(6):3016–3035, 2012.

[50] R. Carlson. Adjoint and self-adjoint differential operators on graphs. *Electronic Journal of Differential Equations*, 6(1998):1–10, 1998.

[51] M. Cassier and M.-I. Weinstein. High contrast elliptic operators in honeycomb structures. *Multiscale Modeling & Simulation*, 19(4):1784–1856, 2021.

[52] P.-L. Castro. On the Schwarz alternating method. III: a variant for nonoverlapping subdomains. In T. Chan, R. Glowinski, J. Périaux, and O. Widlund, editors, *Third Int. Symposium on Domain Decomposition Methods for Partial Differential Equations*, Philadelphia, PA, 1990. SIAM.

[53] A.-H Castro Neto, F. Guinea, N.-M.-R. Peres, K.-S. Novoselov, and A.-K Geim. The electronic properties of graphene. *Reviews of modern physics*, 81(1):109, 2009.

[54] Jean Cazalis. *Nonlinear quantum systems at dissociation: the example of graphene.* PhD thesis, Université PSL (Paris Sciences & Lettres), 2022.

[55] M. Chamaillard. *Effective boundary conditions for thin periodic coatings.* PhD thesis, Université Paris Saclay, 2016.

[56] S.-N. Chandler-Wilde and J. Elschner. Variational approach in weighted sobolev spaces to scattering by unbounded rough surfaces. *SIAM journal on mathematical analysis*, 42(6):2554–2580, 2010.

[57] S.-N. Chandler-Wilde and P.-B. Monk. Existence, uniqueness, and variational methods for scattering by unbounded rough surfaces. *SIAM Journal on Mathematical Analysis*, 37(2):598–618, 2005.

[58] S.-J. Chapman, D.-P. Hewett, and L.-N. Trefethen. Mathematics of the faraday cage. *Siam Review*, 57(3):398–417, 2015.

[59] H.-T. Chen, A.-J Taylor, and N. Yu. A review of metasurfaces: physics and applications. *Reports on progress in physics*, 79(7):076401, 2016.

[60] G. Ciaramella and L. Mechelli. An overlapping waveform-relaxation preconditioner for economic optimal control problems with state constraints. *arXiv preprint arXiv:2103.14849*, 2021.

[61] D. Cioranescu, A. Damlamian, G Griso, and D Onofrei. The periodic unfolding method for perforated domains and neumann sieve models. *Journal de mathématiques pures et appliquées*, 89(3):248–277, 2008.

[62] I.-S. Ciuperca, M. Jai, and C. Poignard. Approximate transmission conditions through a rough thin layer: the case of periodic roughness. *European J. Appl. Math.*, 21(1):51–75, 2010.

[63] X. Claeys. On the theoretical justification of Pocklington's equation. *Math. Models Methods Appl. Sci.*, 19(8):1325–1355, 2009.

[64] J. Coatléven. *Analyse mathématique et numérique de quelques problèmes d'ondes en milieu périodique.* PhD thesis, Ecole Polytechnique X, 2011.

[65] D.-L. Colton and R. Kress. *Inverse Acoustic ans electromagnetic scattering theory.* Springer-Verlag, second edition, 1998.

[66] J. Dalibard. La matière topologique et son exploration avec des gaz quantiques. `https://www.college-de-france.fr/site/jean-dalibard/course-2017-2018.htm`. Accessed: 2022-08-23.

[67] M. Dambrine and G. Vial. A multiscale correction method for local singular perturbations of the boundary. *ESAIM: Mathematical Modelling and Numerical Analysis*, 41(1):111–127, 2007.

[68] M. Dauge, P. Dular, L. Krähenbühl, V. Péron, R. Perrussel, and C. Poignard. Corner asymptotics of the magnetic potential in the eddy-current model. *Mathematical Methods in the Applied Sciences*, 37(13):1924–1955, 2014.

[69] M. Dauge, S. Tordeux, and G. Vial. Selfsimilar perturbation near a corner: matching versus multiscale expansions for a model problem. In *Around the research of Vladimir Maz'ya. II*, volume 12 of *Int. Math. Ser. (N. Y.)*, pages 95–134. Springer-Verlag, New York, 2010.

[70] B. Delourme. High-order asymptotics for the electromagnetic scattering by thin periodic layers. *Mathematical Methods in the Applied Sciences*, 38(5):811–833, 2015.

[71] B. Delourme, S. Fliss, P. Joly, and E. Vasilevskaya. Trapped modes in thin and infinite ladder like domains: existence and asymptotic analysis. *INRIA Research Report*, 2016.

[72] B. Delourme, S. Fliss, P. Joly, and E. Vasilevskaya. Trapped modes in thin and infinite ladder like domains. part 2: asymptotic analysis and numerical application. *Asymptotic Analysis*, (Preprint):1–36, 2019.

[73] B. Delourme, H. Haddar, and P. Joly. Approximate models for wave propagation across thin periodic interfaces, 2011.

[74] B. Delourme, H. Haddar, and P. Joly. Approximate models for wave propagation across thin periodic interfaces. *Journal de mathématiques pures et appliquées*, 98(1):28–71, 2012.

[75] B. Delourme, H. Haddar, and P. Joly. On the well-posedness, stability and accuracy of an asymptotic model for thin periodic interfaces in electromagnetic scattering problems. *Mathematical Models and Methods in Applied Sciences*, 23(13):2433–2464, 2013.

[76] B. Delourme, P. Joly, and E. Vasilevskaya. Existence of guided waves due to a lineic perturbation of a 3d periodic medium. *Applied Mathematics Letters*, 69:146–152, 2017.

[77] B. Delourme, E. Lunéville, J.-J. Marigo, A. Maurel, J.-F. Mercier, and K. Pham. A stable, unified model for resonant faraday cages. *Proceedings of the Royal Society A*, 477(2245):20200668, 2021.

[78] B. Delourme, K. Schmidt, and A. Semin. On the homogenization of thin perforated walls of finite length. *Asymptotic Analysis*, 97(3-4):211–264, 2016.

[79] P. Delplace, D. Ullmo, and G Montambaux. Zak phase and the existence of edge states in graphene. *Physical Review B*, 84(19):195452, 2011.

[80] B. Després. *Méthodes de décomposition de domaine pour les problèmes de propagation d'ondes en régimes harmoniques*. PhD thesis, Université Dauphine - Paris IX, 1991.

[81] P. Donato, A. Lamacz, and B. Schweizer. Sound absorption by perforated walls along boundaries. *Applicable Analysis*, pages 1–15, 2020.

[82] D. Drissi. *Simulation des silencieux d'échappement par une méthode d'éléments finis homogénéisés*. PhD thesis, Université de Tunis, 2003.

[83] A. Drouot. The bulk-edge correspondence for continuous honeycomb lattices. *Communications in Partial Differential Equations*, 44(12):1406–1430, 2019.

[84] A. Drouot. Microlocal analysis of the bulk-edge correspondence. *Communications in Mathematical Physics*, 383(3):2069–2112, 2021.

[85] A. Drouot and M.-I. Weinstein. Edge states and the valley hall effect. *Advances in Mathematics*, 368:107142, 2020.

[86] M. Duruflé, V. Péron, and C. Poignard. Time-harmonic maxwell equations in biological cells—the differential form formalism to treat the thin layer. *Confluentes Mathematici*, 3(02):325–357, 2011.

[87] M. Duruflé, V. Péron, and C. Poignard. Thin layer models for electromagnetism. *Communications in Computational Physics*, 16(1):213–238, 2014.

[88] T. Duyckaerts, A. Grigis, and A. Martinez. Resonance widths for general helmholtz resonators with straight neck. *Duke Mathematical Journal*, 165(14):2793–2810, 2016.

[89] M.-S.-P. Eastham. *The spectral theory of periodic differential equations*. Edinburgh : Scottish Academic Press, Edinburgh-London, distributed by chatto and windus edition, 1973.

[90] S. Ervedoza and E. Zuazua. On the numerical approximation of exact controls for waves, 2012.

[91] P. Exner. Lattice kronic-penney models. *Physical review letters*, 74(18):3503, 1995.

[92] M. Faraday. I. experimental researches in electricity.—fifteenth series. *Philosophical Transactions of the Royal Society of London*, (129):1–12, 1839.

[93] C. Fefferman, J. Lee-Thorp, and M.-I. Weinstein. *Topologically protected states in one-dimensional systems*, volume 247. American Mathematical Society, 2017.

[94] C. Fefferman and M.-I. Weinstein. Honeycomb lattice potentials and dirac points. *Journal of the American Mathematical Society*, 25(4):1169–1220, 2012.

[95] C.-L. Fefferman, S. Fliss, and M.-I. Weinstein. Discrete honeycombs, rational edges and edge states. *arXiv preprint arXiv:2203.03775*, 2022.

[96] C.-L. Fefferman, J.-P. Lee-Thorp, and M.-I. Weinstein. Topologically protected states in one-dimensional continuous systems and dirac points. *Proceedings of the National Academy of Sciences*, 111(24):8759–8763, 2014.

[97] C.-L. Fefferman and M.-I. Weinstein. Wave packets in honeycomb structures and two-dimensional dirac equations. *Communications in Mathematical Physics*, 326(1):251–286, 2014.

[98] C.-L. Fefferman and M.-I. Weinstein. Continuum schroedinger operators for sharply terminated graphene-like structures. *arXiv preprint arXiv:1810.03497*, 2018.

[99] A. Figotin and V. Gorentsveig. Localized electromagnetic waves in a layered periodic dielectric medium with a defect. *Physical Review B*, 58(1):180, 1998.

[100] A. Figotin and A. Klein. Localization of classical waves .1. Acoustic waves. *Comm. Math. Phys.*, 180(2):439–482, January 1996.

[101] A. Figotin and A. Klein. Localized classical waves created by defects. *J. Statist. Phys.*, 86(1-2):165–177, 1997.

[102] A. Figotin and A. Klein. Midgap defect modes in dielectric and acoustic media. *SIAM J. Appl. Math.*, 58(6):1748–1773 (electronic), 1998.

[103] A. Figotin and P. Kuchment. Band-gap structure of spectra of periodic dielectric and acoustic media. I. Scalar model. *SIAM J. Appl. Math.*, 56(1):68–88, 1996.

[104] A. Figotin and P. Kuchment. Band-gap structure of spectra of periodic dielectric and acoustic media. II. Two-dimensional photonic crystals. *SIAM J. Appl. Math.*, 56(6):1561–1620, 1996.

[105] A. Figotin and P. Kuchment. Spectral properties of classical waves in high-contrast periodic media. *SIAM Journal on Applied Mathematics*, 58(2):683–702, 1998.

[106] S. Fliss. A Dirichlet-to-Neumann approach for the exact computation of guided modes in photonic crystal waveguides. *SIAM J. Sci. Comput.*, 35(2):B438–B461, 2013.

[107] S. Fliss and P. Joly. Solutions of the time-harmonic wave equation in periodic waveguides: asymptotic behaviour and radiation condition. *Archive for Rational Mechanics and Analysis*, 219(1):349–386, 2016.

[108] S. Fliss, P. Joly, and V. Lescarret. A dirichlet-to-neumann approach to the mathematical and numerical analysis in waveguides with periodic outlets at infinity. *Pure and Applied Analysis*, 3(3):487–526, 2021.

[109] S. Fliss, P. Joly, and J.-R. Li. *Exact boundary conditions for wave propagation in periodic media containing a local perturbation.* Bentham Science Publishers. E-Book Series Progress in Computational Physics (PiCP), Volume 1, 12 2009.

[110] R.-R. Gadyl'shin. Existence and asymptotics of poles with small imaginary part for the helmholtz resonator. *Russian Mathematical Surveys*, 52(1):1, 1997.

[111] R.-R. Gadyl'shin. On an analog of the helmholtz resonator in the averaging theory. *Comptes Rendus de l'Académie des Sciences-Series I-Mathematics*, 329(12):1121–1126, 1999.

[112] M.-J. Gander. Optimized Schwarz Method. *SIAM Journal on Numerical Analysis*, 44(2):699–731, 2006.

[113] M.-J. Gander and E. Hairer. Nonlinear convergence analysis for the parareal algorithm. In *Domain decomposition methods in science and engineering XVII*, pages 45–56. Springer, 2008.

[114] M.-J. Gander and E. Hairer. Analysis for parareal algorithms applied to hamiltonian differential equations. *Journal of Computational and Applied Mathematics*, 259:2–13, 2014.

[115] M.-J. Gander and L. Halpern. Méthodes de décomposition de domaines. notions de base. *Techniques de l'ingénieur Analyse numérique des équations différentielles et aux dérivées partielles*, base documentaire : 42620210.(ref. article : af1375), 2012.

[116] M.-J. Gander, L. Halpern, and F. Nataf. Optimized Schwarz methods. In *Domain decomposition methods in sciences and engineering (Chiba, 1999*, pages 15–27, 2001.

[117] M.-J. Gander, L. Halpern, and F. Nataf. Optimal schwarz waveform relaxation for the one dimensional wave equation. *SIAM Journal on Numerical Analysis*, 41(5):1643–1681, 2003.

[118] M.-J. Gander and F. Kwok. Schwarz methods for the time-parallel solution of parabolic control problems. In *Domain decomposition methods in science and engineering XXII*, pages 207–216. Springer, 2016.

[119] M.-J. Gander, F. Kwok, and B.-C. Mandal. Convergence of substructuring methods for elliptic optimal control problems. In P.E. Bjørstad, S.C. Brenner, L. Halpern, H.H. Kim, R. Kornhuber, T. Rahman, and O.B. Widlund, editors, *Domain decomposition methods in science and engineering*, volume 125 of *Lect. Notes Comput. Sci. Eng.*, pages 291–300. Springer, Berlin, 2018.

[120] M.-J. Gander, F. Kwok, and G. Wanner. Constrained optimization: From lagrangian mechanics to optimal control and pde constraints. In *Optimization with PDE Constraints*, pages 151–202. Springer, 2014.

[121] M.-J. Gander and J. Kwok, F.and Salomon. Paraopt: A parareal algorithm for optimality systems. *SIAM Journal on Scientific Computing*, 42(5):A2773–A2802, 2020.

[122] M.-J. Gander and Y. Liu. Is there more than one dirichlet–neumann algorithm for the biharmonic problem? *SIAM Journal on Scientific Computing*, 43(3):A1881–A1906, 2021.

[123] M.-J. Gander, F. Magoulès, and F. Nataf. Optimized Schwarz methods without overlap for the Helmholtz equation. *SIAM J. Sci. Comput.*, 24(1):38–60, 2002.

[124] M.-J. Gander and M. Petcu. Analysis of a krylov subspace enhanced parareal algorithm for linear problems. In *ESAIM: Proceedings*, volume 25, pages 114–129. EDP Sciences, 2008.

[125] S. Giani and I.-G. Graham. Adaptive finite element methods for computing band gaps in photonic crystals. *Numerische Mathematik*, 121(1):31–64, 2012.

[126] R. Glowinski, J.-L. Lions, and J. He. *Exact and Approximate Controllability for Distributed Parameter Systems: A Numerical Approach*. Encyclopedia of Mathematics and its Applications. Cambridge University Press, 2008.

[127] D. Gontier. Edge states in ordinary differential equations for dislocations. *Journal of Mathematical Physics*, 61(4):043507, 2020.

[128] G.-M. Graf and M. Porta. Bulk-edge correspondence for two-dimensional topological insulators. *Communications in Mathematical Physics*, 324(3):851–895, 2013.

[129] H. Grandjean. *Effective boundary conditions for thin periodic coatings*. PhD thesis, Propagation d'une onde de choc dans un liquide aéré: modélisation et application aux rideaux de bulles, Doctoral dissertation, Université de Bretagne occidentale-Brest., 2012.

[130] D. Grieser. Spectra of graph neighborhoods and scattering. *Proc. Lond. Math. Soc. (3)*, 97(3):718–752, 2008.

[131] B.-B. Guzina, O. Oudghiri-Idrissi, and S. Meng. Asymptotic anatomy of the berry phase for scalar waves in two-dimensional periodic continua. *Proceedings of the Royal Society A*, 478(2262):20220110, 2022.

[132] T. Hagström, R.-P. Tewarson, and A. Jazcilevich. Numerical experiments on a domain decomposition algorithm for nonlinear elliptic boundary value problems. *Appl. Math. Lett.*, 1(3):299–302, 1988.

[133] F.-D.-M. Haldane and S. Raghu. Possible realization of directional optical waveguides in photonic crystals with broken time-reversal symmetry. *Physical review letters*, 100(1):013904, 2008.

[134] L. Halpern and J. Szeftel. Optimized and quasi-optimal Schwarz waveform relaxation for the one-dimensional Schrödinger equation. *Math. Models Methods Appl. Sci.*, 20(12):2167–2199, 2010.

[135] F. Hecht. New development in freefem++. *Journal of numerical mathematics*, 20(3-4):251–266, 2012.

[136] M. Heinkenschloss. A time-domain decomposition iterative method for the solution of distributed linear quadratic optimal control problems. *Journal of Computational and Applied Mathematics*, 173(1):169–198, 2005.

[137] M. Heinkenschloss and H. Nguyen. Balancing Neumann-Neumann methods for elliptic optimal control problems. In *Domain decomposition methods in science and engineering*, volume 40 of *Lect. Notes Comput. Sci. Eng.*, pages 589–596. Springer, Berlin, 2005.

[138] R. Hempel and K. Lienau. Spectral properties of periodic media in the large coupling limit: Properties of periodic media. *Communications in Partial Differential Equations*, 25(7-8):1445–1470, 2000.

[139] D.-P. Hewett and I.-J. Hewitt. Homogenized boundary conditions and resonance effects in faraday cages. *Proceedings of the Royal Society A: Mathematical, Physical and Engineering Sciences*, 472(2189):20160062, 2016.

[140] P.-D Hislop and A. Martinez. Scattering resonances of a helmholtz resonator. *Indiana University mathematics journal*, pages 767–788, 1991.

[141] P.-D. Hislop and I.-M. Sigal. *Introduction to spectral theory: With applications to Schrödinger operators*, volume 113. Springer Science & Business Media, 2012.

[142] V. Hoang. The limiting absorption principle for a periodic semi-infinite waveguide. *SIAM Journal on Applied Mathematics*, 71(3):791–810, 2011.

[143] V. Hoang, M. Plum, and C. Wieners. A computer-assisted proof for photonic band gaps. *Z. Angew. Math. Phys.*, 60(6):1035–1052, 2009.

[144] C.-L. Holloway and E.-F Kuester. A homogenization technique for obtaining generalized sheet-transition conditions for a metafilm embedded in a magnetodielectric interface. *IEEE Transactions on Antennas and Propagation*, 64(11):4671–4686, 2016.

[145] C.-L. Holloway, E.-F. Kuester, J. Baker-Jarvis, and P. Kabos. A double negative (dng) composite medium composed of magnetodielectric spherical particles embedded in a matrix. *IEEE Transactions on Antennas and Propagation*, 51(10):2596–2603, 2003.

[146] C.-L. Holloway, E.-F. Kuester, J.-A. Gordon, J. O'Hara, J. Booth, and D.-R. Smith. An overview of the theory and applications of metasurfaces: The two-dimensional equivalents of metamaterials. *IEEE antennas and propagation magazine*, 54(2):10–35, 2012.

[147] A.-M. Il′in. *Matching of asymptotic expansions of solutions of boundary value problems*, volume 102 of *Translations of Mathematical Monographs*. American Mathematical Society, Providence, RI, 1992. Translated from the Russian by V. Minachin [V. V. Minakhin].

[148] C. Japhet. *Méthodes de décomposition de domaine et conditions aux limites artificielles en mécanique des fluides: méthode optimisée d'ordre 2*. PhD thesis, Université Paris Nord - Paris XIII, 1998.

[149] J.-D. Joannopoulos, R.-D. Meade, and J.-N. Winn. *Photonic Crystal - Molding the Flow of Light*. Princeton Univeristy Press, 1995.

[150] S.-G. Johnson and J-D. Joannopoulos. *Photonic Crystal - The road from theory to practice*. Kluwer Acad. Publ., 2002.

[151] P. Joly. An elementary introduction to the construction and the analysis of perfectly matched layers for time domain wave propagation. *SeMA Journal*, 57(1):5–48, 2012.

[152] P. Joly and A. Semin. Construction and analysis of improved Kirchoff conditions for acoustic wave propagation in a junction of thin slots. In *Paris-Sud Working Group on Modelling and Scientific Computing 2007–2008*, volume 25 of *ESAIM Proc.*, pages 44–67. EDP Sci., Les Ulis, 2008.

[153] P. Joly and S. Tordeux. Matching of asymptotic expansions for wave propagation in media with thin slots. I. The asymptotic expansion. *Multiscale Model. Simul.*, 5(1):304–336 (electronic), 2006.

[154] P. Joly and S. Tordeux. Matching of asymptotic expansions for waves propagation in media with thin slots. II. The error estimates. *M2AN Math. Model. Numer. Anal.*, 42(2):193–221, 2008.

[155] I.-V. Kamotskii and S.-A. Nazarov. Spectral problems in singularly perturbed domains and selfadjoint extensions of differential operators. *Translations of the American Mathematical Society-Series 2*, 199:127–182, 2000.

[156] A. Khrabustovskyi. Opening up and control of spectral gaps of the Laplacian in periodic domains. *J. Math. Phys.*, 55(12):121502, 23, 2014.

[157] A. Khrabustovskyi and E. Khruslov. Gaps in the spectrum of the Neumann Laplacian generated by a system of periodically distributed traps. *Math. Methods Appl. Sci.*, 38(1):11–26, 2015.

[158] A. Kirsch. Diffraction by periodic structures. In *Inverse problems in mathematical physics*, pages 87–102. Springer, 1993.

[159] A. Kirsch. A scattering problem for a local perturbation of an open periodic waveguide. *Mathematical Methods in the Applied Sciences*, 2022.

[160] A. Kirsch and A. Lechleiter. A radiation condition arising from the limiting absorption principle for a closed full-or half-waveguide problem. *Mathematical Methods in the Applied Sciences*, 41(10):3955–3975, 2018.

[161] M. Kohmoto and Y. Hasegawa. Zero modes and edge states of the honeycomb lattice. *Physical Review B*, 76(20):205402, 2007.

[162] V.-A. Kondrat′ev. Boundary-value problems for elliptic equations in conical regions. *Dokl. Akad. Nauk SSSR*, 153:27–29, 1963.

[163] V.-A. Kozlov, V.-G. Mazya, and J. Rossmann. *Elliptic boundary value problems in domains with point singularities*, volume 52 of *Mathematical Surveys and Monographs*. American Mathematical Society, Providence, RI, 1997.

[164] R. Krug, G. Leugering, A. Martin, M. Schmidt, and D. Weninger. Time-domain decomposition for optimal control problems governed by semilinear hyperbolic systems. *SIAM Journal on Control and Optimization*, 59(6):4339–4372, 2021.

[165] P. Kuchment. *Floquet theory for partial differential equations*, volume 60 of *Operator Theory: Advances and Applications*. Birkhäuser Verlag, Basel, 1993.

[166] P. Kuchment. *7. The Mathematics of Photonic Crystals*, chapter 7, pages 207–272. 2001.

[167] P. Kuchment. Quantum graphs. I. Some basic structures. *Waves Random Media*, 14(1):S107–S128, 2004. Special section on quantum graphs.

[168] P. Kuchment and B.-S. Ong. On guided waves in photonic crystal waveguides. In *Waves in periodic and random media (South Hadley, MA, 2002)*, volume 339 of *Contemp. Math.*, pages 105–115. Amer. Math. Soc., Providence, RI, 2003.

[169] P. Kuchment and B.-S. Ong. On guided electromagnetic waves in photonic crystal waveguides. In *Operator theory and its applications*, volume 231 of *Amer. Math. Soc. Transl. Ser. 2*, pages 99–108. Amer. Math. Soc., Providence, RI, 2010.

[170] P. Kuchment and Y. Pinchover. Integral representations and Liouville theorems for solutions of periodic elliptic equations. *J. Funct. Anal.*, 181(2):402–446, 2001.

[171] P. Kuchment and O. Post. On the spectra of carbon nano-structures. *arXiv preprint math-ph/0612021*, 2006.

[172] P. Kuchment and H. Zeng. Convergence of spectra of mesoscopic systems collapsing onto a graph. *J. Math. Anal. Appl.*, 258(2):671–700, 2001.

[173] F. Kwok. On the time-domain decomposition of parabolic optimal control problems. In *Domain Decomposition Methods in Science and Engineering XXIII*, pages 55–67. Springer, 2017.

[174] J.-E. Lagnese and G. Leugering. Time-domain decomposition of optimal control problems for the wave equation. *Systems & control letters*, 48(3-4):229–242, 2003.

[175] J.-E. Lagnese and G. Leugering. *Domain decomposition methods in optimal control of partial differential equations*, volume 148 of *International Series of Numerical Mathematics*. Birkhäuser Verlag, Basel, 2004.

[176] V. Laude. Phononic crystals. In *Phononic Crystals*. de Gruyter, 2020.

[177] N. Lebbe, K. Pham, and A. Maurel. Stable gstc formulation for maxwell's equations. *IEEE Transactions on Antennas and Propagation*, pages 1–1, 2022.

[178] A. Lechleiter and R. Zhang. A convergent numerical scheme for scattering of aperiodic waves from periodic surfaces based on the floquet–bloch transform. *SIAM Journal on Numerical Analysis*, 55(2):713–736, 2017.

[179] J.-P. Lee-Thorp, M.-I. Weinstein, and Y. Zhu. Elliptic operators with honeycomb symmetry: Dirac points, edge states and applications to photonic graphene. *Archive for Rational Mechanics and Analysis*, 232(1):1–63, 2019.

[180] J. Lin and H. Zhang. Mathematical theory for topological photonic materials in one dimension. *arXiv preprint arXiv:2101.05966*, 2021.

[181] J.-L. Lions. *Optimal control of systems governed by partial differential equations.*, volume 170. Springer, Berlin, 1971.

[182] J.-L. Lions and O. Pironneau. Sur le contrôle parallèle des systèmes distribués. *C. R. Acad. Sci. Paris Sér. I Math.*, 327(12):993–998, 1998.

[183] B. Lombard, A. Maurel, and J.-J. Marigo. Numerical modeling of the acoustic wave propagation across a homogenized rigid microstructure in the time domain. *Journal of Computational Physics*, 335:558–577, 2017.

[184] Y. Maday and G. Turinici. The parareal in time iterative solver: a further direction to parallel implementation. In *Domain decomposition methods in science and engineering*, pages 441–448. Springer, 2005.

[185] A.-L. Madureira and F. Valentin. Asymptotics of the Poisson problem in domains with curved rough boundaries. *SIAM J. Math. Anal.*, 38(5):1450–1473 (electronic), 2006/07.

[186] J.-J. Marigo and A. Maurel. Two-scale homogenization to determine effective parameters of thin metallic-structured films. *Proceedings of the Royal Society A: Mathematical, Physical and Engineering Sciences*, 472(2192):20160068, 2016.

[187] J.-J. Marigo and A. Maurel. An interface model for homogenization of acoustic metafilms, 2017.

[188] J.-J. Marigo, A. Maurel, K. Pham, and A. Sbitti. Effective dynamic properties of a row of elastic inclusions: the case of scalar shear waves. *Journal of elasticity*, 128(2):265–289, 2017.

[189] J.-J. Marigo, A. Maurel, K. Pham, and A. Sbitti. Effective dynamic properties of a row of elastic inclusions: the case of scalar shear waves. *Journal of elasticity*, 128(2):265–289, 2017.

[190] P.-A. Martin. On acoustic and electric faraday cages. *Proceedings of the Royal Society A: Mathematical, Physical and Engineering Sciences*, 470(2171):20140344, 2014.

[191] A. Maurel, J.-J. Marigo, J.-F. Mercier, and K. Pham. Modelling resonant arrays of the helmholtz type in the time domain. *Proceedings of the Royal Society A: Mathematical, Physical and Engineering Sciences*, 474(2210):20170894, 2018.

[192] A. Maurel, J.-F. Mercier, K. Pham, J.-J. Marigo, and A. Ourir. Enhanced resonance of sparse arrays of helmholtz resonators—application to perfect absorption. *The Journal of the Acoustical Society of America*, 145(4):2552–2560, 2019.

[193] D. Maystre. I rigorous vector theories of diffraction gratings. In *Progress in optics*, volume 21, pages 1–67. Elsevier, 1984.

[194] V. Maz'ya, S.-A. Nazarov, and B. Plamenevskij. *Asymptotic theory of elliptic boundary value problems in singularly perturbed domains. Vol. I*, volume 111 of *Operator Theory: Advances and Applications*. Birkhäuser Verlag, Basel, 2000. Translated from the German by Georg Heinig and Christian Posthoff.

[195] G. Meinardus. *Approximation of functions: Theory and numerical methods*, volume 13. Springer Science & Business Media, 2012.

[196] P.-B. Monk. *Finite element methods for Maxwell's equations*. Numerical Mathematics and Scientific Computation. Oxford University Press, New York, 2003.

[197] P.-B. Monk. *Finite element methods for Maxwell's equations*. Numerical Mathematics and Scientific Computation. Oxford University Press, New York, 2003.

[198] P.-B. Monk, C. Rivas, R. Rodríguez, and M.-E. Solano. An asymptotic model based on matching far and near field expansions for thin gratings problems. *ESAIM: Mathematical Modelling and Numerical Analysis*, 55:S507–S533, 2021.

[199] A. Munch. Family of implicit schemes uniformly controllable for the 1-d wave equation. *Comptes Rendus Mathématique*, 339(10):733–738, 2004.

[200] K. Nakada, M. Fujita, G. Dresselhaus, and M.-S. Dresselhaus. Edge state in graphene ribbons: Nanometer size effect and edge shape dependence. *Physical Review B*, 54(24):17954, 1996.

[201] F. Nataf, F. Rogier, and E. De Sturler. Optimal Interface Conditions for Domain Decomposition Methods. Technical Report 301, CMAP Ecole Polytechnique, 1994.

[202] S.-A. Nazarov. Asymptotic behavior of the solution of the Dirichlet problem in an angular domain with a periodically changing boundary. *Mat. Zametki*, 49(5):86–96, 159, 1991.

[203] S.-A. Nazarov. Asymptotic conditions at a point, selfadjoint extensions of operators, and the method of matched asymptotic expansions. *Translations of the American Mathematical Society-Series 2*, 193:77–126, 1999.

[204] S.-A. Nazarov. Asymptotic behavior of the solution and the modeling of the Dirichlet problem in an angular domain with a rapidly oscillating boundary. *Algebra i Analiz*, 19(2):183–225, 2007.

[205] S.-A. Nazarov. The Neumann problem in angular domains with periodic and parabolic perturbations of the boundary. *Tr. Mosk. Mat. Obs.*, 69:182–241, 2008.

[206] S.-A. Nazarov. An example of multiple gaps in the spectrum of a periodic waveguide. *Mat. Sb.*, 201(4):99–124, 2010.

[207] S.-A. Nazarov. Opening of a gap in the continuous spectrum of a periodically perturbed waveguide. *Mat. Zametki*, 87(5):764–786, 2010.

[208] S.-A. Nazarov. The asymptotic analysis of gaps in the spectrum of a waveguide perturbed with a periodic family of small voids. *J. Math. Sci. (N. Y.)*, 186(2):247–301, 2012. Problems in mathematical analysis. No. 66.

[209] S.-A. Nazarov. On the spectrum of the laplace operator on the infinite dirichlet ladder. *St. Petersburg Mathematical Journal*, 23(6):1023–1045, 2012.

[210] S.-A. Nazarov. Bounded solutions in a T-shaped waveguide and the spectral properties of the Dirichlet ladder. *Comput. Math. Math. Phys.*, 54(8):1261–1279, 2014.

[211] S.-A. Nazarov. Umov-mandelshtam radiation conditions in elastic periodic waveguides. *Sbornik: Mathematics*, 205(7):953, 2014.

[212] S.-A. Nazarov and J. Sokołowski. Self-adjoint extensions for the Neumann Laplacian and applications. *Acta Math. Sin. (Engl. Ser.)*, 22(3):879–906, 2006.

[213] J.-C. Nédélec. Mixed finite elements in r3. *Numerische Mathematik*, 35(3):315–341, 1980.

[214] J.-C. Nédélec. *Acoustic and electromagnetic equations*, volume 144 of *Applied Mathematical Sciences*. Springer-Verlag, New York, 2001. Integral representations for harmonic problems.

[215] M. Negreanu and E. Zuazua. Convergence of a multigrid method for the controllability of a 1-d wave equation. *Comptes Rendus Mathematique*, 338(5):413–418, 2004.

[216] H. Nguyen and R. Tsai. A stable parareal-like method for the second order wave equation. *Journal of Computational Physics*, 405:109156, 2020.

[217] S. Ozawa. Spectra of domains with small spherical Neumann boundary. *J. Fac. Sci. Univ. Tokyo Sect. IA Math.*, 30(2):259–277, 1983.

[218] S. Ozawa. Asymptotic property of an eigenfunction of the Laplacian under singular variation of domains—the Neumann condition. *Osaka J. Math.*, 22(4):639–655, 1985.

[219] Ö. Ozdemir, H. Haddar, and A. Yaka. Reconstruction of the electromagnetic field in layered media using the concept of approximate transmission conditions. *IEEE transactions on antennas and propagation*, 59(8):2964–2972, 2011.

[220] G.-P. Panasenko and E. Perez. Asymptotic partial decomposition of domain for spectral problems in rod structures. *Journal de Mathématiques Pures et Appliquées*, 87(1):1 – 36, 2007.

[221] L. Parnovski. Bethe-Sommerfeld conjecture. *Ann. Henri Poincaré*, 9(3):457–508, 2008.

[222] L. Parnovski and A. V. Sobolev. Bethe-Sommerfeld conjecture for periodic operators with strong perturbations. *Invent. Math.*, 181(3):467–540, 2010.

[223] E. Pavel. Contact interactions on graph superlattices. *Journal of Physics A: Mathematical and General*, 29(1):87, 1996.

[224] J.-B. Pendry. Negative refraction makes a perfect lens. *Physical review letters*, 85(18):3966, 2000.

[225] J.-R. Poirier, A. Bendali, and P. Borderies. Impedance boundary conditions for the scattering of time-harmonic waves by rapidly varying surfaces. *Antennas and Propagation, IEEE Transactions on*, 54(3):995–1005, 2006.

[226] J.-R. Poirier, A. Bendali, P. Borderies, and S. Tournier. High order asymptotic expansion for the scattering of fast oscillating periodic surfaces. In *proceedings of waves 2009*, 2009.

[227] O. Post. Spectral convergence of quasi-one-dimensional spaces. *Ann. Henri Poincaré*, 7(5):933–973, 2006.

[228] J. Rauch and M. Taylor. Potential and scattering theory on wildly perturbed domains. *J. Funct. Anal.*, 18:27–59, 1975.

[229] L. Rayleigh. The theory of the helmholtz resonator. *Proceedings of the Royal Society of London. Series A, Containing Papers of a Mathematical and Physical Character*, 92(638):265–275, 1916.

[230] M. Reed and B. Simon. *Methods of modern mathematical physics v. I-IV*. Academic Press, New York, 1972-1978.

[231] C. Rivas, M.-E. Solano, R. Rodríguez, P.-B. Monk, and A. Lakhtakia. Asymptotic model for finite-element calculations of diffraction by shallow metallic surface-relief gratings. *JOSA A*, 34(1):68–79, 2017.

[232] J. Rubinstein and M. Schatzman. Variational problems on multiply connected thin strips. I. Basic estimates and convergence of the Laplacian spectrum. *Arch. Ration. Mech. Anal.*, 160(4):271–308, 2001.

[233] J. Rubinstein and M. Schatzman. Variational problems on multiply connected thin strips. II. Convergence of the Ginzburg-Landau functional. *Arch. Ration. Mech. Anal.*, 160(4):309–324, 2001.

[234] D. Ruprecht. Wave propagation characteristics of parareal. *Computing and Visualization in Science*, 19(1):1–17, 2018.

[235] Y. Saito. The limiting equation for Neumann Laplacians on shrinking domains. *Electron. J. Differential Equations*, pages No. 31, 25 pp. (electronic), 2000.

[236] E. Sánchez-Palencia. *Nonhomogeneous media and vibration theory*, volume 127 of *Lecture Notes in Physics*. Springer-Verlag, Berlin, 1980.

[237] E. Sánchez-Palencia. Un problème d'écoulement lent d'un fluide incompressible au travers d'une paroi finement perforée. In *Homogenization methods: theory and applications in physics (Bréau-sans-Nappe, 1983)*, volume 57 of *Collect. Dir. Études Rech. Élec. France*, pages 371–400. Eyrolles, Paris, 1985.

[238] A. Schiela and S. Ulbrich. Operator preconditioning for a class of inequality constrained optimal control problems. *SIAM J. Optim.*, 24(1):435–466, 2014.

[239] B. Schweizer. Inhomogeneous helmholtz equations in wave guides–existence and uniqueness results with energy methods. *European Journal of Applied Mathematics*, pages 1–27, 2022.

[240] B. Schweizer and M. Urban. Effective maxwell's equations in general periodic microstructures. *Applicable Analysis*, 97(13):2210–2230, 2018.

[241] A. Semin, B. Delourme, and K. Schmidt. On the homogenization of the helmholtz problem with thin perforated walls of finite length. *ESAIM: Mathematical Modelling and Numerical Analysis*, 52(1):29–67, 2018.

[242] J. Shapiro. The bulk-edge correspondence in three simple cases. *Reviews in Mathematical Physics*, 32(03):2030003, 2020.

[243] J. Shapiro and M.-I. Weinstein. Is the continuum ssh model topological? *arXiv preprint arXiv:2107.09146*, 2021.

[244] C.-M. Soukoulis. Wood pile photonic crystal. `https://commons.wikimedia.org/w/index.php?curid=11294534`. Accessed: 2022-08-22.

[245] W.-P. Su, J.-R. Schrieffer, and A.-J. Heeger. Solitons in polyacetylene. *Physical review letters*, 42(25):1698, 1979.

[246] S.-H. Tang and M. Zworski. From quasimodes to resonances. *Mathematical Research Letters*, 5(3):261–272, 1998.

[247] M. Touboul, K. Pham, A. Maurel, J.-J. Marigo, B. Lombard, and C. Bellis. Effective resonant model and simulations in the time-domain of wave scattering from a periodic row of highly-contrasted inclusions. *Journal of Elasticity*, 142(1):53–82, 2020.

[248] P.-H. Tournier, F. Hecht, F. Nataf, M. Bonazzoli, F. Rapetti, V. Dolean, S. Semenov, I. El Kanfoud, I. Aliferis, C. Migliaccio, et al. Microwave tomography for brain stroke imaging. In *2017 IEEE International Symposium on Antennas and Propagation & USNC/URSI National Radio Science Meeting*, pages 29–30. IEEE, 2017.

[249] M.-B. Tran. On domain decomposition methods for optimal control problems. *Applications of Mathematics 2013*, pages 207–214, 2013.

[250] F. Tröltzsch. *Optimal control of partial differential equations: theory, methods, and applications*, volume 112. American Mathematical Soc., 2010.

[251] M. Van Dyke. *Perturbation methods in fluid mechanics*. Applied Mathematics and Mechanics, Vol. 8. Academic Press, New York, 1964.

[252] E. Vasilevskaya. *Open periodic waveguides. Theory and computation.* PhD thesis, Université Paris 13, 2016.

[253] V.-G. Veselago. The electrodynamics of substances with simultaneously negative values of epsilon and mu. *Physics-Uspekhi*, 10(4):509–514, 1968.

[254] G. Vial. *Analyse multi-échelle et conditions aux limites approchées pour un probleme avec couche mince dans un domaine à coin.* PhD thesis, École Normale Supérieure de Cachan, Paris, 2003.

[255] V. Vinoles. *Problèmes d'interface en présence de métamatériaux: modélisation, analyse et simulations.* PhD thesis, Université Paris-Saclay (ComUE), 2016.

[256] M. Vorobets. On the Bethe-Sommerfeld conjecture for certain periodic Maxwell operators. *J. Math. Anal. Appl.*, 377(1):370–383, 2011.

[257] P.-R. Wallace. The band theory of graphite. *Physical review*, 71(9):622, 1947.

[258] M. Xiao, Z.-Q. Zhang, and C.-T. Chan. Surface impedance and bulk band geometric phases in one-dimensional systems. *Physical Review X*, 4(2):021017, 2014.

[259] Y. Xu and X. Chen. Optimized schwarz methods for the optimal control of systems governed by elliptic partial differential equations. *Journal of Scientific Computing*, 79(2):1182–1213, 2019.

[260] Sylvain Zalczer. *Propriétés spectrales de modèles de graphène périodique et désordonné*. PhD thesis, Université de Toulon, 2020.

[261] R. Zhang. A high order numerical method for scattering from locally perturbed periodic surfaces. *SIAM Journal on Scientific Computing*, 40(4):A2286–A2314, 2018.

[262] R. Zhang. Numerical methods for scattering problems in periodic waveguides. *Numerische Mathematik*, 148(4):959–996, 2021.

[263] R. Zhang. Exponential convergence of perfectly matched layers for scattering problems with periodic surfaces. *SIAM Journal on Numerical Analysis*, 60(2):804–823, 2022.

[264] J. Zhou Hagström, A. Maurel, and K. Pham. The interplay between fano and fabry–pérot resonances in dual-period metagratings. *Proceedings of the Royal Society A*, 477(2255):20210632, 2021.

[265] E. Zuazua. Propagation, observation, and control of waves approximated by finite difference methods. *SIAM review*, 47(2):197–243, 2005.